

---

Electronic Thesis and Dissertation Repository

---

12-14-2016 12:00 AM

# Modelling and Analysis of Smart Grids for Critical Data Communication

Abdulfattah Noorwali  
*The University of Western Ontario*

Supervisor  
Dr. Raveendra Rao  
*The University of Western Ontario* Joint Supervisor  
Dr. Abdallah Shami  
*The University of Western Ontario*

Graduate Program in Electrical and Computer Engineering  
A thesis submitted in partial fulfillment of the requirements for the degree in Doctor of Philosophy  
© Abdulfattah Noorwali 2016

Follow this and additional works at: <https://ir.lib.uwo.ca/etd>



Part of the [Digital Communications and Networking Commons](#), and the [Systems and Communications Commons](#)

---

## Recommended Citation

Noorwali, Abdulfattah, "Modelling and Analysis of Smart Grids for Critical Data Communication" (2016). *Electronic Thesis and Dissertation Repository*. 4440.  
<https://ir.lib.uwo.ca/etd/4440>

This Dissertation/Thesis is brought to you for free and open access by Scholarship@Western. It has been accepted for inclusion in Electronic Thesis and Dissertation Repository by an authorized administrator of Scholarship@Western. For more information, please contact [wlsadmin@uwo.ca](mailto:wlsadmin@uwo.ca).

# Abstract

Practical models for the subnetworks of smart grid are presented and analyzed. Critical packet-delay bounds for these subnetworks are determined, with the overall objective of identifying parameters that would help in the design of smart grid with least end-to-end delay.

A single-server non-preemptive queueing model with prioritized critical packets is presented for Home Area Network (HAN). Closed-form expressions for critical packet delay are derived and illustrated as a function of: i) critical packet arrival rate, ii) service rate, iii) utilization factor, and iv) rate of arrival of non-critical packets. Next, wireless HANs using FDMA and TDMA are presented. Upper and lower bounds on critical packet delay are derived in closed-form as functions of: i) average of signal-to-interference-plus-noise ratio, ii) random channel scale, iii) transmitted power strength, iv) received power strength, v) number of EDs, vi) critical packet size, vii) number of channels, viii) path loss component, ix) distances between electrical devices and mesh client, x) channel interference range, xi) channel capacity, xii) bandwidth of the channel, and xiii) number of time/frequency slots. Analytical and simulation results show that critical packet delay is smaller for TDMA compared to FDMA. Lastly, an Intelligent Distributed Channel-Aware Medium Access Control (IDCA-MAC) protocol for wireless HAN using Distributed Coordination Function (DCF) is presented. The protocol eliminates collision and employs Multiple Input Multiple Output (MIMO) system to enhance system performance. Simulation results show that critical packet delay can be reduced by nearly 20% using MA-Aware protocol compared to IDCA-MAC protocol. However, the latter is superior in terms throughput.

A wireless mesh backbone network model for Neighbourhood Area Network (NAN) is presented for forwarding critical packets received from HAN to an identified gateway. The routing suggested is based on selected shortest path using Voronoi tessellation. CSMA/CA and CDMA protocols are considered and closed-form upper and lower bounds on critical packet delay are derived and examined as functions of i) signal-to-noise ratio, ii) signal interference, iii) critical packet size, iv) number of channels, v) channel interference range, vi) path loss components, vii) channel bandwidth, and viii) distance between MRs. The results show that critical packet delay to gateway using CDMA is lower compared to CSMA/CA protocol.

A fiber optic Wide Area Network (WAN) is presented for transporting critical packets received from NAN to a control station. A Dynamic Fastest Routing Strategy (DFRS) algorithm is used for routing critical packets to control station. Closed-form expression for mean critical packet delay is derived and is examined as a function of: i) traffic intensity, ii) capacity of fiber links, iii) number of links, iv) variance of inter-arrival time, v) variance of service time, and vi) the latency of links. It is shown that delay of critical packets to control station meets acceptable standards set for smart grid.

**Keywords:** Delay, HAN, Modelling, NAN, Smart Grid, and WAN.

# Acknowledgements



“O Allah, to You is praise as befits the Glory of Your Face and the greatness of your Might.” All the praises, and foremost thanks are due to Allah for helping me in completing my PhD study. Without His guidance and blessings, nothing is possible. If I would count up the favours of Allah, never would I be able to number them. Prayers and peace of Allah be upon the noble Prophet Mohammad and upon his family and companions, the honorable followers.

I would like to thank all people who have helped me in getting my PhD thesis between covers.

First, I would like to express my deep appreciation to my thesis supervisor Dr. Raveendra Rao. His office door is always open for discussion, encouragement, insightful guidance, consistent support, invaluable advice, and constructive criticism. I appreciate his time and ideas that have helped me to be highly productive. With his involvement and patience, I have been able to write my Ph.D thesis successfully. Also, I would like to thank my co-supervisor Dr. Abdallah Shami for his continuous encouragement, kindness and support at all stages of my PhD study.

I would also like to show my sincere gratitude and deep thanks to my parents, my grandmother, my wife, my siblings and my children. Their dua’a, support, encouragement, smile, and countless sacrifices are the basis of my continuing personal development. The inexhaustible kindness and love I have received are invaluable. They deserve all the credits.

I would also like to express my thanks to all my fantastic friends and colleagues for their kind support and encouragement. Special thanks go to my friends at Western with whom I had the privilege to work and the discussions with them have benefited me immensely.

Last but not the least, I would like to thank Umm Al-Qura University for the scholarship and financial support through Saudi Cultural Bureau in Canada, without which this work would not have been possible.

***Abdulfattah Noorwali***

# Dedication

**To:** *my parent, my grandmother, my wife, my siblings, and my children*

# Table of Contents

<b>Abstract</b>	<b>i</b>
<b>Acknowledgements</b>	<b>iii</b>
<b>Dedication</b>	<b>iv</b>
<b>List of Tables</b>	<b>viii</b>
<b>List of Figures</b>	<b>ix</b>
<b>List of Abbreviations</b>	<b>xii</b>
<b>List of Symbols</b>	<b>xv</b>
<b>1 Introduction</b>	<b>1</b>
1.1 Introduction to Smart Grids	1
1.2 Literature Survey and Motivation	3
1.3 Structure of Smart Grid	8
1.3.1 Three Subnetworks of Smart Grid	10
1.4 Thesis Objectives	12
1.4.1 Modelling and Analysis of Home Area Network (HAN)	12
1.4.2 Modelling and Analysis of Channel-Aware MAC Protocol for HAN	13
1.4.3 Modelling and Analysis of Neighbourhood Area Network	13
1.4.4 Modelling and Analysis of Wide Area Network	14
1.5 Thesis Organization	15
<b>2 Background</b>	<b>17</b>
2.1 Introduction	17
2.2 Key Terms	17
2.3 Network Models and Assumptions	18
2.3.1 Generating Functions	20
2.3.2 Wireless Interference	20
2.3.3 Channel Capacity	22
2.3.4 Routing and Communication	23
2.3.5 Communication Access Schemes	23
2.3.6 Optical Communication	23
2.3.7 MATLAB Simulator	24
2.4 Smart Grid Components	24
2.4.1 Home Area Network	25

2.4.2	Neighborhoods Area Network . . . . .	33
2.4.3	Wire-Line Network . . . . .	37
2.5	Summary and Conclusions . . . . .	41
<b>3</b>	<b>Single-Server Non-Preemptive Priority Queueing Model for HAN . .</b>	<b>42</b>
3.1	Introduction . . . . .	42
3.2	Model of Non-preemptive Single Server Queueing System . . . . .	43
3.2.1	State of Queueing System . . . . .	46
3.2.2	Queueing System Contents . . . . .	46
3.3	Delay Analysis of Queueing System . . . . .	49
3.4	Average Packet Delay and Contents for HAN . . . . .	50
3.5	Numerical Results and Discussion . . . . .	51
3.6	Summary and Conclusions . . . . .	55
<b>4</b>	<b>Modelling and Delay Analysis of Wireless HAN . . . . .</b>	<b>56</b>
4.1	Introduction . . . . .	56
4.2	Model of Wireless HAN . . . . .	57
4.2.1	Channel Models and Fading Statistics . . . . .	60
4.2.2	Centralized Multiple-Access Schemes for Scheduling Transmissions	60
4.3	Delay Analysis . . . . .	63
4.3.1	Lower Bound on the Delay . . . . .	63
4.3.2	Upper Bound on the Delay . . . . .	65
4.3.3	Capacity Estimation over Wireless Fading Channels . . . . .	65
4.3.4	Delay Analysis for Multiple Access Schemes . . . . .	67
4.4	Numerical Results and Discussions . . . . .	68
4.5	Summary and Conclusions . . . . .	74
<b>5</b>	<b>Intelligent Distributed Channel-Aware MAC Protocol for HAN . . .</b>	<b>76</b>
5.1	Introduction . . . . .	76
5.1.1	Background . . . . .	77
5.2	HAN Environment Description . . . . .	78
5.2.1	CSMA/CA Scheme . . . . .	78
5.2.2	MAC System Description . . . . .	79
5.2.3	Tuning In/Tuning Out Specifications . . . . .	80
5.3	Intelligent Distributed Channel-Aware MAC Protocol . . . . .	80
5.3.1	Interference Cancellation . . . . .	81
5.3.2	Zig-Zag Decoding . . . . .	81
5.3.3	Simulation Results and Analysis . . . . .	83
5.3.4	IDCA-MAC Protocol Operation . . . . .	84
5.4	Overall Evaluation . . . . .	88
5.5	Summary and Conclusions . . . . .	90

<b>6</b>	<b>Modelling and Delay Analysis of NAN</b>	<b>91</b>
6.1	Introduction	91
6.1.1	Background	91
6.2	Model of WMBN	95
6.2.1	Voronoi Tessellation Definition	96
6.2.2	Inter-Channel Interference Model	96
6.2.3	Wireless Interference	97
6.2.4	Scheduling Transmissions	99
6.2.5	Straight-Line Path Routing (SLPR) Algorithm	104
6.3	Delay Analysis	105
6.3.1	Parallel Transmission in CSMA/CA	105
6.3.2	Transmission using CDMA Protocol	107
6.4	Numerical Results and Discussions	108
6.5	Conclusions and Summary	111
<b>7</b>	<b>Modelling and Delay Analysis of WAN</b>	<b>112</b>
7.1	Introduction	112
7.2	Expression for Delay in WAN	113
7.3	Proposed Dynamic Routing Strategy (DFRS)	114
7.3.1	Problem Formulation to Determine Optimal Path	114
7.4	End-To-End Delay Analysis in WAN	117
7.4.1	Transition State	119
7.4.2	Average Delay Analysis	120
7.4.3	Multiple Access Scheme for Scheduling Transmissions	121
7.5	Numerical Results and Discussion	122
7.5.1	Overall Evaluation of Critical Packet Delay	123
7.6	Conclusions and Summary	126
<b>8</b>	<b>Conclusions</b>	<b>127</b>
8.1	Introduction	127
8.2	Summary of Contributions	127
8.3	Suggestions for Future Work	129
	<b>Curriculum Vitae</b>	<b>143</b>



# List of Tables

Section		Page
1.1	A list of notable research efforts in smart grid . . . . .	7
2.1	Traffic (packets/second)-cum-Routing Matrix . . . . .	38
2.2	Wire Link Capacities . . . . .	39
2.3	Table for computing delays over each of the links in the network . . . . .	40
3.1	Parameters used to determine average number of packets in the system (Fig. 2.4) and average packet delay (Fig. 2.5) as a function of $\lambda_{HP}$ . . . .	52
3.2	Parameters used to determine average packet delay (Fig. 2.6) as a function of service rate, $\mu$ . . . . .	53
3.3	Parameters used to determine average packet delay as a function of system utilization factor, $\rho_T$ . . . . .	54
5.1	Extended RTS frame structure for IDCA-MAC protocol . . . . .	79
5.2	Extended CTS frame structure for IDCA-MAC protocol . . . . .	79
5.3	ICDA-MAC protocol parameters used in the simulation [62] . . . . .	83
6.1	Model parameters used in simulation of WMBN . . . . .	108
6.2	Parameters used for plotting critical delay as a function of $CIR$ (Fig. 5.10) . . . .	108
6.3	Parameters used for plotting critical delay as a function of $\beta$ (Fig. 5.11) . . . .	108
6.4	Parameters used for plotting of critical packet delay as a function of number of critical packets $n$ (Fig. 5.11) . . . . .	109
7.1	Parameters used in the fiber-optic WAN model used for numerical computations . . . . .	123

# List of Figures

Section		Page
1.1	Annual business losses from power grid problem. . . . .	3
1.2	Chronological research effects in smart grid communications. . . . .	6
1.3	General view of power grid/smart grid. . . . .	7
1.4	A conceptional model of smart grid. . . . .	9
1.5	A pictorial view of a smart grid. . . . .	9
1.6	An expanded view of smart grid model. . . . .	11
2.1	IEEE 802.11 Channel Blocks. . . . .	21
2.2	Example of how distance is considered. . . . .	21
2.3	Powers signals decay effects to $i$ channel into $u$ node. . . . .	22
2.4	Transmissions around $u$ node. . . . .	22
2.5	The structure components of M/M/1 model. . . . .	26
2.6	FDMA frequency bands. . . . .	28
2.7	TDMA Time Slots. . . . .	29
2.8	Type of data generated by electrical devices. . . . .	29
2.9	FDMA Transmission Function. . . . .	30
2.10	TDMA Transmission Function. . . . .	31
2.11	Fading types. . . . .	32
2.12	Definitions of Voronoi Cell Shapes. . . . .	34
2.13	CSAM/CA timing diagram. . . . .	36
2.14	CDMA time/frequency slots. . . . .	36
2.15	Wire-Line Network. . . . .	37
2.16	Wire-Line Network Example. . . . .	38
3.1	Non-preemptive queueing model between ED and MC. . . . .	44
3.2	Model of HAN in smart grid. . . . .	44
3.3	Queueing model between a set of $n$ EDs and MC. . . . .	51
3.4	Average number of packets in the system as a function of HP arrival rate ( $\lambda_{HP}$ ). . . . .	52
3.5	Average packet delay as a function of HP arrival rate ( $\lambda_{HP}$ ). . . . .	53
3.6	Average packet delay as a function of service rate ( $\mu$ ), for $\lambda_{HP} = 8$ and $\lambda_{PB} = 1$ . . . . .	54
3.7	Average packet delay as a function of $\rho_T$ , for $\lambda_{HP} = 2$ and $\lambda_{PB} = 1$ . . . . .	55
4.1	Model of typical wireless HAN and its multipath environment. . . . .	57
4.2	Spectrum allocation in IEEE 802.11 networks . . . . .	58
4.3	General view of wireless HAN communication network. . . . .	58
4.4	Path loss model for transmission between ED and MC. . . . .	59

4.5	Time-frequency plot for modified FDMA. . . . .	61
4.6	Time-frequency plot for modified TDMA. . . . .	62
4.7	Channel block showing interference from each active channel. . . . .	64
4.8	Channel capacity as a function of SNR for Nakagami, Rayleigh, and Gaussian channels. . . . .	67
4.9	Critical delay bounds for HAN with modified FDMA as a function of SNR ( $\bar{\gamma}$ ) for $CIR = 2$ , $Q_{HAN} = 25$ , $n = 200$ , $\beta = 2$ . . . . .	69
4.10	Critical delay bounds for HAN with modified TDMA as a function of SNR ( $\bar{\gamma}$ ) for $CIR = 2$ , $Q_{HAN} = 25$ , $n = 200$ , $\beta = 2$ . . . . .	70
4.11	Critical delay bounds for HAN as a function of $CIR$ for: $Q_{HAN} = 25$ , $n = 200$ , $\beta = 3$ , and $\bar{\gamma} = 5$ dB. . . . .	71
4.12	Critical delay bounds for HAN as a function of $\beta$ for $Q_{HAN} = 25$ , $n = 200$ , $CIR = 8$ , and $\bar{\gamma} = 5$ dB. . . . .	71
4.13	Critical delay bounds for HAN as a function of $n$ for $Q_{HAN} = 25$ , $\beta = 3$ , $CIR = 8$ , and $\bar{\gamma} = 5$ dB. . . . .	72
4.14	Critical delay bounds for HAN ( $A = 1$ ) as a function of $CIR$ for: $Q_{HAN} = 25$ , $n = 200$ , $\beta = 3$ , and $\bar{\gamma} = 100$ . . . . .	73
4.15	Critical delay bounds for HAN ( $A = 1$ ) as a function of $\beta$ for $Q_{HAN} = 25$ , $n = 200$ , $CIR = 8$ , and $\bar{\gamma} = 100$ . . . . .	73
4.16	Critical delay bounds for HAN ( $A = 1$ ) as a function of $n$ for $Q_{HAN} = 25$ , $\beta = 3$ , $CIR = 8$ , and $\bar{\gamma} = 100$ . . . . .	74
5.1	Structure of HAN with EDs and MC equipped with multiple antennas. . . . .	81
5.2	Collision scenario of transmitting more than one packet over the channel. . . . .	82
5.3	Two transmitted packets with collision. . . . .	83
5.4	Timing diagram of MAC decision process when secondary transmission time is less than the primary [62]. . . . .	86
5.5	Timing diagram of MAC decision process for the case of partial weight sensing [62]. . . . .	86
5.6	Timing diagram of MAC decision process for the case of splitting data through transmission [62]. . . . .	87
5.7	Timing diagram of MAC decision process for the case of collision [62]. . . . .	87
5.8	Throughput of the system as a function of number of electrical devices [62]. . . . .	88
5.9	Critical packet delay of the system using IDCA-MAC protocol as a function of number of electrical devices [62]. . . . .	89
5.10	Throughput of the system as a function of CW size [62]. . . . .	89
6.1	Structure and location of NAN in smart grid. . . . .	92
6.2	Conceptional model of Wireless Mesh Backbone network. . . . .	94
6.3	Example of Voronoi structure. . . . .	95
6.4	Wireless mesh backbone network in the Voronoi diagram. . . . .	96
6.5	Straight-line path in Voronoi diagram. . . . .	98
6.6	Division of ring area for WMBN. . . . .	98
6.7	Channel block showing interference from each active channel. . . . .	100
6.8	Packet delay bounds as a function of number of critical packets. . . . .	101

6.9	CDMA: Time, frequency and code slots. . . . .	102
6.10	Delay bounds as a function of the $CIR$ . . . . .	110
6.11	Delay bounds as a function of the $SNR$ . . . . .	110
6.12	Delay bounds as a function of number of critical packets $n$ . . . . .	111
7.1	Structure of high-speed WAN. . . . .	115
7.2	Network model scenario. . . . .	115
7.3	Death and birth process of a WAN in a smart grid. . . . .	120
7.4	TDMA time slots. . . . .	121
7.5	Critical packet delay as a function of threshold WAN $QoS$ . . . . .	124
7.6	Critical packet delay in WAN as a function of capacity of links $C_l$ . . . . .	124
7.7	Critical packet delay as a function of adjacent channel load $y_{i,j}$ . . . . .	125
7.8	Critical packet delay a function of link utilization $\rho_l$ . . . . .	125
7.9	Critical packet delay as a function of number of available channels $b_l$ . . . . .	126
8.1	End-to-end delay of smart grid as a function of number of EDs for: $Q_{HAN} = 25$ , $Q_{NAN} = 25$ , $b_l = 1 - 15$ , $\beta = 3$ , $r = 8000$ , $d^{edge} = 100m$ , $d^{vertex} = 200m$ , $L = 1000$ , $W = 22MHz$ , $r_o = 5m$ , $\varphi = 3$ , $\bar{\gamma} = 200$ , $\lambda = 500packts/sec$ , $\mu = 600packets/sec$ , $C_l = 100Mbs$ , $QoS = 50Mbits$ , and $r_{i,j} = 10Km$ . . . . .	130
8.2	NetMIMO . . . . .	131

# List of Abbreviations

AL	Access Layer
AP	Access Point
CDMA	Code Division Multiple Access
CIR	Channel Interference Range
CL	Core Layer
CSMA/CA	Carrier Sense Multiple Access/Collision Avoidance
DCF	Distributed Coordination Function
DFRS	Dynamic Fastest Routing Strategy
DL	Distribution Layer
DRX	Delay-Responsive Cross Layer
ED/EDs	Electrical Device/Electrical Devices
EDN	Electrical Device Network
EISA	Energy Independence and Security Act
FDMA	Frequency Division Multiple Access
FIFO	First Input First Output
GPSR	Greedy Perimeter Stateless Routing
GTS	Guaranteed Time Slots
HAN/HANs	Home Area Network/Home Area Networks
HOL	Head-of-Line
HP	High Priority
ICR	Inter-Channel-Interference Range
ICT	Information and Communication Technologies
IEEE	Institute of Electrical and Electronics Engineers

i.i.d	independent and identically distributed
IP	Internet Protocol
LAN	Local Area Network
LoS	Line of Sight
MAC	Medium Access Control
MBN	Mesh Backbone Network
MA-Aware	Media Access Aware
MC/MCs	Mesh Client/Mesh Clients
MR/MRs	Mesh Router/Mesh Routers
MWM	Maximum Weighted Matching
NAV	Network Allocation Vector
NAN	Neighbourhood Area Network
NIST	National Institute of Standards and Technology
PB	Periodic Base
PC	Point Coordinator
PCF	Point Coordination Function
PDF	Probability Distribution Function
PHY	Physical Layer
PGF	Probability Generating Function
PLC	Power Line Communication
QAM	Quadrature Amplitude Modulation
QGA	QoS-aware GTS
QoS	Quality of Service

SNR	Signal-to-Noise Ratio
SLPR	Straight-Line Path Routing
TDMA	Time Division Multiple Access
TUs	Time Units
WAN	Wide Area Network
WDN	Wired Distribution Network
WHAN	Wireless Home Area Network
WiFi	Colloquial English synonym for “WLAN”
WLAN	Wireless Local Area Network
WMN	Wireless Mesh Network
WMBN	Wireless Mesh Backbone Network

# List of Symbols

$a$	Time slot
$\varphi$	Path-loss exponent
$\alpha$	Random channel scale
$b_{i,a}$	Number of class $i$ arrivals in slot $a$
$b_{T,a}$	Total number of arrivals in slot $a$
$B(z_1, z_2)$	Joint pgf of the number of per-slot-class ( $i = 1, 2$ ) arrivals
$B_T(z)$	pgf of the total number of arrivals per-slot
$B_{HP}(z)$	pgf of number of HP arrivals
$B_{PB}(z)$	pgf of number of PB arrivals
$\beta$	$SNR$ threshold
$C_{AWGN}$	Capacity of AWGN channel
$C_{Fading}$	Capacity of fading channel
$C_R$	Capacity of Rayleigh channel
$C_N$	Capacity of Nakagami channel
$Cov[...]$	Covariance of two stochastic variables
$CIR$	Channel interference range
$C_l$	Capacity over link $l$
$C_{i,u}$	Capacity of channel $i$ at node $i$
$C_{ell}$	Voronoi cell



$d$	Distance between two active channels $(i, j)$
$D_{hop}$	One-hop communication delay in WMBN
$d_{edge}$	Minimum distance from mesh router to its cell edge
$d^{vertex}$	Maximum distance from mesh router to its cell vertex
$\Delta_{EDN}$	Delay in Electrical device network
$\Delta_{FD}$	Delay in FDMA system
$\Delta_{end-to-end}$	End-to-end delay
$\Delta_{end-to-end}^l$	Lower bound on end-to-end delay
$\Delta_{end-to-end}^u$	Upper bound on end-to-end delay
$\Delta_{TD}$	Delay in TDMA system
$E_l$	Average number of packets in each link
$E_{lt}$	Average number of packets in transit
$E_{lq}^{G/G/b_l}$	Number of packets that are waiting in queue
$E_q^{G/G/b_l}$	Approximate number of packets in queue
$f_k$	Group of different frequency bands
$\gamma$	Instantaneous $SNR$
$\bar{\gamma}$	Average $SNR$
$\gamma_{u,i}$	$SNR$ on channel $i$ at node $u$
$\Gamma(..., ...)$	Complementary incomplete gamma function
$h^l$	Minimum number of hops
$h^u$	Maximum number of hops
$I$	Interference
$I_{u,i,j}$	Interference caused by simultaneous $j$ transmissions on channel $i$ at node $u$
$k$	Number of available channels
$L$	Packet size
$L_l$	Distance of link $l$ in Km
$\lambda_l$	Arrival rate over link $l$
$\lambda_{HP}$	Arrival rate of high priority packets
$\lambda_{PB}$	Arrival rate of periodic base packets
$\lambda_T$	Total arrival rate

$M$	Number of time slots
$\mu$	Service rate
$\mu_k$	Death rate corresponding to $\lambda_l$
$n$	Number of reports to be transmitted
$N_o$	PSD of White Gaussian noise
$\omega$	Waiting time
$\omega_{CD}$	Waiting time in CDMA system
$\omega_{FD}$	Waiting time in FDMA system
$\omega_{TD}$	Waiting time in TDMA system
$\Omega$	Expected value of random channel scale
$P_t^{(t)}$	Transmitted power
$P_l(0)$	Probability of no packets in the system
$P_r^{(t)}$	Received power
$P_R(\gamma)$	Probability density function of SNR for Rayleigh channel
$P_N(\gamma)$	Probability density function of SNR for Nakagami channel
PGF	Probability generating function
$Q_{EDN}$	Number of channels in the EDN
$Q_{HAN}$	Number of channels in the HAN
$Q_{NAN}$	Number of channels in the NAN
$Q_{WAN}$	Number of channels in the WAN
$QoS$	Quality of Service in bits
$r^{(ref)}$	Reference distance
$r_{i,j}$	Path length of link between $i$ and $j$
$\rho_{HP}$	Load due to HP packets
$\rho_l$	Load over link $l$
$\rho_{PB}$	Load due to PB packets
$\rho_T$	Total load
$S$	Number of scheduled transmissions
$s(t)$	Transmitted signal
$\sigma_a^2$	Variance of inter-arrival time

$\sigma_s^2$	Variance of service time
$SNR$	Signal-to-noise ratio
$T$	Transmission time
$T_{\text{avg}}$	Average packet delay
$\tau_{CD}$	Transmission time in CDMA system
$\tau_{FD}$	Transmission time in FDMA system
$\tau_l$	Propagation delay over link $l$
$\tau_{TD}$	Transmission time in TDMA system
$T_s$	Mean service time
$T_{\text{mean}}^{(G/G/l)}$	Average packet delay in WAN for $G/G/l$ system
$T_{\text{mean}}^{(G/G/b_l)}$	Average packet delay in WAN for $G/G/b_l$ system
$T_l^{(G/G/l)}$	Transmission time over link $l$ in $G/G/l$ system
$T_l^{(G/G/b_l)}$	Transmission time over link $l$ in $G/G/b_l$ system
$u_l$	Utilization of the fiber optic link $l$
$u_{i,a}$	System contents of class $i$ traffic at the beginning of random slot $a$
$u_{T,a}$	Total system contents at the beginning of random slot $a$
$U_a(z_1, z_2)$	Joint pgf of HP and PB classes at the beginning of slot $a$
$U(z_1, z_2)$	Steady-state joint pgf of the system contents HP and PB classes at a random slot
$V_a^2$	Coefficient of variation of inter-arrival time
$Var[b_T]$	Variance of total number of arrivals
$V_s^2$	Coefficient of variation of service time
$W$	Channel bandwidth
$y$	Total load in WAN
$\bar{y}$	Average total load in a WAN
$y_{i,j}$	Traffic load between a pairs of nodes $(i, j)$
$Z_{\text{CSMA/CA}}^l$	Minimum number of scheduled channels in CSMA/CA system
$Z_{\text{CSMA/CA}}^u$	Maximum number of scheduled channels in CSMA/CA system
$Z_{\text{CDMA}}^l$	Minimum number of scheduled channels in CDMA system
$Z_{\text{CDMA}}^u$	Maximum number of scheduled channels in CDMA system

# Chapter 1

## Introduction

### 1.1 Introduction to Smart Grids

Power grid is a term used to describe electricity system that supplies power to Electrical Devices (EDs), located at customers' site, through four operations: generation, transmission, distribution, and control station. It has become critical to connect a communication network/system between the control station and customers for the purpose of gathering and analyzing real-time data about customers to monitor and effect corrective measures. This has become all the more important after the events like the North American power outages that occurred between 1998 and 1999, which left nearly 3.5 million customers without electricity in specific cases for long durations of time.

Efficient communication network infrastructure is therefore the catalyst that elevates especially interconnectivity between different utilities and is in turn essential for avoiding unexpected disconnections from power grid. Such a communication infrastructure is referred to as intelligent network or smart grid. Smart grid gathers information from customers to enable automated delivery of power to them in an efficient way and protects customers from disconnection to power grid.

In [1], a communication network architecture is presented that still needs innovative solutions to integrate it effectively with the power grid. EDs often suffer from unreliable power supply during peak hours. Meanwhile, power grids are becoming larger and more complex, encompassing thousands of EDs, requiring a more stable power supply system. These concerns have contributed to the emergence of the first smart grid (2005) by Italy's Telegestore Project, which serves nearly 27 million users. This grid is based on smart meters connected via low-bandwidth Power Line Communication (PLC) systems. Since then, works on smart grids have been expanded to analyze the performance of the electrical network over large geographic areas and to deal with anomalies. In December

2007, the USA applied efforts to create and deploy a smart grid, with the Energy Independence and Security Act (EISA) encouraging utility companies to begin deployment of smart grids. In this regard, a Federal Smart Grid Task Force was established with the objective of modernizing the power grid for enabling quick response to demand, and for providing high-quality power to customers. As a result, smart grid was deployed in 2008 in Colorado, USA, for connecting customers to power grid through a control station. In 2012, work on smart grid designs culminated in the specification of standards for smart grid and were published by the American National Institute of Standards and Technology (NIST) [2]. The logical connections among different system domains are discussed in these standards. It is highlighted that communication networks should support current and future electrical devices for purposes of monitoring, fault detection, fault isolation, addressability, service discovery, routing, quality of service, and security [3].

One of the most significant challenges facing smart grid architects is that of providing end-to-end communication services. Power equipment should have the ability to send large amounts of information in order to facilitate communication between power plants and consumers. Such networks should provide robust connectivity between EDs and the control stations. This connectivity should aid in decision making based on reports received from EDs, to track power faults and respond to them instantaneously.

To put the scale of the problem into perspective, it is estimated [4], that the annual business loss due to problems of power grid at 150 billion dollars as shown in Fig. 1.1. The United States grid consists of nearly 3,200 electric utilities operating with about 70,000 power plants serving around 315 million consumers using nearly 157,000 miles of high voltage electric transmission lines [1]. The average age of the power grid transmission line is 50-60 years [3]. Between 1988 and 1998, the demand for electricity in the U.S grew by 30%, yet only 15% new transmission capacity was created [4]. The severity of potential costs does not pertain to the scale only. Environmental factors are also critical, as around 40% of America's total CO<sub>2</sub> emissions are due to electricity production [5]. The added layer of intelligence through smart grid requires independent processors in each ED and at each substation and power plant. These processors must have a robust operating system and be able to act as agents that can communicate and cooperate with each other using a large distributed computing platform. When this does not happen due to delay, losses due to miscommunication start to accumulate [6] and can potentially

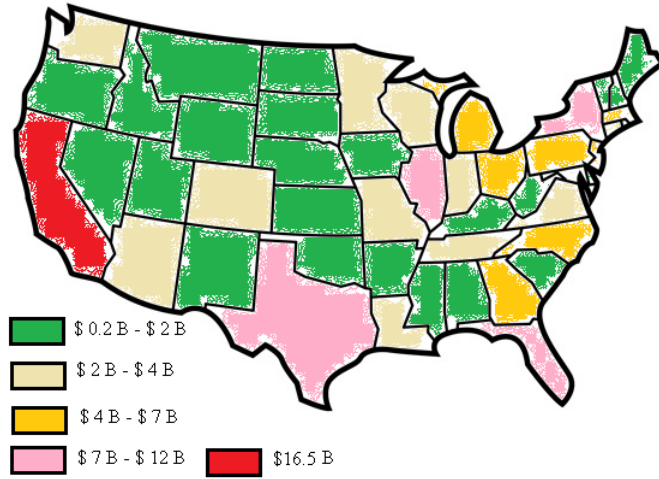


Figure 1.1: Annual business losses from power grid problem.

lead to system instability.

A sobering example of how fast the critical data need to be transmitted for quick and corrective action can be seen in the case of the missing Malaysian aircraft (MH 370), in April 2014. The aircraft disappeared from radar screens, but the response system was unable to make a quick decision and relay it quickly enough. Similarly in a smart grid, the power status information generated by EDs are critical and required to be conveyed for decision making with a guaranteed minimum value of delay. The different types of critical data are [7]: i) alarms on power level usage, ii) status on power fault detection, iii) quality of power, and iv) weather and environment. The end-to-end delay being the critical metric in smart grids is a function of various parameters such as node energy and network characteristics. The hypothesis in this work is that there always exists room for improvement.

## 1.2 Literature Survey and Motivation

Recently, smart grid has been studied in numerous works. Sood, in 2009, [5, 6] examined the interconnection between several power system applications and network availability with the aim of enhancing power generation using smart grids. Souryal et al. [8] presented a study to assess and deploy wireless technologies for smart grids. In their work,

they analyzed the performance of smart grid using IEEE 802.11 standard. Also, they devised a model link layer network to measure reliability, delay, and throughput between relays and customers. However, their model was simply based on channel effects and collisions and it did not take into account end-to-end service, and the domains of operations and customers. In [9], the challenge of managing network demand is investigated using the characteristics of smart meters, bandwidth requirement, and delay via the Ethernet. Hamid et al. [10] examined a multigate network, a tree-based structure, to provide reliable two-way communication between meters and a data collector node. They introduced a scheduling scheme to balance traffic among a set of gateways. Delay effects were not considered. Galli et al. [11] proposed a method for modelling smart grids and addressed the issue of data transmission over Power Line Communication(PLC) system. One of the first efforts that addressed end-to-end services in a smart grid was examined by Sauter et al. [12]. They addressed a combination of gateways between application servers and customer nodes using PLC system and an IP-based network. The generic solution they proposed encouraged researchers to further study end-to-end connections between applications and servers. As data security gained more attention, Sauter et al.[13, 14, 15] discussed issues of privacy and protection of information confidentiality in smart grids. In [16], a dynamic operation of cellular- based smart network is examined for reducing operational expenditures and CO<sub>2</sub> emissions. Base stations in the network are designed to control retailers' ability to procure electricity. Mohammad [17] considered a wireless mesh network for collection of data from electrical equipment, and investigated its performance to determine the number of relays that would reduce the choice of overhead. The numbers of clients, communication bandwidth and distance factors are considered by Mohammad [18] in the design of mesh network using optimization methods.

The trade-off between wireless coverage and capacity is addressed by Hongjian [19] and methods for improving the spectral efficiency and coverage for communication infrastructure in smart grids are also discussed. Lopez et al. [20] investigated bidirectional real-time communication strategies for modelling distribution large of smart grid. The results show that flexible and cost-effective solutions are possible in smart grid. Kulkarni [21] discussed interconnection of networking system in smart grid with the aim of improving robustness, scalability, and fault detection. It is shown that deployment of a mesh radio-based protocol can help smart meters to discover the best connectivity

to a concentrator closet to them. In [22], Fateh studied hybrid hierarchical smart grid that combined wired and wireless systems with the aim of minimizing installation and operational costs. Results showed that wireless link bandwidth is a limiting factor when optimizing cost. Later, Yi et al. [23] used wireless mesh network for smart grids and investigated its delay performance for critical communications. However, they did not consider the constraints associated with real-time scenarios in smart grid. Kong et al. [24] considered a wireless neighbourhood area network based on IEEE 802.15.4g standard and assumed that smart meters are divided into groups and take turns sharing wireless channels using the slotted Aloha protocol. Their objective is limited to quantifying the QoS metric as a function of number of concentrators per  $10 \text{ km}^2$  of geographical area.

A smart grid, in general, must be interoperable and communicate with subsystems that are distributed and allows multiple applications to communicate with each other. Smart grids generate billions of data points from thousands of devices, requiring continuous on-the-spot analysis for prioritizing. This leads to timing challenges in smart grids. These challenges become more complex in the light of architectural design, limited bandwidth resource, shadowing effect, number of channels, channel interference etc. All these factors contribute to unacceptable packet loss and delays in smart grid. In an attempt to address these challenges, Gupta et al. [25] obtained a tighter upper bound on delay for a Neighbourhood Area Network (NAN) with single-hop traffic and general interference constraints. They estimated the expected delay for independent arrival streams using Maximum Weighted Matching (MWM) scheduling policy. Irfan et al. [26, 27] introduced a data distribution technique called Delay-Responsive Cross Layer (DRX) that uses application layer to perform cross-layer predictions for the end-to-end delay. The technique can be used for applications in smart grid. They did not address realistic scenarios in which interfering nodes exist and the claims in their work is based on simulations without theoretical support. Gowdemy et al. [56, 29] studied critical communication with respect to consumer needs and investigated throughput, delay, and scalability of NAN in smart grid using Greedy Perimeter Stateless Routing (GPSR) strategy. They showed that the upper bound on delay of 100 ms can be achieved. However, the simulation scenario was limited to a single-hop IEEE 802.15.4 network. Neal et al. [30] used an optimization tool to implement minimal communication structure requirements for smart grid subject to delay and pricing constraints. They used concepts from queuing theory to quantify



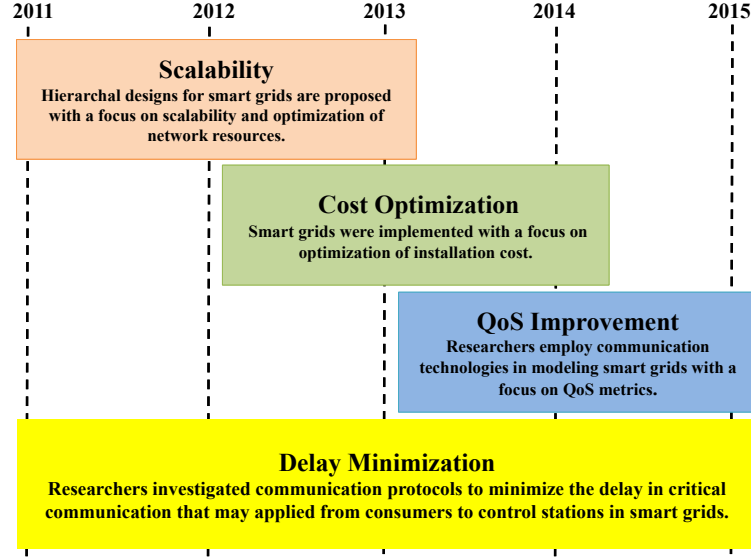


Figure 1.2: Chronological research effects in smart grid communications.

parameters to control delay in smart grid. They did not consider practical constraints such as channel capacity limits, data distributions etc. Al-Anabgi et al. [31] proposed an algorithm to allow the transmission of data using Guaranteed Time Slots (GTS) which can be used to reduce end-to-end delay of critical data in a HAN. This algorithm although is aimed at minimizing the delay of critical data, its application is limited to IEEE 802.15.4 networks.

Table 1.1: A list of notable research efforts in smart grid

Feature	[10]	[12]	[17]	[19]	[22]	[21]	[25]	[26, 27]	[56, 29]	[31]	Proposed Model
<b>Architecture</b>	Multi-gate network- based on hybrid tree routing	PLC with IP based	Cooperative modelling	Various relaying strategies	Hierarchical networks	Mesh-radio-based solution	Maximum weighted matching	DRX based on IEEE 802.15.4	Greedy Perimeter Stateless Routing	Guaranteed Time Slots	Interconnected networks based on IEEE 802.11
<b>Reliability</b>	Reduce network congestion	Data security	Local wireless mesh architecture	Improving the spectral efficiency	Minimizing the installation and operational costs	Maintain connectivity	Allows for simultaneous transmissions	Monitors the applications	Select optimum time slot allocation	Increase number of paths	Minimizing delay and provides real-time platform
<b>Scalability</b>	✓	X	X	✓	✓	✓	X	X	X	X	✓
<b>Delay</b>	X	X	X	X	X	X	X	✓	✓	✓	✓
<b>Complexity</b>	High	High	Low	High	Low	High	Moderate	High	High	Moderate	Low
<b>Cost</b>	X	X	✓	✓	✓	X	X	X	X	X	X

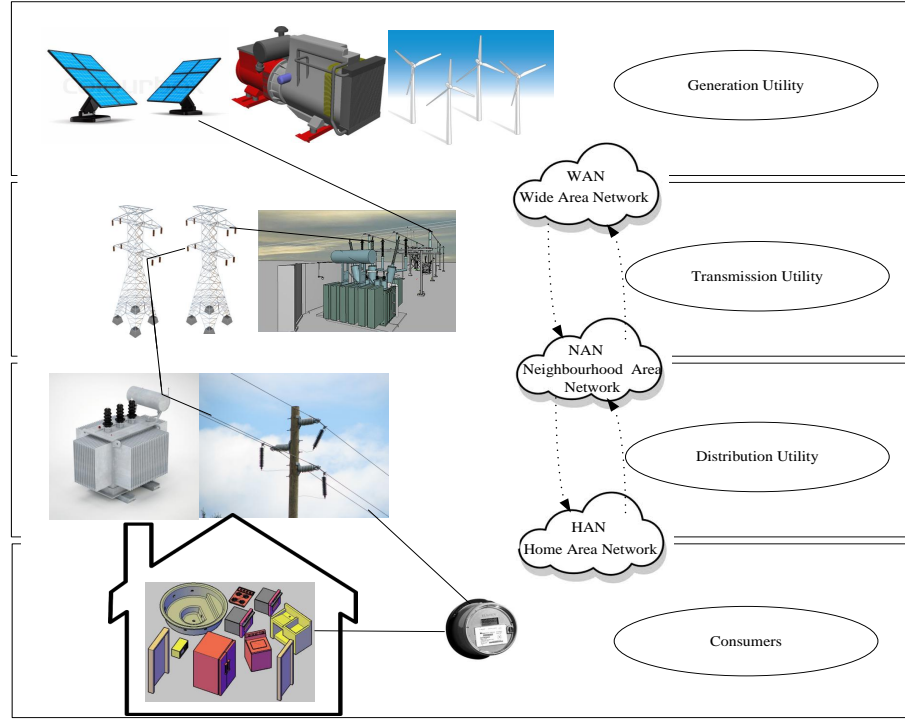


Figure 1.3: General view of power grid/smart grid.

A summary of chronological research efforts in smart grid communications in the areas of scalability, cost optimization, QoS improvement, and delay minimization is depicted in Fig. 1.2. Table 1.1 provides a list of research efforts in smart grids and can be used to identify gaps in research that need to be addressed in the areas of architecture, reliability, scalability, delay, and cost of smart grids. It is noted that critical

data communication in smart grid plays a major role and has been studied in bits and pieces. An examination of a comprehensive model of smart grid, with major focus on critical communication delay analysis (consumers to the control station) is lacking in the literature.

### 1.3 Structure of Smart Grid

A comprehensive model of smart grid must address consumers' demand, economic balance of power generation and supply, and time required to respond to remotely located consumers. Also, the model must effect successful operation, power transfers, and reduce energy losses. In order to understand and fulfil these expectations, a general view of power grid/smart grid is shown in Fig. 1.3 in which electrical devices (customers) are served through three stages of utility: generation, transmission, and distribution. Smart grid serves as an interface between customers and utility power grid. Customers generate real-time data regarding quality of supply and consumption of power received from the power grid. The data generated is then transmitted to a control station via smart grid. The control station analyzes data received from customers and effects controls in utility to restore/maintain/ correct power supply to customers.

A conceptual hierarchical structure of smart grid is shown in Fig. 1.4 and consists of three layers of communications with interfaces between layers. The first layer is the Access Layer (AL) where data is gathered from customers or EDs. The network associated with this layer is HAN, The data generated at AL is then passed on to Distribution Layer (DL). The network associated at this layer is NAN. Finally, data from DL is passed on to Core Layer (CL) and the network associated at this layer is WAN. The data from the WAN is finally sent to the control station. In essence, smart grid is modeled as a network consisting of these subnetworks, namely, HAN, NAN, and WAN. Thus, in this thesis modelling and analysis of these three subnetworks of smart grid for critical data communication is addressed.

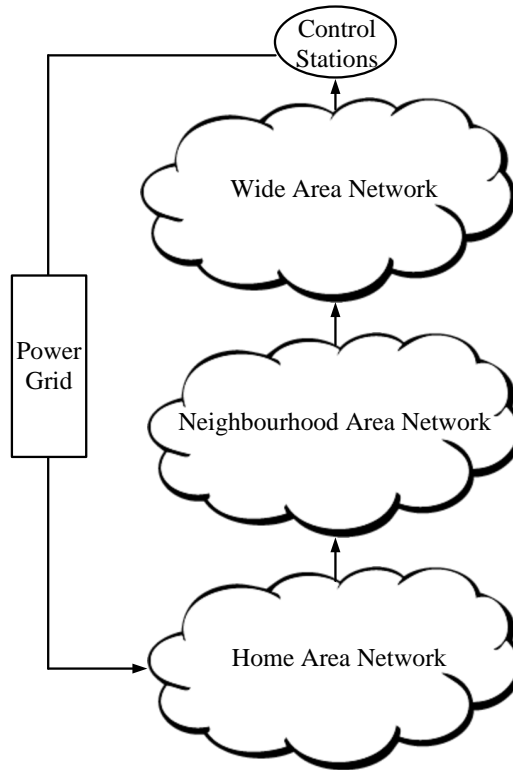


Figure 1.4: A conceptional model of smart grid.

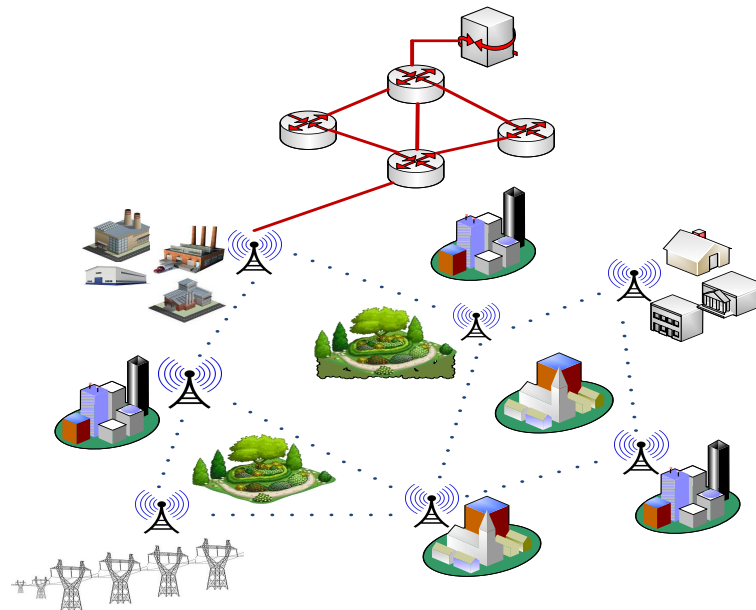


Figure 1.5: A pictorial view of a smart grid.

Fig. 1.5 shows a pictorial view of smart grid. In order to avoid collision between subnetworks of smart grid, IEEE 802.11 technology can be used as a possible wireless

choice for all three layers since the standard [32] allows simultaneous use of three disjoint spectrum bands: 2.4 GHz, 3.6 GHz, and 5 GHz. This standard is widely used in homes to attain high-bandwidth connections and requires small amounts of electrical power. This fact is a motivating factor in the modelling and analysis of smart grid (the HANs, NANs, and WANs). The emphasis in this thesis is focused on establishing bounds on critical communication delay between EDs and the control station.

### **1.3.1 Three Subnetworks of Smart Grid**

As expanded view of smart grid with three subnetworks with interface nodes is shown in Fig. 1.6. The EDs in HAN subnetworks generate routine and critical data in the form of report of packets and are required to be communicated to the control station via NAN and WAN. The MCs serve as interface nodes between HAN and NAN. The MCs are assumed to be connected to a set of MRs that are strategically located in NAN. In the NAN subnetwork, packets collected from HAN subnetwork move from MR to MR to identified gateways. The gateway nodes in NAN serve as interface nodes to WAN subnetworks. The packet received in WAN then move through high-speed WAN to identified gateway nodes in it which are connected to the control station. Thus, the gateway is WAN serve as interface nodes to the control stations. The packets received at the control station are analyzed to effect corrective measure at EDs through the power grid.

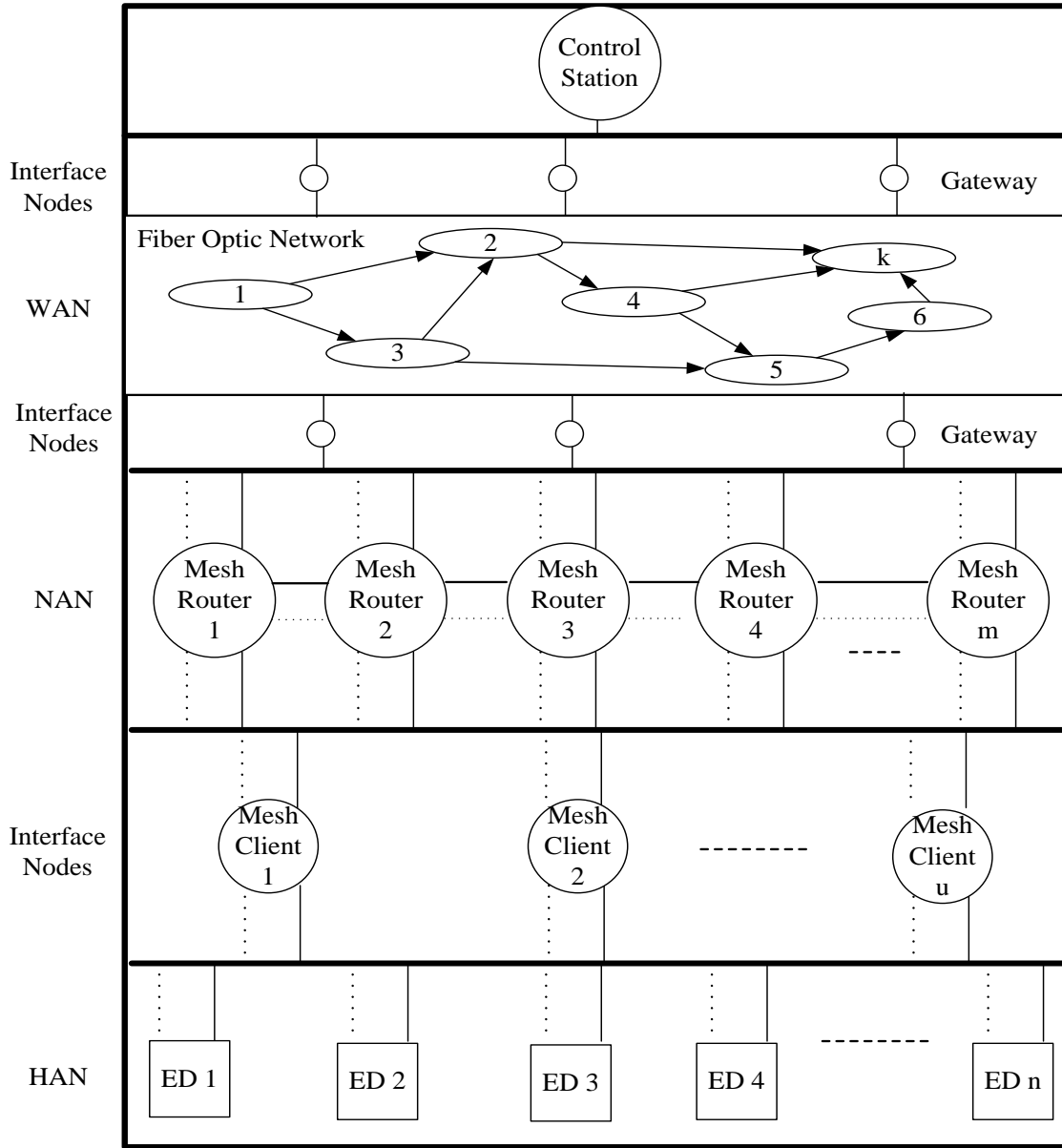


Figure 1.6: An expanded view of smart grid model.

In this generalized model, there are two possible ways to convey messages from electrical devices to control stations: via wires or wirelessly, as shown in Fig. 1.6. Although a generalized model of smart grid is shown, each subnetwork in it must be carefully modelled to understand the parameters that influence the delay in the transmission of critical data from EDs to the control station to effect corrective measures. These sub-networks are modelled theoretically and by MATLAB simulator. MATLAB is a well-established simulator, authenticated platform and licensed to be used for studying models such as

queueing theory and wireless/wired communication network models. Also, because most of the work is based on communication models MATLAB is used for the entire thesis and found it easier for the author and consistent. In this content, in the next section, the objectives of this thesis are sketched.

## 1.4 Thesis Objectives

In this section, the problems addressed in the thesis with specific objectives are described; with particular emphasis to critical data communication between EDs and the control station.

### 1.4.1 Modelling and Analysis of Home Area Network (HAN)

In HAN, wireless communication is considered between EDs and their respective Mesh Clients (MCs). In addition, the traffic from each ED is modeled as a combination of routine and critical data/reports. A single-server non-preemptive priority queueing system is suggested to prioritize critical reports and transmit using Head-of-Line (HOL) scheduling strategy. Mesh Clients (MCs) examine channel status to allocate the most available subchannels that do not interfere with each other. After prioritization of packets that are ready to be transmitted, each MC polls EDs in its domain to allocate maximum number of available channels using: i) FDMA and ii) TDMA techniques, until all reports at EDs have been transmitted. In the model, PCF is considered and an Interference model is used to avoid collisions. The specific objectives are:

- To develop a probabilistic model to represent the multi-class traffic generated by an ED in HAN and to use it as input to a single-server non-preemptive queueing system with HOL scheduling strategy and to derive closed-form expressions for average packet delay and mean buffer length for each class of traffic. Subsequently, to generalize this result to the case of a set of EDs connected to an MC and to identify parameters that influence critical packet/report delay in HAN.
- To present models of wireless HAN using: i) FDMA and ii) TDMA communication resource allocation strategies.

- To develop theoretical upper and lower bounds on critical packet delay in HANs as a function of i) average signal-to-noise ratio; ii) transmitted signal strength; iii) random channel scale; iv) number of slots/bands; v) path loss component; vi) distance between EDs and MC; vii) channel capacity and viii) channel bandwidth.
- To develop a software package to simulate wireless HAN and to compare analytical results with simulations.

### **1.4.2 Modelling and Analysis of Channel-Aware MAC Protocol for HAN**

The wireless HAN can be modeled to have a single collision domain if deployed in DCF mode for communication between a set of EDs and an MC. Further, if MIMO technology is used further enhancements in critical packet delay and throughput can be achieved. In this content, the specific objectives are:

- To use an Intelligent Distributed Channel Aware Medium Access Control (IDCA-MAC) protocol for wireless HAN employing MIMO technology.
- To use an algorithm to recover lost packets due to a collision in the MIMO based wireless HAN using IDCA-MAC protocol.
- To develop and implement wireless HAN in software for estimating and identifying parameters that influence critical packet delay.

### **1.4.3 Modelling and Analysis of Neighbourhood Area Network**

The NAN can be modeled as a set of strategically located MRs. The interface nodes, MCs, from HAN are assumed to be connected to MRs via wired links. It is noted that several MCs may be connected to each MR in HAN. The objective in NAN is to move packets from MR to MR, one hop at a time until the packet reaches a gateway node in NAN which serves as the interface node to WAN. There may exist several gateway nodes in NAN. Since the packet has to traverse quickly to a gateway to minimize delay, the Voronoi tessellation concept is used to determine an efficient straight-line routing strategy between an MR and gateway node. The concept involves finding the distance



between the location of each MR to its virtual bound edge which is smaller than the distance to its vertex. For wireless transmission, each MR is responsible for sensing and allocating channel based on modified Carrier Sense Multiple Access/Collision Avoidance (CSMA/CA) and Code Division Multiple Access (CDMA) in Distributed Coordination Function (DCF) mode. The Signal to Noise plus the Interference Ratio (SINR) plays an important role in the allocation of channel for transmission of packet. Consequently, the maximum number of packets that can be assigned in a time slot leads to minimal delay. In a nutshell, the packet has to move from an MR to an MR in a straight-line path until it is received at the gateway. The specific objectives are summarized below:

- To propose a Wireless Mesh Backbone Network (WMBN) model for NAN and to specify communication protocol and routing strategy.
- To provide an end-to-end shortest path routing using the Voronoi tessellation for transmissions of packets from MR to gateway node.
- To present an optimum solution for transmission of critical packets to gateway node with minimal delay, subject to channel characteristics.
- To derive closed-form expressions for upper and lower bounds on delay as a function of: i) signal-to-noise ratio, ii) signal interference, iii) critical packet size, iv) number of channels, v) channel interference range, vi) path loss components, vii) channel bandwidth, and viii) distance between MRs.

#### **1.4.4 Modelling and Analysis of Wide Area Network**

The WAN covers large areas and the distance between two nodes is typically measured in kilometres. The links connecting nodes in WAN are high-speed cables. In this thesis, the links are modeled as fiber optic cables. Optical communication provides up to 15 “superchannels” with high data rates. A Dynamic Fastest Routing Strategy (DFRS) is presented in WAN for routing packets to minimize delay and traffic congestion. The specific objectives are summarized below:

- To propose a topological design of WAN that adapts to faster routes to achieve minimum end-to-end delay.

- To propose a Dynamic Fastest Routing Strategy (DFRS) for WAN with  $n$  number of nodes and  $m$  number of links that enables the packets to choose the best routes from source node to gateway.
- To derive a closed-form expression for critical packet delay in WAN as a function of : i) traffic intensity, ii) capacity of fiber links, iii) number of links, iv) variance of inter-arrival time, v) variance of service time, and vi) the latency of links.

## 1.5 Thesis Organization

The thesis is divided into seven chapters. In chapter 2, background on the thesis is provided. It determines the key terms used in the thesis, and describes different communication components used in modelling smart grid.

In Chapter 3, a single-server non-preemptive queueing model is proposed and analyzed for handling multi-priority traffic generated by EDs in smart grids. Closed-form expressions for average packet delay for a two-class (high priority and periodic base) traffic are derived and illustrated. The average packet delay is a function of i) critical packet arrival rate; ii) service rate; iii) utilization factor; and iv) rate of arrival of periodic base. It is shown using numerical results that the proposed model can be used to estimate critical packet delay in the HAN subnetwork of smart grid.

In Chapter 4, a wireless HAN model is proposed to achieve minimum communication delay for transmission of critical packet from EDs to MC. The delay performances of models using i) FDMA and ii) TDMA are presented. In the analysis, multi-path reception and path loss exponent factor are also considered and closed-form expressions for delay are derived. The critical packet delay is a function of the i) Signal-to-Interference-Plus-Noise Ratio; ii) interferences; iii) number of critical packets; iv) size of the packet in bits; v) number of scheduled channels; channel interference range; and vi) power transmitted. Analytical and simulation results show that critical packet delay is smaller for TDMA compared to FDMA.

Chapter 5 focuses on practical modelling of HAN. The objective is to propose a model that allows simultaneous transmission of multiple packets at (higher/lower) rates depending on condition of wireless channel between EDs and MC. A protocol named IDCA-MAC for HAN that used MIMO technology is proposed, evaluated, and compared

with conventional MA-Aware protocol. The IDCA-MAC protocol and the entire model for HAN are explained in detail and simulated using NS-2 simulator and MATLAB. Simulation results show that critical packet delay increases by nearly 20% using IDCA-MAC protocol compared to MA-Aware protocol.

In Chapter 6, a WMBN model is deployed for NAN and it serves as the distribution layer that receives data from HAN and forwards it to the upper core layer. The main objective is to move the packet from router to router until it reaches identified gateways subject to the criterion of minimum delay. The routing suggested is based on selected shortest path using Voronoi tessellation. CSMA/CA and CDMA protocols are considered and closed-form upper and lower bounds on critical packet delay are derived and examined as functions of i) signal-to-noise ratio; ii) signal interference; iii) critical packet size; iv) number of channels; v) channel interference range; vi) path loss components; vii) channel bandwidth; and viii) distance between MRs. The results show that critical packet delay to gateway using CDMA is lower compared to CSMA/CA protocol.

In Chapter 7, a fiber optic WAN is presented for transporting critical packets received from NAN to a control station. A DFRS algorithm is used for routing critical packets to control station. Closed-form expression for mean critical packet delay is derived and is examined as a function of: i) traffic intensity; ii) capacity of fiber links; iii) number of links; iv) variance of inter-arrival time; v) variance of service time; and vi) the latency of links. It is shown that delay of critical packets to control station meets acceptable standards set for smart grid.

In Chapter 8, the conclusions of this thesis and the conclusions from results obtained are summarized. Also, areas for further research in the light of the needs of power grid/smart grid are outlined.

# Chapter 2

## Background

### 2.1 Introduction

In this chapter, an overview on smart grid with focus on its sub-networks communication infrastructures is presented. Smart grids are comprised of several interconnected layers of networks: i) HAN, ii) NAN, and iii) WAN. Two communication technologies are possible to convey data between these sub-networks: wire-line and wireless. However, wire-line communication technologies required new infrastructure compared to wireless communication networks. The idea of using mixture of these two technologies in modelling smart grid is a common practice in studying sensitive end-to-end delay from consumers to the control station.

This chapter identify key terms used in the research. Then, it determines the assumptions considered in the thesis, describes different communication components used in modelling smart grid, and discusses the effective communication technologies.

### 2.2 Key Terms

Many smart grid EDs are delay sensitive; therefore, a certain value of end-to-end delay should be guaranteed. End-to-end delay is the main smart grid network issue that needs to be investigated. However, it is tightly bounded by many other factors such as node energy and network capacity. This research attempts to model a smart grid communication network to address these network challenges and issues. Therefore, during this thesis, terms used need to be defined.

**Throughput** – This term is used to describe the successful of transmission of data in pits per second (bits/s) over a medium to a receiver.

**Delay** – This term is used to describe the time takes for the data to be received at receiver side and it measures in second (s).

**Channel Capacity** – This term is used to describe the measures capabilities of carrying data over a channel.

**Quality of Service** – This term is used to describe the quality required in bits over a wire-line network.

**Channel Interference Range** – This term is used to describe number channels that are overlapping with an active channel.

**Interference** – This term is used to describe the action of distortion when two or more users are transmitting simultaneously using one channel.

**Routing** – This terms is used to describe the forwarding data between nodes and it can be proactive and reactive strategies.

**Voronoi**– This term is used to describe a technique that helps to find shortest routing path to destination.

## 2.3 Network Models and Assumptions

The vision of proposing this work for a PhD thesis is to develop bounds on delay for transmitting critical packets in smart grid to control station. The desire for this thesis concurs with the expectations of those in the industry, which is that a model be able to detect, predict and to provide timely service restoration to take further decisions on how to isolate potential breaches.

Because delay of transmitting critical packets from electrical devices through smart grids is important, modeling of end-to-end communication networks is taken into consideration in this study. To study end-to-end communiation, the sum of queueing and transmission delay factors at intermediate nodes must be considered. Thus, our work seeks to derive closed-form expressions to evaluate the delay between EDs at the customer side and the final destination of the control station.

For more detail, three parts have been considered:

1. Modeling and delay analysis for HAN.
2. Modeling and delay analysis of a mesh backbone network in NAN.

### 3. Modeling and delay analysis of a wireline network in WAN.

In developing these interconnected networks, wireless delay factors (architecture design, scheduling, queueing, node transmission power, routing, limited bandwidth, number of channels, and channel interference) are considered to obtain an example solution for critical delay messages. This thesis work investigates wireless network delay performance to support different critical time applications in a few steps. In the first step, an expression for delay from electrical devices to mesh clients/access points (APs) is obtained. There are several devices located randomly at customers' locations. Thus, a model of wireless network that schedules different priority traffic arriving from electrical devices to mesh clients is proposed. Then, calculation of the delay subject to queueing models, signal interferences, the number of electrical devices, the number of channels, and the power of node transmission is given. After that, it is assumed that the mesh client conveys messages to the mesh router without any loss because it is connected directly to the mesh router. In a wireless mesh backbone network, the packet has to move from routers to the identified gateway. So, in this step, the delay calculation is obtained between mesh routers and the gateway, subject to Voronoi cell shapes, routing metrics, signal interference, node power transmission, router locations, noise, number of mesh routers, number of channels, and distance. To illustrate, two extreme real-world application scenarios are considered to find the acceptable upper and lower bounds on delay. Thus, an analytical wireless network model is proposed for understanding the interconnected wireless networks. To validate the work in the first part, a platform scenario environment is implemented using the certified planning network professional, the MATLAB simulator. The work will then be examined and analyzed by comparing theoretical work with simulation results. Finally, this work presents a delay analysis to check whether the performance analyzed meets the desired goals of wireless networks in smart grids, and the results approached will be compared with the work obtained in the literature that uses the same conditions.

In the following sub-sections, required communication components for smart grid are discussed.

### 2.3.1 Generating Functions

Generating functions in probability theory play an important role for the sum of discrete random variables [33]. This tools help in differentiating types of packets generated by EDs and they are independents. Indeed, Probability Generating Function (PGF) provides simple form of sums and limit of these random variables. If  $X$  and  $Y$  are two independents distribution, PGF transforms a sum into a product to be handled. Therefore, the PGF can be calculated as:

$$G_x(z) = \sum_{k=0}^{\infty} p_k s^k = E(z^k), \quad (2.1)$$

where  $p_k = P(X = k)$ ,  $k = 0, 1, 2, \dots$ , and  $X$  takes a finite number of values. For example, the PGF of Poisson distribution is calculated as:

$$G_x(z) = \sum_{k=0}^{\infty} p_k z^k = \sum_{k=0}^{\infty} \frac{1}{k!} \lambda^k e^{-\lambda} z^k = e^{\lambda(z-1)} \quad (2.2)$$

### 2.3.2 Wireless Interference

Different spectrum are considered to model the design. Therefore, no wireless interference across different layers. Nevertheless, each individual layer has radio channel environment effects such as path loss, channel overlap, and environmental noise. Inter-channel interference issue is clearly explained in Fig. 2.1. Fig. 2.1 is an example of channels bandwidth and how they are overlapped to each other [56].

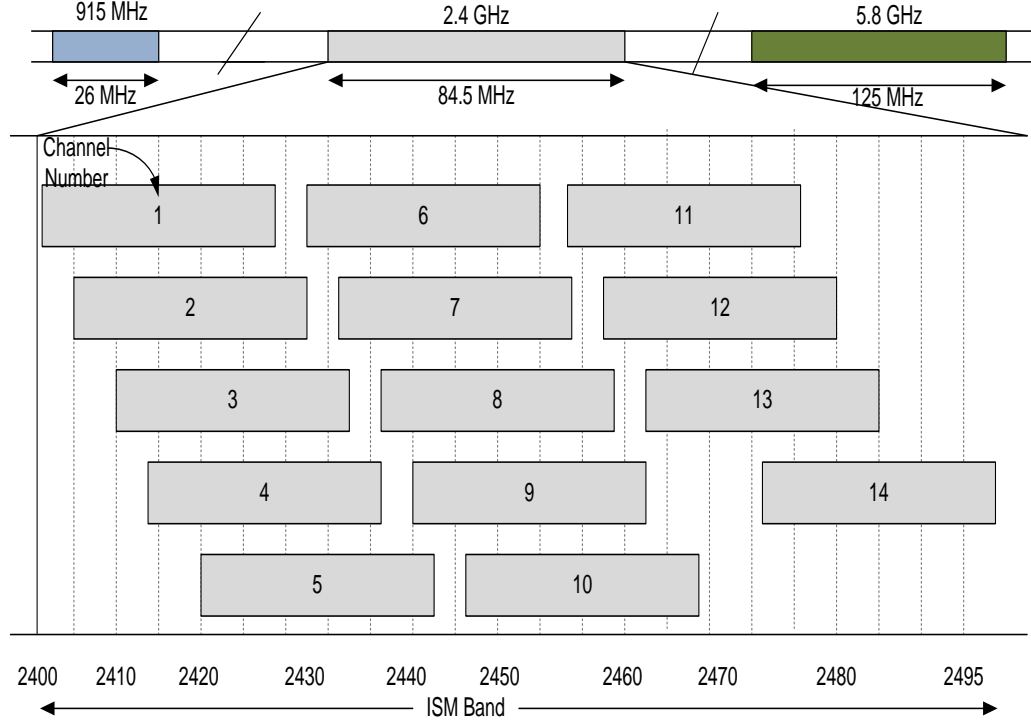


Figure 2.1: IEEE 802.11 Channel Blocks.

In addition, wireless signal decay for the path loss as  $P_r$  is defined in (2.3) see Fig. 2.2.

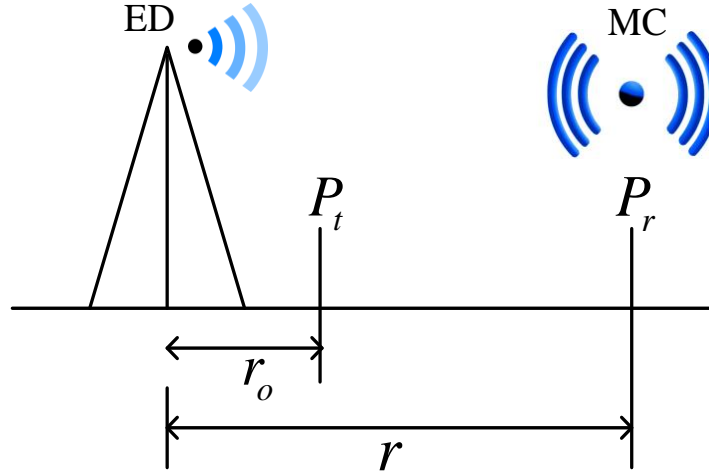


Figure 2.2: Example of how distance is considered.

$$P_r = P_o \left( \frac{r}{r_o} \right)^{-\varphi}, \quad (2.3)$$



where  $\varphi$  is the path loss.

Since all transmissions affect  $u$  node that using channel  $i$ , Fig. 2.3 and Fig. 2.4 illustrate the total effects of the power signal into  $i$  channel.

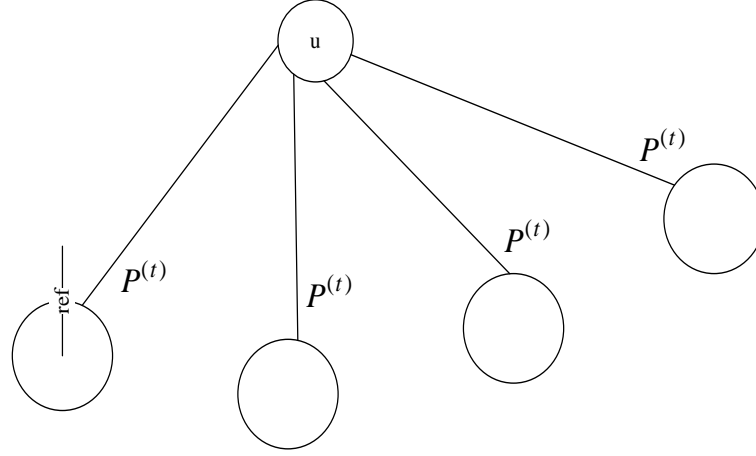


Figure 2.3: Powers signals decay effects to  $i$  channel into  $u$  node.

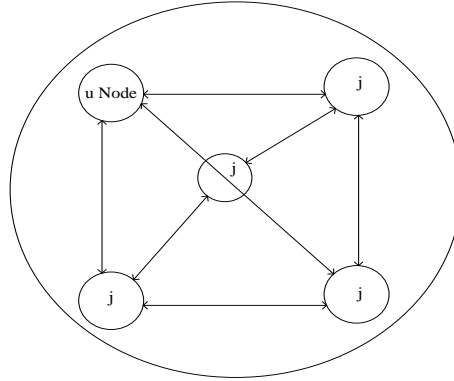


Figure 2.4: Transmissions around  $u$  node.

Indeed, IEEE 802.11 has two access schemes: random access control, which is Distributed Coordination Function (DCF), and centralized access control, which is Point Coordination Function (PCF). DCF has two working mechanisms: two way handshaking, or four way handshaking.

### 2.3.3 Channel Capacity

In transmitting information at rate  $R$ , the channel is used every  $t$  seconds. The channel capacity is then measured in bits per channel use. In 1948, Claude E. Shannon and V.

Kawadia [55] defined the notion of channel capacity and provided a mathematical model by which it could be computed. The expression used to determine channel capacity can be described as follows:

$$C = B \log_2(1 + SNR), \quad (2.4)$$

where  $B$  is channel bandwidth, SNR is the signal to noise ratio.

### 2.3.4 Routing and Communication

*Straightline Routing* algorithm is considered in this work because critical packets  $n$  will be forwarded along path close to the cells connected to other mesh routers. This path line must traverse a sequence of cells until reaches gateway [71]. To avoid interference, upper bound delay case is considered and conservative communication strategy is developed.

### 2.3.5 Communication Access Schemes

Even though each node in the network is required to forward packets to another node, the communication in smart grid could carry periodic or bursty traffic. Therefore, communications is required to estimates the channel condition and schedule to send priority packets at a data rate not exceeding the channel capacity before periodic packets. Transmission schedule schemes in each wireless local area network require adjustments to differentiate between types of data.

### 2.3.6 Optical Communication

Optical fiber is the channel cables used for optical communications [84]. For instance, if a group of nodes are connected with these cables, transmitter node will transmit infra-red wavelengths with speed of light ( $3 \times 10^8$ ) m/s to the receiver side. Both sides must be equipped with modulation and demodulation techniques for signal conversion. In addition, each cable is capable to handle up to 15 channels. The issue of routing is addressed in Chapter 8.

### 2.3.7 MATLAB Simulator

In this thesis, the simulation model for studying delay performance of interconnected network systems and scenarios is based on Matrix Laboratory (MATLAB) simulator [34] that includes channel interference range, number of channels, and signal to interference ratio. MATLAB is a multi-paradigm numerical computing environment and fourth-generation programming language. It is a commercially available simulator for communication systems and networks. It has great flexibility in supporting design and analysis of communication networks. Also, it supports devices, protocols, and applications. In comparison with other simulators, MATLAB has more detailed simulation models, and provide better configuration as it has more advanced ability to simulate physical links and antennas. It is built with various toolboxes such as MuPAD symbolic engine and Simulink that add graphical multi-domain simulation and model-based design for dynamic and embedded systems. These properties give MATLAB the ability to be adopted to smart grid communication networks and provide analysis for various applications.

## 2.4 Smart Grid Components

A comprehensive model of smart grid must address consumers' demand, economic balance of power generation and supply, and time required to respond to remotely located consumers. Also, the model must effect successful operation, power transfers, and reduce energy losses. In order to understand and fulfil these expectations, a general view of power grid/smart grid is shown in Fig. 1.3 in which electrical devices (customers) are served through three stages of utility: generation, transmission, and distribution. Smart grid serves as an interface between customers and utility power grid. Customers generate real-time data regarding quality of supply and consumption of power received from the power grid. The data generated is then transmitted to a control station via smart grid. The control station analyzes data received from customers and effects controls in utility to restore/maintain/ correct power supply to customers.

This fact is a motivating factor in the modelling and analysis of smart grid (the HANs, NANs, and WANs). The emphasis in this thesis is focused on establishing bounds on critical communication delay between EDs and the control station. Therefore, wireless

technology is assumed considered for HAN and NAN, and wire-line communication is considered for WAN.

### 2.4.1 Home Area Network

In HAN, the traffic generated at electrical devices is either periodic or bursty. Bursty traffic is the most critical information that needs to be transmitted to the control station, for it may indicate that the device is running abnormally. It can be thought as a multi-class queues model. For instance, old devices sometimes consume more power or have less than enough power to run efficiently. This might affect the performance of the whole power grid, and sometimes a sudden shut down might occur.

This part of the research focuses on how to prioritize high priority packets and establish bounds on delay between the electrical devices and their mesh client. Thus, a Point Coordination Function (PCF) accessing mode is studied since PCF access functions have the advantage of providing better delay times. Three main issues arise in accessing channels in HAN. The first issue is differentiating between the scheduled bursty priority traffic and periodic traffic. The second issue is identifying the effects of allocating channels for priority traffic while doing simultaneous transmissions. The last issue is establishing an expression for delay between electrical devices and their mesh clients. In this subnetwork, electrical devices use a different wireless spectral band than what is being used in the backbone. Indeed, IEEE 802.11 allows users to use wireless networks with three bands: 2.4G, 3.6G, and 5G. The reason for not using the same band in the two sub-networks, HAN and backbone, is to avoid collisions. In this thesis, the scenario of abnormal events occurring in power grids nearest to the clients is considered. The coverage of this area is managed by Local Area Networks (LANs) that are monitored by the mesh client node.

Generated packets in ED are queued in a single queue server using Kendall's notation [47] in the form  $A/S/C$ , where  $A$  is the distribution function of the inter-arrival times,  $S$  is the distribution function of the service times, and  $C$  the number of the servers. Mathematically, it can be proved by Markov chains. For example,  $M/M/1$  queue is a model where packets arrival rate follows Poisson distribution and service rate follows exponential distribution with one server and infinity queue size as shown in Fig. 2.5. There are various scheduling discipline can be used; however, First Input First Output

(FIFO) is assumed to be used in molding discrete server queue. In addition, packets with high priority have to be served first. Therefore, there are two types of priority queues are available: preemptive, where server can be interrupted, and non-preemptive, where server cannot be interrupted. Thus, non-preemptive single server queue is preferred because server should not be interrupted when it is transmitting packets to MC. Here, it is required that the utilization factor of the system  $\rho = \lambda/\mu < 1$ , otherwise the queue length will explode.

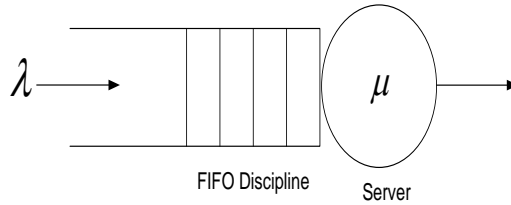


Figure 2.5: The structure components of M/M/1 model.

Two different classes are considered to differentiate two type of packets: i) high priority class and ii) low priority class. Therefore, the expected total number of packets is:

$$E[u]_T = E[u_1] + E[u_2], \quad (2.5)$$

where  $E[u_1]$  is the expected number of high priority packets, and  $E[u_2]$  is the expected number of low priority packets. Based on little theory [47], the expected number of high priority packets is given as:

$$E[u_1] = \lambda_1 \times E[d_1], \quad (2.6)$$

where  $\lambda_1$  is the arrival rate of high priority packets and  $E[d_1]$  is the expected delay of high priority packet. Once the packets are prioritized, wireless transmission medium is considered. MC polls EDs using FDMA or TDMA to schedule transmissions [55]. FDMA is responsible for allocating a single channel to only one ED at a time. However, redefining the entire bandwidth as a group of different frequency bands in order to increase the number of simultaneous transmissions and to avoid interference is considered. For instance, some EDs will be allocated to different frequency bands with inter-channel separation. The remaining EDs have to wait for some period of time. Thus, there is an

allocation waiting time and there is also a queue for the critical packets in each ED. On the other hand, TDMA schedules transmission in a wireless LAN that lets each packet fit into one time slot duration  $\tau$  only. To formulate the problem mathematically,  $n$  reports will be generated at time  $t = 0$ . Then, the objective is to represent the minimal achievable time  $\Delta_{HAN}$  to send this report to the mesh client. The mesh client uses the PCF mode to poll electrical devices to schedule data transmission from electrical devices. The wireless channel of transmission should not be overlapped, meaning it can accommodate, at most, one packet at any time, as well as simultaneous transmissions. A comparison of the measurement level between the signal power and noise gives the signal-to-noise ratio

$$SNR = \frac{\text{signal power}}{\text{noise power}}. \quad (2.7)$$

Consequently, to satisfy the desired power signal to the noise power, the  $SNR$  threshold  $\beta$  should be  $\geq 1$ .

$$\gamma_{u,i} = \frac{P^{(t)}}{N + \sum_{\{j\}} I_{u,i,j}}, \quad (2.8)$$

where  $i$  is the current occupied transmission channel and  $I_{u,i,j}$  refers to the interference caused by the simultaneous transmissions  $j$  on channel  $i$  at node  $u$ .

In particular, electrical devices will transmit  $n$  reports, which include the status information, to the Mesh Client inside the network. It is known that TDMA and Carrier Sense Multiple Access (CSMA) are currently employed access schemes in IEEE 802.11 protocols [32].

Delay performance using the TDMA scheme as opposed to the Frequency Division Multiple Access (FDMA) scheme as the latter is designed for different objectives other than communication delay.

#### 2.4.1.1 FDMA and TDMA Schemes

FDMA is responsible for allocating a single channel to only one client at a time, as shown in Fig. 2.6. FDMA is technically simple to implement; however, much of the bandwidth will be wasted, almost always being allocated to somebody even if the client not transmitting. In this access method, there is no waiting time, as shown in (2.9) since

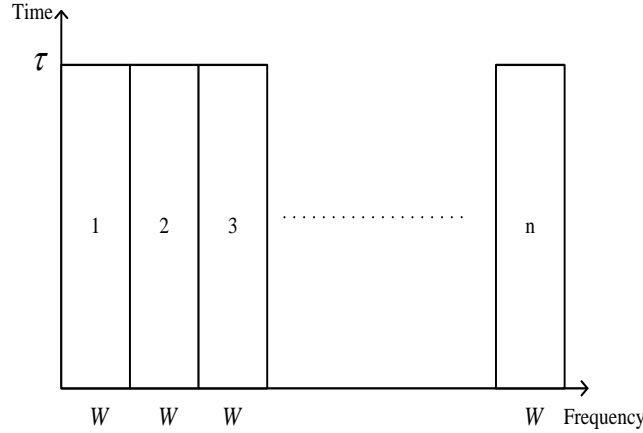


Figure 2.6: FDMA frequency bands.

there is no queue for the data in which to wait.

$$\omega_{FD} = o \quad (2.9)$$

On the other hand, in TDMA the signal will be divided into a number of long slots. Fig. 2.7 shows that every short time of a channel will be allocated and then move to another channel until all clients are allocated. Here, there is waiting time that needs to be considered, which can be represented as the following:

$$\omega_{TD} = \frac{1}{M} \sum_{m=1}^M (m-1) \frac{T}{M}; \omega_{TD} = \frac{T}{2} \left(1 - \frac{1}{M}\right), \quad (2.10)$$

where  $M$  is the time slots. However, this will benefit burst data. This data could split up in time and TDMA will prepare this data to send.

This burst data would take a short slot of time and wouldn't be noticed or affect other allocations. Meanwhile all other appliances would allocate to different available time slots. This would be known as time division multiple access. Appliances in HAN would carry two types of data: periodic data and bursty data, as shown in Fig. 2.8,

Fig. 2.10 shows that TDMA would serve a certain number of electrical devices, allowing them to access the system, and at the same time increase the efficiency of transmissions. Another advantage is that TDMA will offer efficient utilization for hierarchical

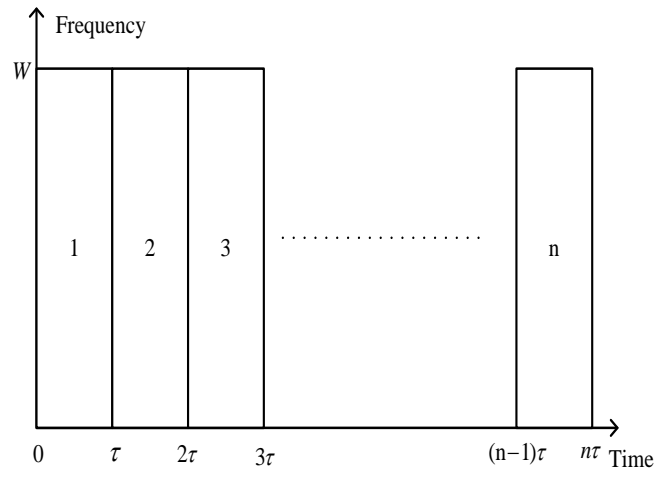


Figure 2.7: TDMA Time Slots.

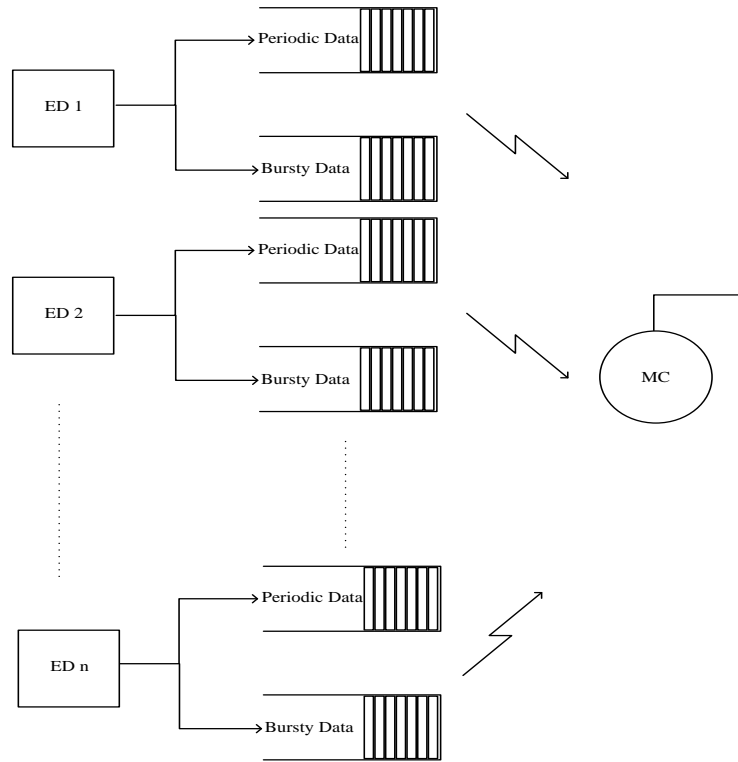


Figure 2.8: Type of data generated by electrical devices.



structures.

To illustrate transmission function, and regarding allocation users into the channel, as shown in Fig. 2.9, the process in FDMA looks simple to implement since each electrical

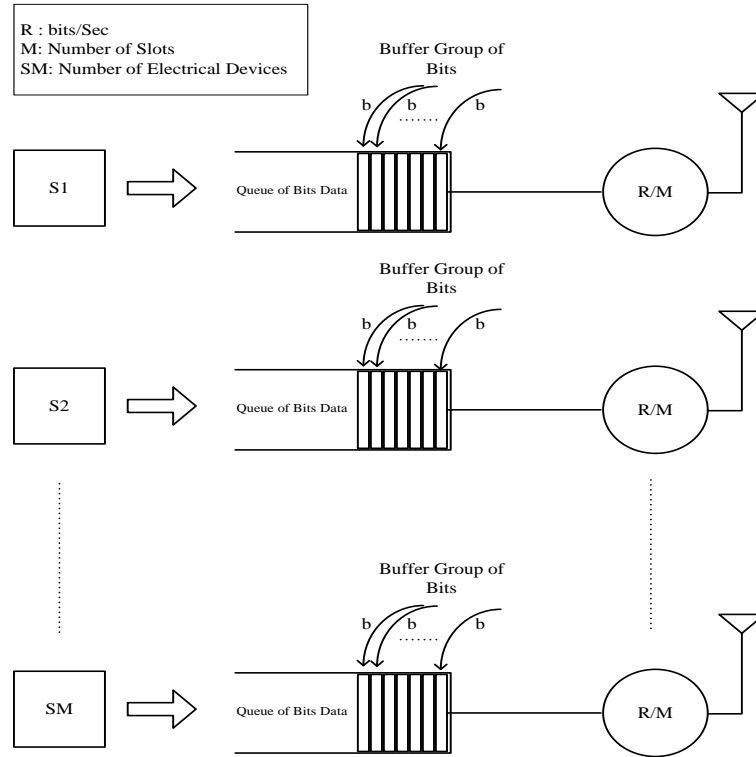


Figure 2.9: FDMA Transmission Function.

device will allocate a single channel at a time. However, the FDMA process wastes the entire transmission time in the channel as denoted by (2.11), and (2.12):

$$D_{FD} = T \quad (2.11)$$

$$\tau_{FD} = T \quad (2.12)$$

For a clear explanation, Fig. 2.7 shows that TDMA will save resources and time. Since waiting time is the disadvantage in TDMA, each electrical device will take only a short duration to complete the transmission as:

$$\tau_{TD} = \frac{T}{M} \quad (2.13)$$

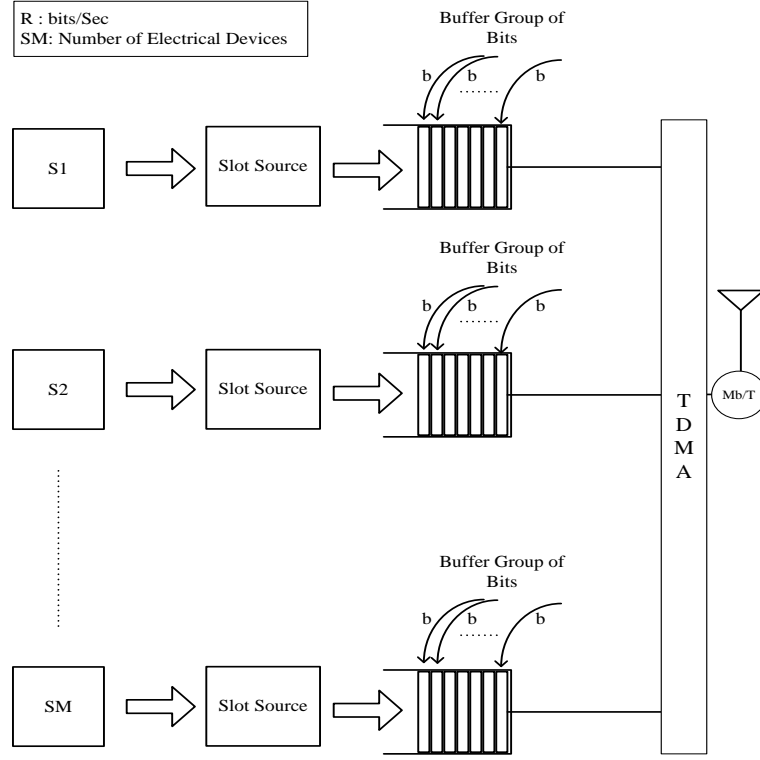


Figure 2.10: TDMA Transmission Function.

The entire length of time will be divided into  $M$  number of devices to allow them to share the same period of time. Consequently, the delay time in this system would be carried out as:

$$D = \omega + \tau \quad (2.14)$$

Therefore, subtracting (2.11), and (2.10), the overall delay that electrical devices would take to access the channel is:

$$D_{TD} = D_{FD} - \frac{T}{2} \left( 1 - \frac{1}{M} \right) \quad (2.15)$$

The bottom line proven here is, as discussed above, that TDMA is the most suitable access process for electrical devices in HAN to access the channel. Raleigh and Nakagami distributions are also considered to describe channel fading. For analytical purpose in this work, it is assumed that all nodes transmit power  $P_t$ , and receive power equals  $P_r$ .

### 2.4.1.2 Small Scale Fading

The small scale fading is used to describe the distortion on the transmitted signal due to random delay, reflection, diffraction, and scattering. The change is in the amplitude of the signal and its phase. The variation is small because it is comparatively fast. Different types of fading is shown in Fig. 2.11 [54].

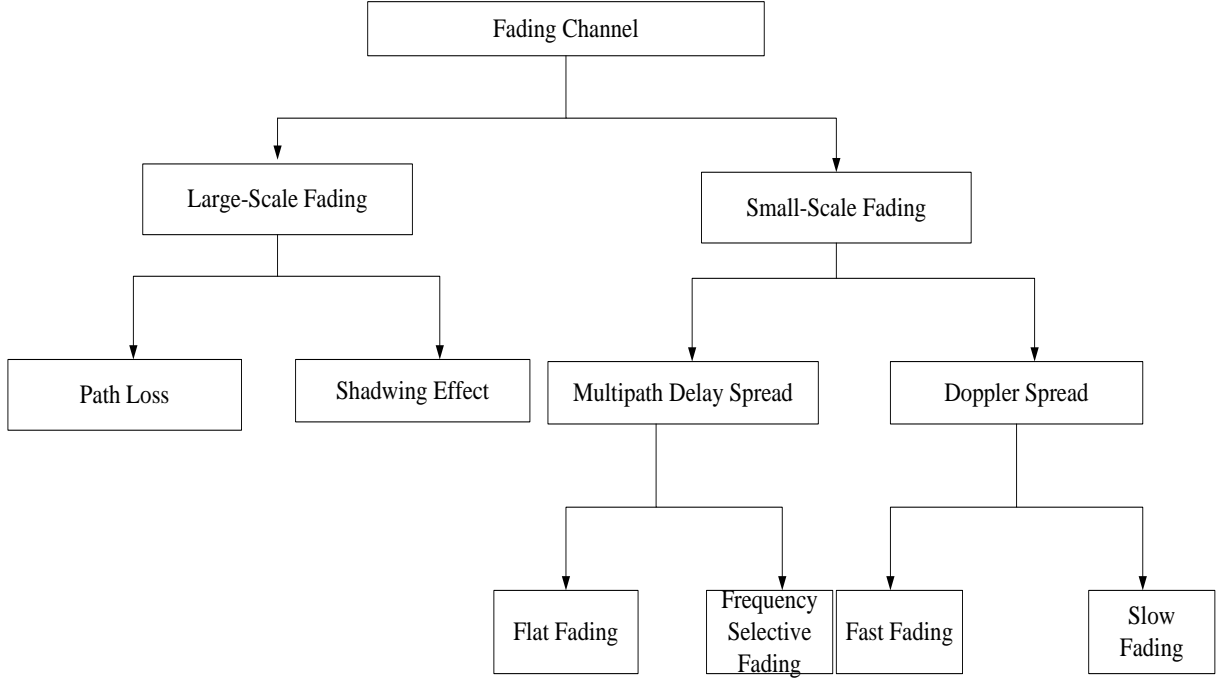


Figure 2.11: Fading types.

Thus, the Probability Density Function (PDF) of  $\gamma_{u,i}$  in small scale fading is presented as:

$$p(\gamma) = \frac{p\sqrt{\frac{\Omega\gamma}{\bar{\gamma}}}}{2\sqrt{\frac{\gamma\bar{\gamma}}{\Omega}}}, \quad (2.16)$$

where  $\alpha$  is the signal scale,  $\Omega$  is the mean squared value of  $\alpha$ ,  $\gamma = \alpha^2 E_s / N_o$ , and its average  $\bar{\gamma} = \Omega E_s / N_o$ . The magnitude of the received signal is affected in the case of there is no Line-of-Sight (LoS) between EDs and MC, which is called Rayleigh distribution. The PDF of  $\alpha$  used to model the multi-path fading is given as:

$$P_R(\alpha) = \frac{\alpha}{\Omega} \exp\left(-\frac{\alpha}{2\Omega}\right), \quad \alpha \geq 0. \quad (2.17)$$

Therefore, the PDF of the instantaneous  $\gamma$  is obtained as:

$$P_R(\gamma) = \frac{1}{\bar{\gamma}} \exp\left(-\frac{\gamma}{\bar{\gamma}}\right), \quad \gamma \geq 0. \quad (2.18)$$

If there is LoS signal component, the wireless channel can be modelled as Nakagmi distribution. It is used to model multipath channel as a function of fading parameter  $k$ . Various model can be generated by giving different value to  $k$ . For example, when  $k = 1$ , it means there is no LoS and leads to Rayleigh distribution. As  $k \rightarrow \infty$ , fading channel approaches Additive White Gaussian Noise (AWGN) channel. The PDF is consequently obtained as:

$$P_N(\gamma) = \left(\frac{k}{\bar{\gamma}}\right)^k \frac{\gamma^{k-1}}{\Gamma(k)} \exp\left(-k\frac{\gamma}{\bar{\gamma}}\right), \quad \gamma \geq 0. \quad (2.19)$$

## 2.4.2 Neighborhoods Area Network

In this section, a wireless mesh network is deployed as the backbone network. It serves as a distribution layer that receives data from the electrical devices via mesh clients and forwards these data to the wire-line network.

To illustrate, as discussed in the previous HAN layer, data will be collected by mesh clients. In a mesh backbone sub-network, each mesh router will have one or more mesh clients that are connected directly by a wire-line. The mesh routers are wirelessly interconnected and the main objective is to move the packet from router to router until the packet reaches the identified gateway.

In the following subsection, the methodology and preliminary results are presented.

The  $n$  report packets collected from mesh clients, with each packet of length  $L$  bits, is forwarded to the router in the backbone network. Mesh routers are located distributively among Voronoi cells. The long link distances between routers are subject to attenuation and communication challenges. This work examines the transportation delay of transmitting reports between mesh routers and gateway node.

### 2.4.2.1 Routing Technology

Routing technology is used in selecting a path for traffic in a network. There are two types of routing: i) proactive mode and ii) reactive mode. In reactive routing, router keeps

silence until routing is needed; however, in proactive mode router updates matrix table with the suitable paths all the time. Proactive is needed in NAN for selecting shortest path route to destination. Among these routing strategies, Voronoi tessellation provides realistic routing in large scale demography compared to other existing routing techniques. By putting the routers in a well-planned location, it allows for communication coverage for HANs and provides a realistic example for location distribution measurements. Voronoi irregular cells are a suitable choice as they have the advantage of allowing to select shortest path between sources and last destination. Fig. 2.12 illustrates the example of the cells in a Voronoi diagram [23]. Each irregular cell shape of Voronoi contains the location of a mesh router.

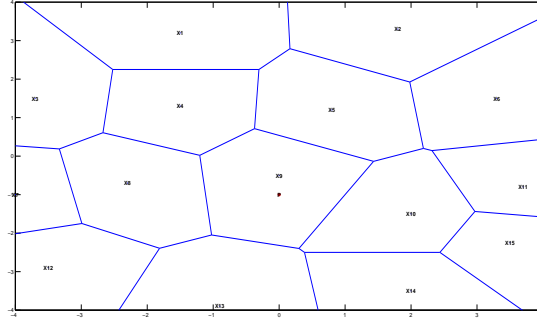


Figure 2.12: Definitions of Voronoi Cell Shapes.

In such a case, both mesh routers and mesh clients are co-located. Because mesh routers are widely distributed over mesh backbone networks, long-distance information will be considered. The best communication case occurs when the receiver is located close to the transmitter. In this case, it is assumed that the amount of interference at the mesh receiver is minimal. Based on Voronoi cells, the distance between a mesh router in the network and its edge is less than the distance between the router and its vertex:  $d^{edge} < d^{vertex}$ . So, the minimum distance between two mesh routers is  $2d^{edge}$ .

When the distance between two mesh routers is  $< 20$  m, interference will be ignored because minimum distance between the two routers is considered. After that, estimation of the capacity is required. To determine the capacity of the link between these routers, the Shannon theorem is considered.

The next step is to determine the reduction of the signal strength when the signal is transmitted through a space. Depending on the environmental space, the path loss  $\varphi$

will vary between 2 and 4. Knowing that  $X_u - X_{v_j}$  is the distance between two nodes, then based on  $d^{(ref)}$ , the capacity of the link is given as:

$$C_{i,u} = B \log_2 \left( 1 + \frac{P(t) \left( \frac{|X_u - X_{v_j}|}{d^{(ref)}} \right)^{-\varphi}}{N + \sum_j I_{u,i,j}} \right), \quad (2.20)$$

where  $d^{(ref)}$  is the reference distance where the transmitted power has no losses.

#### 2.4.2.2 CSMA/CA and CDMA Schemes

Wireless communication in NAN is taken place under Distributed Coordination Function (DCF) mode. DCF synchronous data to be transferred through the channel based on CSMA/CA protocol [32]. CSMA/CA as shown Fig. 2.13 is responsible to monitor the channel if it is idle or not while there is no possible to detect collision if it occurred. In order to allow this protocol to work perfectly, Short Inter-frame Space (SIFS), which is a required period for giving the priority to other stations, use different type of frames such as Acknowledgement (ACK) frame, CTS frame, and any frame exchanges. For completing one transmission, handshaking frames, which are Request to Send (RTS) and Clear To Send (CTS), require to operate with CSMA/CA. If the data arrived without any error, the receiver will reply back with ACK packet. The length of RTS frame is 20 bytes, which is much shorter than data frame, while the length of Data frame is 2300 bytes long. Moreover, CTS has only 14 bytes length. For avoiding collision, CSMA/CA must sense the channel in order to perform a transmission while the backoff counter is random. The duration that required to complete one successful transmission is imported in duration field that is suppose to be adjusted in Network Allocation Vector (NAV). The Slot Time used in 802.11 to define Inter-frame Space period (IFS), which is responsible to determine the backoff time in range 0 to 7. When the backoff counter becomes zero, CSMA/CA will sense the channel in the way of doing the transmission.

On the other hand, CDMA is modeled and used to form a spread spectrum communication [55]. In CDMA, the signal is spread over a wider frequency band, as shown in Fig. 2.14. Thus, CDMA allows each MR in NAN to transmit simultaneously using coding

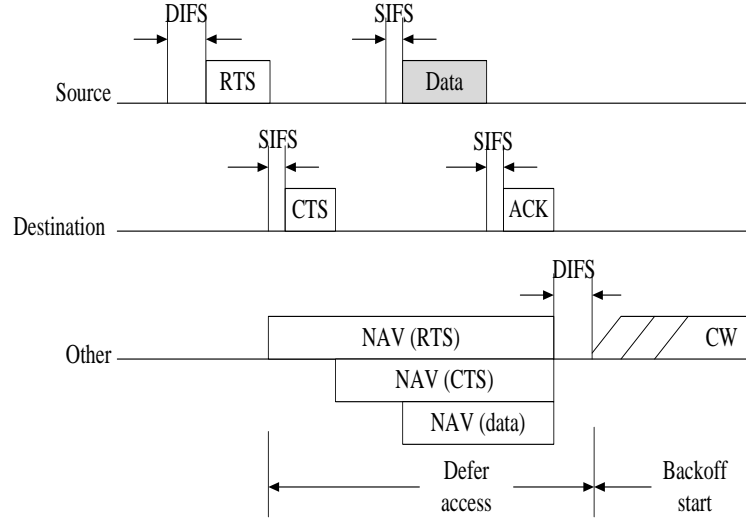


Figure 2.13: CSAM/CA timing diagram.

theory. This enables the time of transmission to overlap. In contrast, TDMA allows EDs to share a channel by taking turns, whereas FDMA allows EDs to share a channel on different frequency bands. CDMA, however, allows few packets to be transmitted to the available channels, but only the desired signal will be extracted. The rest is considered to be noise. From a delay perspective, unlike other access schemes, CDMA does not require synchronization among the nodes. Shadowing effects are neglected in this study because

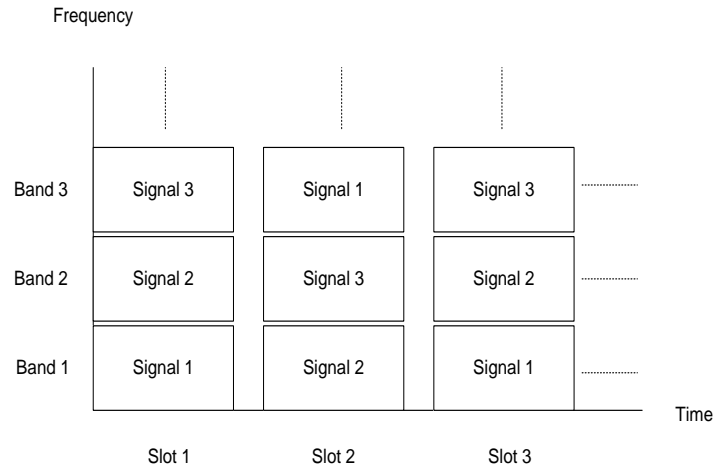


Figure 2.14: CDMA time/frequency slots.

the nodes are not located randomly in the site. However, environmental noise Additive White Gaussian Noise (AWGN) and inter-channel interference are included.

### 2.4.3 Wire-Line Network

The objective of this chapter is to present the third layer, which is wire-line network as it is shown in Fig. 2.15. It is basically to find the delay of this network.

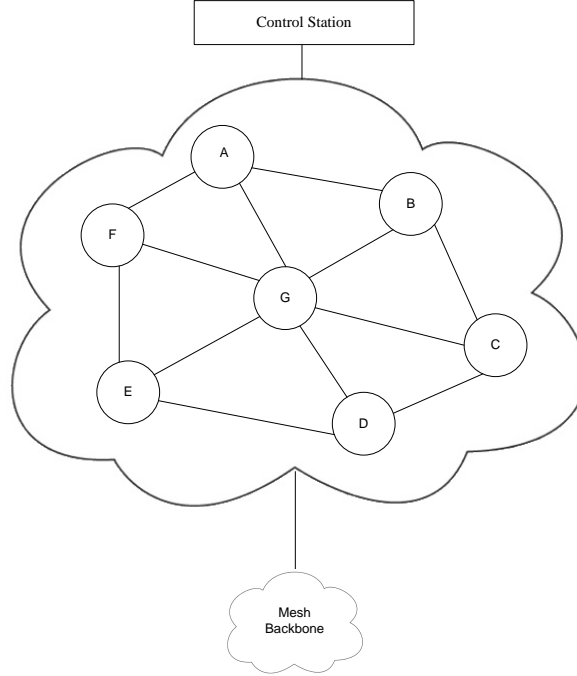


Figure 2.15: Wire-Line Network.

The way to find the delay in wire-line network is based on routing scheme, traffic matrices and queueing theorem [47]. For instance, let us consider the wired network shown in Fig. 2.16, and the traffic-cum-routing matrix is shown in table 2.1. In addition, let assume the average packet length to be 1500 bits. The Capacity of the links are given in table 2.2.



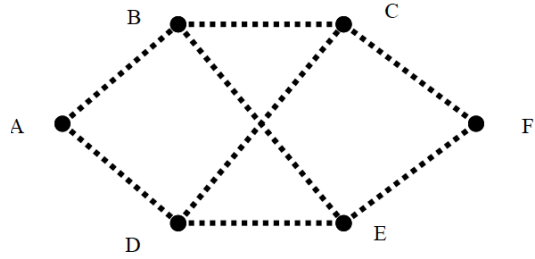


Figure 2.16: Wire-Line Network Example.

Table 2.1: Traffic (packets/second)-cum-Routing Matrix

	A	B	C	D	E	F
A	X	15 AB	20 ABC	5 AD	25 ABE	2 ABEF
B	15 BA	X	10 BC	12 BCD	10 BE	5 BEF
C	20 CBA	10 CB	X	5 CD	15 CFE	10 CF
D	5 DA	12 BCB	5 DC	X	10 DE	5 DCF
E	25 EBA	10 EB	15 EFC	10 ED	X	10 EF
F	2 FEBA	5 FEB	10 FC	5 FCD	10 FE	X

Table 2.2: Wire Link Capacities

Wire Links	Capacity (M bps)
AB, BA	2
BC, CB	2
CF, FC	10
FE, EF	5
DE, ED	2
BE, EB	2
DC, CD	2
AD,DA	2

To determine the average packets delay in the network, delay will be calculated for each link by applying the following:

$$T_i = \frac{1}{\mu C_i - \lambda_i} \quad (2.21)$$

Then, it is observing that traffic from A to B traffic (15 packets/sec) uses link AB, A to C traffic (20 packets/sec) uses link AB, A to E traffic (25 packets/sec) uses link AB, and A to F traffic (2 packets/sec) uses link AB. Adding all of them, they give:  $\lambda_1 = 15 + 20 + 25 + 2 = 62$  packets/sec. By applying this to all links, delay calculation is provided for each link as it's shown in table 2.3.

Table 2.3: Table for computing delays over each of the links in the network

$i$	Link	Capacity $C_i$ Mbps	Traffic, $\lambda_i$ Packets/Sec	$T_i$ ms
1	AB	2	62	786.6
2	BC	2	42	772.4
3	CF	10	30	150.7
4	EF	5	32	302.9
5	AD	2	5	752.8
6	DC	2	22	762.6
7	BE	2	42	774.4
8	DE	2	10	755.7
9	BA	2	62	786.6
10	CB	2	42	774.4
11	FC	10	30	150.7
12	FE	5	32	302.9
13	DA	2	5	752.8
14	CD	2	22	762.6
15	EB	2	42	774.4
16	ED	2	10	755.7

Based on above table, total number of packets/sec arriving in the network is 490 packets/sec. Finally, the average packet delay for the network is calculated using following (2.22), which is equal to 0.6372ms

$$\text{Average Delay} = \sum_i^{16} \frac{\lambda_i}{\lambda} \quad (2.22)$$

In this thesis, high speed communication is required for critical data; thus, fiber optic cables is considered for high-speed network.

## 2.5 Summary and Conclusions

In this chapter, background on smart grid components is provided. In next chapter, traffic modelling and analysis of prioritizing packets are given to ensure successful transmission with minimal delay.

# Chapter 3

## Single-Server Non-Preemptive Priority Queueing Model for HAN <sup>1,2</sup>

### 3.1 Introduction

Traffic modelling and analysis are important in the development of smart grids. Electrical Devices (EDs), located remotely in HAN, generate packets with a variety of priority classes. Traffic with High Priority (HP) packets is delay-sensitive and needs to be delivered to a control station with least delay for enabling corrective measures. The intrinsic problem thus is the need to ensure successful transmission of HP traffic with minimal delay. Since each priority class is an independent discrete event, Probability Generating Function (PGF) can be used as it is useful for dealing with sums of random variables easily. The packets generated by an ED can be modelled as either High Priority (HP) or as Periodic Base (PB). While PB packets carry routine information, HP packets carry critical information. The communication from an ED to a designated Mesh Client (MC) is assumed to be wireless. In this chapter, the primary objective is to present a queueing model for HAN and subject it to delay-analysis.

- 
1. A. Noorwali, M. Alsharef, R. Rao, and A. Shami, "Delay Analysis of Discrete-Time Non-Preemptive Priority Queues in EDN of Smart Grids," Proceedings of 2016 International conference on Communications Computer Science and Information Technology (ICCCSIT), Dubai, pp. 2–7, March 2016.
  2. A. Noorwali, R. Rao, and A. Shami, "Wireless EDN in Smart Grids Communication: Modelling, Prioritizing, and Delay Analysis," International Journal on Networking and Communication, vol. 5, no. 4, pp.1–12, June 2016.

EDs generate two classes of traffic: HP and PB packets. HP packets need to be transmitted as soon as they are generated as they affect the operation of power grid and contain control information about power supply conditions [1, 2]. The random HP traffic can be modeled as a Poisson process [35, 36, 45, 38, 39]. Multiple classes' of traffic are needed for modelling network traffic in smart grids. Recently, researchers [38, 39, 40, 41] have investigated priority queuing with multiple classes of traffic. In these, Poisson arrival process is assumed for each class of traffic to simplify the analysis. Also, PB traffic is dropped and only transmission of HP traffic is considered. Consequently, this assumption ignores the importance of PB traffic which is typically periodic and carries routine information about the operation, power consumption, energy loss, and power factors for monitoring reasons. Therefore, mixture of periodic and random traffic model within an ED is needed. This is critical for real time applications.

In this chapter, a queueing system based on HP and PB traffic generated within an ED is developed. A priority queuing called Head-of-Line (HOL) for scheduling purposes is considered. HOL [41] is a static priority scheme that always gives priority to delay-sensitive class of traffic. In the first step, a queueing model for smart grid access network is presented. The Probability Generating Functions (PGFs) are then derived for this system to obtain mean buffer length and mean queuing delay for each class of traffic [42]. The proposed queueing model for HAN is examined both analytically and using simulations.

## 3.2 Model of Non-preemptive Single Server Queueing System

The traffic from ED to MC can be modeled as a discrete single server queueing system [43, 44] as shown in Fig. 3.1.

The HP traffic is assumed to follow Poisson distribution, and PB is assumed to be deterministic and independent of HP traffic. In addition, the service time  $\tau$  is assumed in this study to be equal to 1 slot. Each ED is connected wirelessly to its MC as shown in Fig. 3.2.

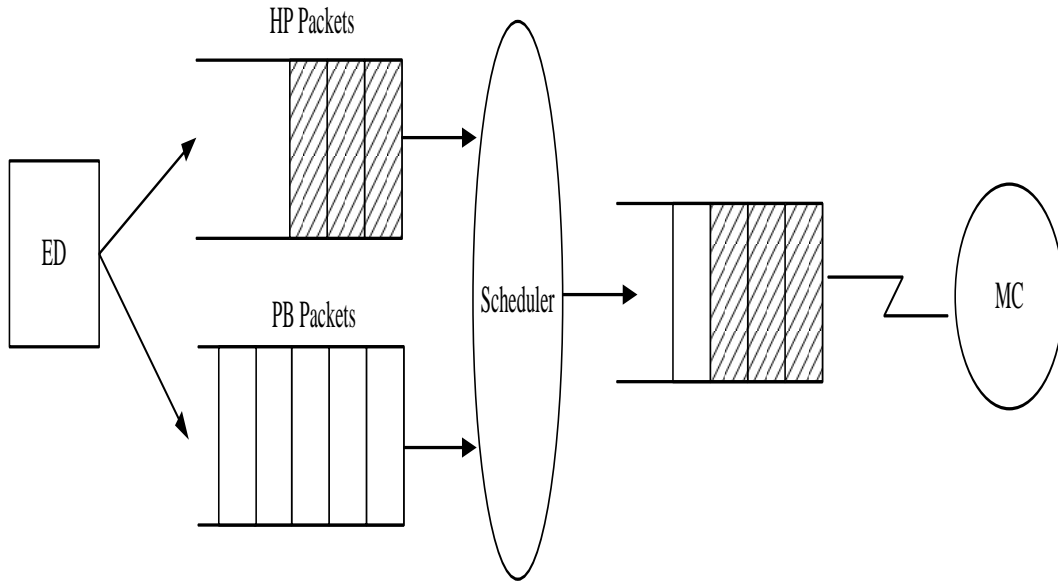


Figure 3.1: Non-preemptive queueing model between ED and MC.

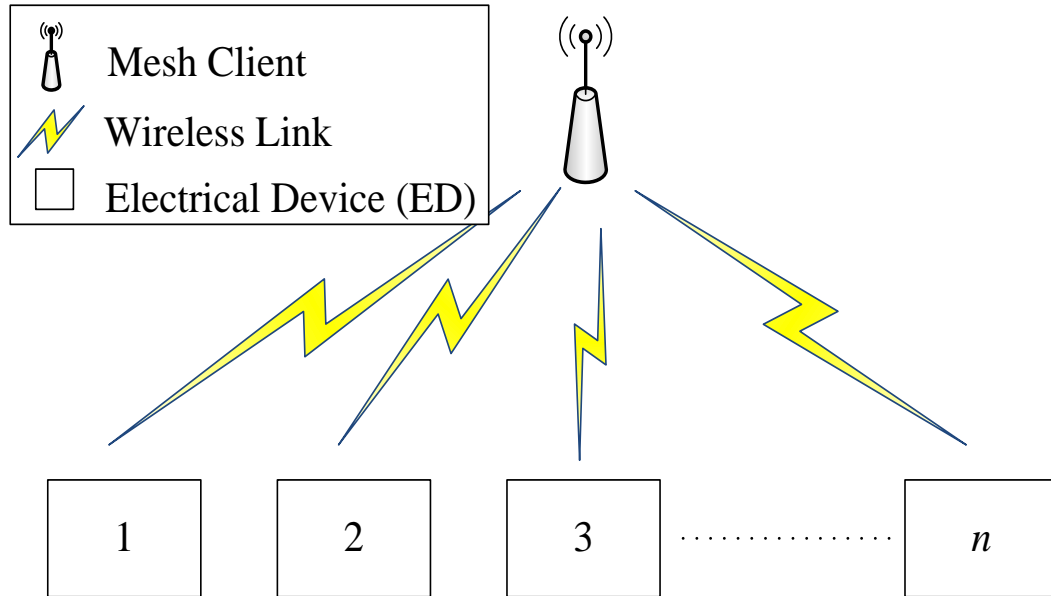


Figure 3.2: Model of HAN in smart grid.

The number of arrivals of each priority class  $i$  during slot  $a$  is denoted as  $b_{i,a}$  ( $i = 1, 2$ ), where  $i = 1$  refers to HP and  $i = 2$  refers to PB traffic, respectively. The joint probability mass function is characterized as:

$$b(k, m) \triangleq \text{Prob} [b_{1,a} = k, b_{2,a} = m], \quad k, m = 0, 1, \dots$$

One of the greatest strengths of PGF is that it turns a sum into a product. Thus, the joint PGFs can be written as:

$$B(z_1, z_2) \triangleq E \left[ z_1^{b_{1,a}}, z_2^{b_{2,a}} \right]. \quad (3.1)$$

Consequently, the total number of packets arriving during a slot is denoted by  $b_{T,a} \triangleq b_{1,a} + b_{2,a}$ . Further, the PGFs for the total of all packets arriving is given as  $B_T(z) \triangleq E \left[ z^{b_{T,a}} \right] = B(z_1, z_2)$ . For instance, the packet arrival from HP-class and PB-class during a slot can be described as  $B_1(z) \triangleq E \left[ z^{b_{1,a}} \right] = B(z, 1)$ , and  $B_2(z) \triangleq E \left[ z^{b_{2,a}} \right] = B(1, z)$ ; respectively. Furthermore, the arrival rate of each class- $i$  ( $i = 1, 2$ ) packets is denoted as  $\lambda_i = B_i'(1)$ ; thus, the total arrival rate is given by  $\lambda_T = \lambda_{HP} + \lambda_{PB} = B_T'(1) = B_1'(1) + B_2'(1)$ . The stability condition of the queueing system is defined as  $\rho_T = \lambda_T / \mu$ , which should be  $< 1$  for a stable system [41].  $\mu$  is the service rate,  $\lambda_{PB} = E[X]/A$ ,  $E[X] = \sum_{a=1}^A a P_a$  is the mean size of the PB class,  $A$  is the total time, and  $P_a$  is the probability that every packet has arrived at an  $a$  slot. Because class  $i = 2$  is presumed to be deterministic, the probability that packets arrive at slot  $a$  is equal to 1. Therefore, the arrival process is jointly Poisson and deterministic. Thus, the PGF  $B(z_1, z_2)$  is given by:

$$B(z_1, z_2) = e^{\lambda_{HP}(z_1-1)} + \frac{\lambda_{PB}}{1-z_2}. \quad (3.2)$$

In addition, the service rate is the transmission time over the wireless link. Thus, whether the PDF is consequently following a Poisson distribution depends on the FIFO discipline. For the priority seeks, if HP packets (in the high priority queue) are generated, the PB will not be served until the HP buffer is empty. In this work, priority scheduling is presumed to be non-preemptive, which means the HP traffic will not be interrupted by any newly generated traffic from PB-class. At the end of the slot in which the HP packet was transmitted, the packet at the HOL of PB jumps to the queue. Note that both



classes will follow the single queue with the FIFO discipline.

### 3.2.1 State of Queuing System

The state of the system at the beginning of time slot  $a$  can be represented by the system buffers as  $u_{i,a} = (i = 1, 2)$ , where  $u_{1,a}, u_{2,a} \leq \infty$ . Consequently, the future state of the process depends only on its present state and not on its sequence of past states. This stochastic process is called Markovian [85]. For instance, the future departure from each buffer will depend only on the present departure. This departure indicates that independently generated packets have been successfully transmitted. Therefore, the first step in our queuing system is to introduce a joint PGF process of  $u_{1,a}, u_{2,a}$  denoted by  $U_a(z_1, z_2) \triangleq E \left[ z_1^{b_{1,a}}, z_2^{b_{2,a}} \right]$ . All possible transitions occur in the current state when there is discussion of at least one channel being allocated to a particular ED. Therefore, the vector  $r = [b_{1,a}, b_{2,a}, u_{1,a}, u_{2,a}]$  is defined to increment and decrement the arrival and the departure. For instance, the arrival packets occur when HP and PB have generated packets into the buffer, and are following mutually exclusive events. To illustrate, when  $u_{1,a} = u_{2,a} = 0$  the transition happens in a state where the amount of arrival is indicated by:  $[b_{1,a} - 1, b_{2,a}, 0, 0]$  and/or  $[b_{1,a}, b_{2,a} - 1, 0, 0]$ . In addition, the transitions happen in a state of buffers  $u_{1,a}$ , and  $u_{2,a}$  when one of the following happens  $[b_{1,a}, b_{2,a}, u_{1,a} - 1, u_{2,a}]$ , and/or  $[b_{1,a}, b_{2,a}, u_{1,a}, u_{2,a} - 1]$ . When the buffer in HP-class is empty at the beginning of time slot  $a$ , a packet from buffers BP-class is subsequently served. However, if  $b_{1,a} > 1$ , this indicates that the HP buffer is not empty and PB packets will be deferred to the next time slot  $a + 1$ .

### 3.2.2 Queueing System Contents

The content of the system is consequently obtained by using the above relationship between all possible mutually exclusive events. First, the two system queues are empty and the two different classes' packets have arrived. The priority will consequently be given to the HP class, which means high priority packets will depart from the system. After that, when the PB queue has its packets ready to transmit and at the same time HP's packets have arrived, they will be queued in the HP class and leave the system. The second scenario is when both classes generate packets simultaneously to non-empty

queues. HP and PB arrival packets will be queued and all HP packets will leave the system first. On the other hand, when an HP packet arrives at an empty HP queue, it will also have the priority of leaving the system. Due to the priority mechanism, when PB packets arrive at non-empty queues, they will be queued until the previous packets leave the system, and so on. These are characterized by the following:

$$u_{1,a+1} = [u_{1,a} - 1]^+ + b_{1,a}; \quad (3.3)$$

$$u_{2,a+1} = \begin{cases} [u_{2,a} - 1]^+ + b_{2,a} & \text{if } u_{1,a} = 0 \\ u_{2,a} + b_{2,a} & \text{if } u_{1,a} > 0 \end{cases} \quad (3.4)$$

where,  $[.]^+$  denotes the maximum of the argument and 0. Therefore,  $U(z_1, z_2) = \text{Prob} [\text{no service} | u_{1,a} = u_{2,a} = 0] + \text{Prob} [\text{service PB class} | u_{1,a} = 0, u_{2,a} > 0] + \text{Prob} [\text{service HP class} | u_{1,a} > 0]$ . This yields with  $E[X\{Y\}] = E[X|Y]\text{Prob}[Y]$  to  $U_{a+1}(z_1, z_2) = E[z_1^{u_{1,a}} z_2^{u_{2,a}} \{\text{no service}\}] + E[z_1^{u_{1,a}} z_2^{u_{2,a}} \{\text{service class-PB}\}] + E[z_1^{u_{1,a}} z_2^{u_{2,a}} \{\text{service class-HP}\}]$ . Therefore, the PGF of  $U_{a+1}$  is calculated as:

$$\begin{aligned} U_{a+1} &= B(z_1, z_2)(\text{Prob} [\text{no service} | (u_{1,a} = u_{2,a} = 0)]) \\ &\quad + \frac{B(z_1, z_2)}{z_1}(\text{Prob}[\text{service class-HP} | (u_{1,a} > 0)]) \\ &\quad + \frac{B(z_1, z_2)}{z_2}(\text{Prob}[\text{service class-PB} | (u_{1,a} = 0 \ \& \ u_{2,a} > 0)]), \end{aligned} \quad (3.5)$$

where, when the two queues are empty, this leads to:

$$\text{Prob} [\text{no service} | (u_{1,a} = u_{2,a} = 0)] = U(0, 0), \quad (3.6)$$

However, the probability of empty queues when the server is busy equals  $1 - U(0, 0)$  and class-HP is being served with probability  $\frac{\rho_{HP}}{\rho_T}$ , this leads to:

$$\begin{aligned} &\text{Prob}[\text{service class-HP} | (u_{1,a} > 0, u_{2,a} > 0)] \\ &= (1 - U(0, 0)) \frac{\rho_{HP}}{\rho_T} = U_a(z_1, z_2) - U(0, z_2), \end{aligned} \quad (3.7)$$

Finally, the probability of empty queues when the server is busy equals  $1 - U(0, 0)$  and class-PB is served with probability  $\frac{\rho_{PB}}{\rho_T}$ , this leads to:

$$\begin{aligned} & \text{Prob}[\text{service class-PB}](u_{1,a} = 0, u_{2,a} > 0) \\ &= (1 - U(0, 0)) \frac{\rho_{PB}}{\rho_T} = U_a(0, z_2) - U(0, 0). \end{aligned} \quad (3.8)$$

In a stable system, the distribution of system contents determines the relation between  $U_{a+1}(\cdot, \cdot)$  and  $U_a(\cdot, \cdot)$  in steady state[41] is outlined by taking  $a \rightarrow \infty$  as:

$$U(z_1, z_2) \triangleq \lim_{a \rightarrow \infty} U_a(z_1, z_2) = \lim_{a \rightarrow \infty} U_{a+1}(z_1, z_2)$$

Knowing that  $U(0, 0)$  is the probability of having an empty system and equal to  $1 - \rho_T$  [42], the joint PGF of the system content is obtained by:

$$\begin{aligned} U_T(z) &\triangleq \lim_{a \rightarrow \infty} E[z^{u_T, a}] \\ &= U(z_1, z_2) = (1 - \rho_T) \frac{B_T(z)(z-1)}{z - B_T(z)}. \end{aligned} \quad (3.9)$$

For HP-class queue content, and the buffer content can be obtained by calculating the PGF of  $U_{HP}(z)$ . By substituting  $z_2$  by 1 in (3.9) and using de l'Hopital's rule [46], which states that if there is an indeterminate form  $0/0$ , differentiating the numerator and the denominator is required and then limit is applied. Thus, the average number of packets in HP-class queue  $U_1(z)$  is given by:

$$\begin{aligned} U_{HP}(z) &\triangleq \lim_{a \rightarrow \infty} E[z^{u_1, a}] = \\ &(1 - \rho_{HP}) \frac{B_{HP}(z)(z-1)}{(z - B_{HP}(z))}. \end{aligned} \quad (3.10)$$

The PB-class queue content is given by:

$$U_{PB}(z) = U_T(z) - U_{HP}(z) \quad (3.11)$$

### 3.3 Delay Analysis of Queueing System

Packet delay can be defined as the total amount of times that a packet spends in the system. In this section, the packet delay of the two classes will be derived. Since the packets generated by BP are deferred to the next slot  $a + 1$  if they are generated simultaneously with HP packets, the HP class is treated as if they are the only packets that arrive in the system at slot  $a$ . The total delay then is given by:

$$d_{\text{total}} = d_{\text{queue}} + d_{\text{service}}. \quad (3.12)$$

where  $d_{\text{queue}}$  is the expected time that packets spend in the queues, and  $d_{\text{service}}$  is the wireless transmission time  $\tau$ .

The PGF is useful for finding the probabilities and moments of a sum of independent random variables. To find the packet delay, we are required to calculate the moments of HP- and PB- class contents as follows: For the stochastic variables, the average values of the system content can be found by taking first derivative of the respective PGFs in (3.9), and (3.10) for  $z = 1$ .

By definition, the expected value of  $E[u_T] = E[u_{HP}] + E[u_{PB}]$ . Where  $E[u_T]$  is derived by taking the first derivative of  $U_T(z)$  for  $z = 1$  as follows:

$$E[u_T] = \frac{\rho_T}{2} + \frac{\mu \text{Var}[b_T]}{2(1 - \rho_T)} + \frac{\lambda_T^2}{2(1 - \rho_T)} \quad (3.13)$$

where the variance in PGF can be obtained as:  $\text{Var}[b_T] = \text{Var}[b_1] + \text{Var}[b_2] + 2\text{Cov}[b_1, b_2]$ , with  $\text{Var}[b_1] = B_1''(1) + B_1'(1) - (B_1'(1))^2$  with  $\text{Var}[b_2] = 0$ , and  $\text{Cov}[b_1, b_2] = 0$  because both systems are uncorrelated and independent. Therefore, by following the same procedure and applying it in (3.10), we find  $E[u_1]$  as:

$$E[u_{HP}] = \frac{\rho_{HP}}{2} + \left[ \frac{\mu \text{Var}[b_1] + \lambda_{HP}^2 + \lambda_{HP} \lambda_{PB} (\mu(\mu - 1))}{2(1 - \rho_{HP})} \right]. \quad (3.14)$$

Furthermore, the average amount of system content in the BP-class is obtained by:

$$E[u_{PB}] = \frac{\rho_{PB}}{2} + \frac{\mu^2 \lambda_{PB} \text{Var}[b_1] + \lambda_{HP} \lambda_T (\mu(\mu - 1))}{2(1 - \rho_T)(1 - \rho_{HP})} - \frac{\rho_{HP} \lambda_{PB} (\mu - 1)}{2(1 - \rho_{HP})}. \quad (3.15)$$

According to Little's law [47], the expected delay of each class can be obtained by:

$$E[d_i] = \frac{E[u_i]}{\lambda_i}, \quad (3.16)$$

where  $E[u_i]$  is the expected number of packets in class  $i$ , and  $\lambda_i$  is the packet arrival rate for a specific class  $i$ . Therefore, by applying (3.14) into (3.16), we find the average packet delay for HP- class by:

$$E[d_{HP}] = \frac{\mu}{2} + \left[ \frac{\lambda_{HP} + \lambda_{PB} (\mu(\mu - 1))}{2(1 - \rho_{HP})} + \frac{\mu \text{Var}[b_1]}{2\lambda_{HP} (1 - \rho_{HP})} \right]. \quad (3.17)$$

As  $E[d_{HP}]$  is already calculated; thus,  $E[d_{PB}]$  is obtained by:

$$E[d_{PB}] = \frac{\mu}{2} + \frac{\mu^2 \text{Var}[b_1]}{2(1 - \rho_T)(1 - \rho_{HP})} + \frac{\lambda_T}{2(1 - \rho_T)(1 - \rho_{HP})} - \frac{\rho_{HP} (\mu - 1)}{2(1 - \rho_{HP})}. \quad (3.18)$$

### 3.4 Average Packet Delay and Contents for HAN

Thus far the analysis presented is valid for the queueing system shown in Fig. 3.1. In order to extend the results to a typical HAN, shown in Fig. 3.2, consisting of  $n$  EDs and an MC, a modified, queueing system for HAN is shown in Fig. 3.3, where  $\lambda_{HP}^i$  and  $\lambda_{PB}^i$ ,  $i = 1, 2, \dots, n$ , denote HP and PB arrival rates for each ED. Thus, the overall HP arrival rate  $\lambda_{HP}$  and PB arrival rate  $\lambda_{PB}$  are given by:

$$\lambda_{HP} = \lambda_{HP}^1 + \lambda_{HP}^2 + \dots + \lambda_{HP}^n \quad (3.19)$$

$$\lambda_{PB} = \lambda_{PB}^1 + \lambda_{PB}^2 + \dots + \lambda_{PB}^n \quad (3.20)$$

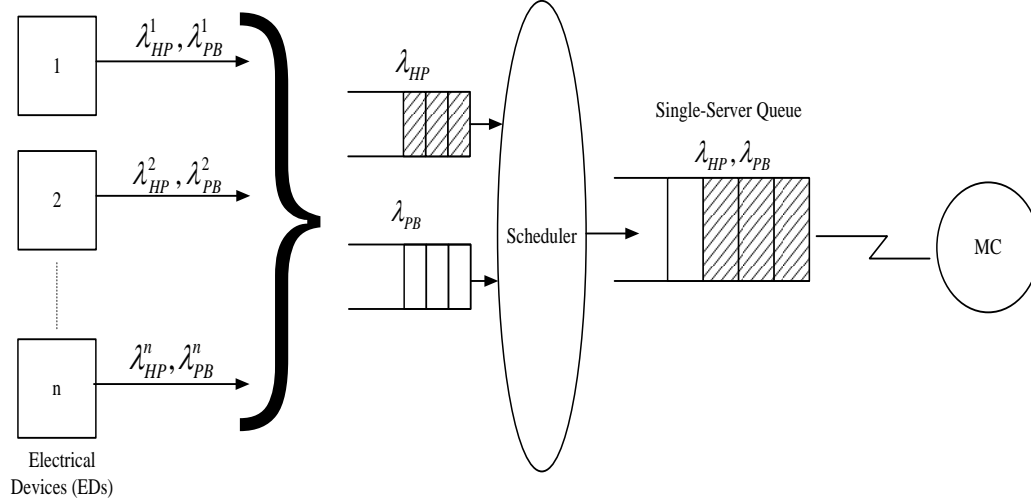


Figure 3.3: Queueing model between a set of  $n$  EDs and MC.

Using (3.19) and (3.20) in (3.17) and (3.18) average packet delay for HAN can be determined. Similarly, using (3.19) and (3.20) in (3.14) and (3.15) the average number of packets in the queueing system in HAN can be determined.

### 3.5 Numerical Results and Discussion

Using the parameters listed in Tables 3.1, 3.2, and 3.3, the content of queues and their delays are examined using closed-form expressions given by (3.14), (3.15), (3.17), and (3.18). Simulation of the queueing system for HAN, shown in Fig. 2.3, is also carried out to validate the analytical results.

The mean value of queue contents for HP and PB classes of traffic are next examined using the parameters given in Table 3.1. The results are shown in Fig. 3.4 as a function of HP arrival rate. When  $\lambda_{HP}$  increases, for a fixed value of  $\lambda_{PB} = 2$ , it is observed that the queue contents mostly of HP packets than PB packets due to HOL scheduling strategy used. For example, at  $\lambda_{HP} = 10$ , the queue consists of 232 HP packets and 80 PB packets on the average. On the other hand, when  $\lambda_{HP}$  increases to 14, the queue consists of 936 HP packets and 182 PB packets on the average.

Table 3.1: Parameters used to determine average number of packets in the system (Fig. 2.4) and average packet delay (Fig. 2.5) as a function of  $\lambda_{HP}$

Parameter	Value
Service rate $\mu$	20 packets/slot
PB Arrival rate $\lambda_{PB}$	2 packets/slot
Slot duration = service time = $\tau$	$4\mu$ sec

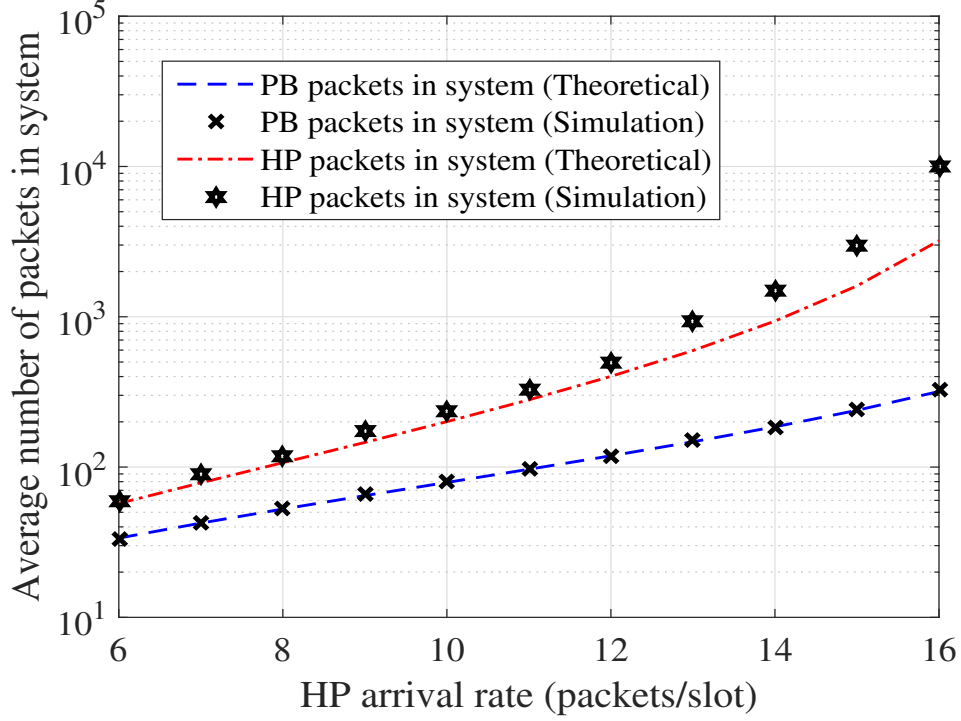


Figure 3.4: Average number of packets in the system as a function of HP arrival rate ( $\lambda_{HP}$ ).

By using the parameters given in Table 2.1, the average PB and HP packet delays as a function of HP arrival rate are plotted in Fig. 3.5 using (3.17) and (3.18). Also, simulation results are shown in the same figure. From Fig. 3.5, it is noted that for  $\lambda_{HP} = 10$ , the mean HP packet delay is  $3m$  sec and the mean PB packet delay is  $40m$  sec. When  $\lambda_{HP}$  increased to 14, the mean PB packet delay is 0.3 sec and mean HP packet delay is  $5m$  sec. Thus, it is observed that the mean PB delay increases exponentially relative to mean HP delay as  $\lambda_{HP}$  increases. This implies that as  $\lambda_{HP}$  increases PB packets suffer more delay due to the HOL scheduling strategy.

Table 3.2: Parameters used to determine average packet delay (Fig. 2.6) as a function of service rate,  $\mu$

Parameter	Value
Service Rate $\mu$	14 - 10 packets/slot
PB Arrival rate $\lambda_{PB}$	1 packet/slot
HP Arrival rate $\lambda_{HP}$	8 packet/slot

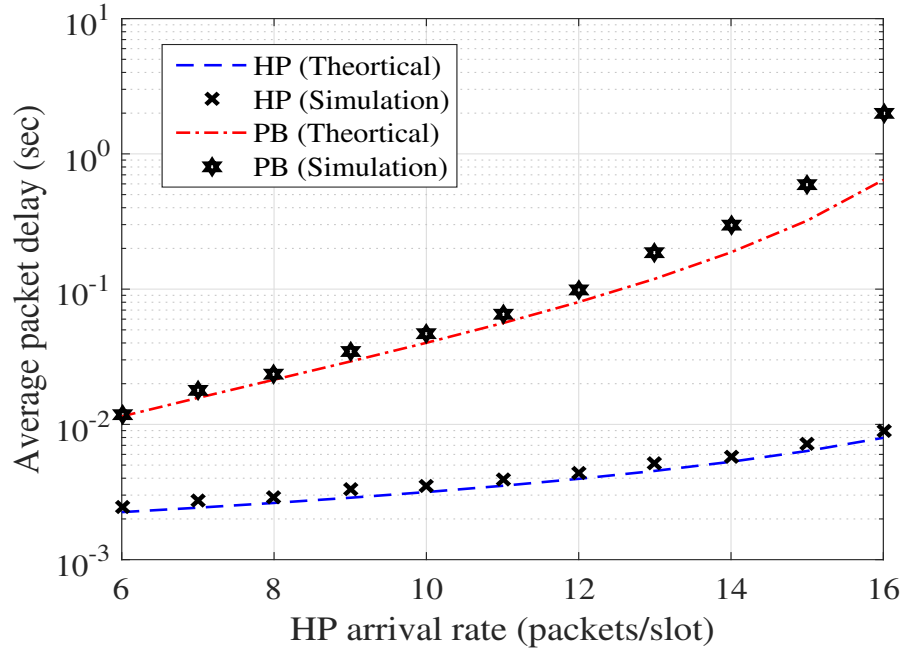


Figure 3.5: Average packet delay as a function of HP arrival rate ( $\lambda_{HP}$ ).

The average delay for both HP and PB traffic are plotted in Fig. 3.6, as a function of service rate ( $\mu$ ) using the parameters given in Table 3.2. It is observed that the mean PB delay decreases as  $\mu$  increases, while mean HP delay almost remains constant. In Fig. 3.7, average HP and PB packet delays are plotted as a function of queueing system utilization factor,  $\rho_T = \left(\frac{\lambda_T}{\mu}\right)$ . It is observed that as  $\rho_T \rightarrow 1$ , the mean packet delays associated with HP and PB traffic increases exponentially. This increase in delay is due to the increase in the number of HP and PB packets in the queue.



Table 3.3: Parameters used to determine average packet delay as a function of system utilization factor,  $\rho_T$

Parameter	Value
HP Arrival rate $\lambda_{HP}$	2 packets/slot
PB Arrival rate $\lambda_{PB}$	1 packet/slot
Utilization $\rho_T$	0.5 - 0.9

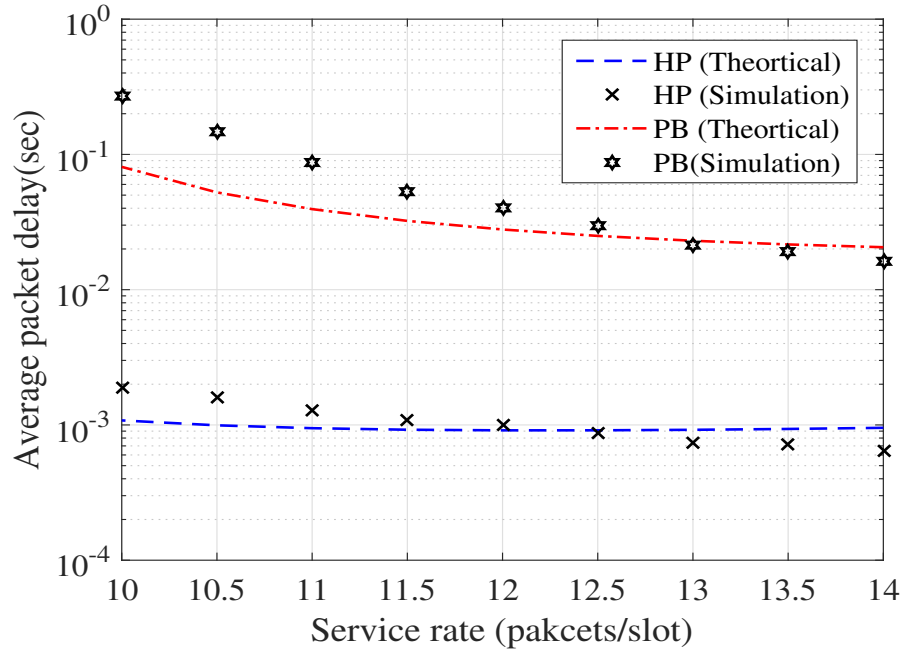


Figure 3.6: Average packet delay as a function of service rate ( $\mu$ ), for  $\lambda_{HP} = 8$  and  $\lambda_{PB} = 1$ .

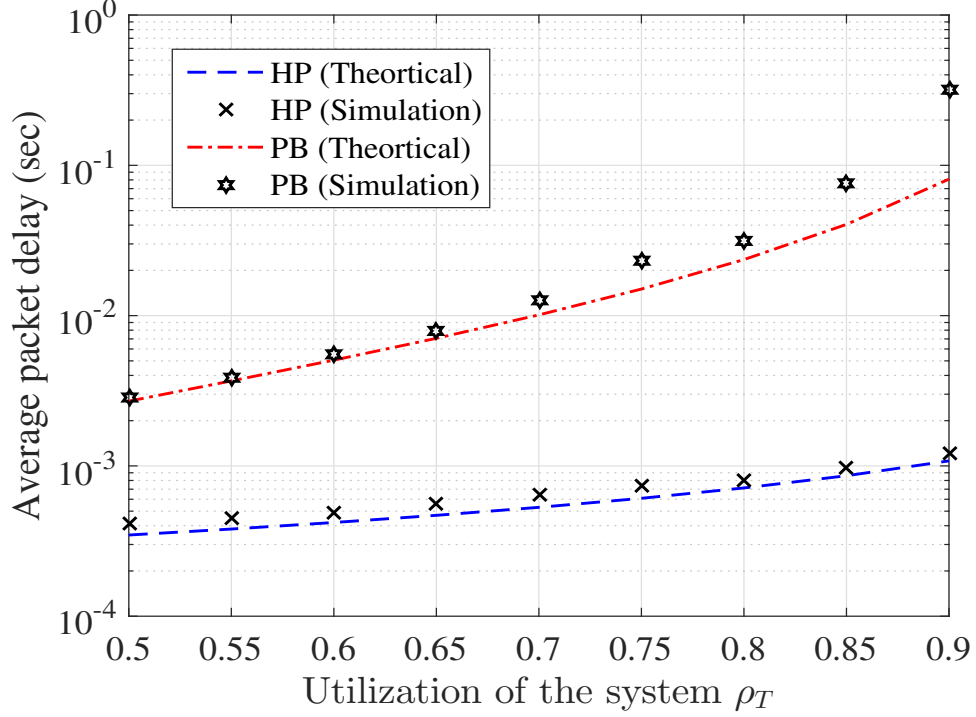


Figure 3.7: Average packet delay as a function of  $\rho_T$ , for  $\lambda_{HP} = 2$  and  $\lambda_{PB} = 1$ .

### 3.6 Summary and Conclusions

In this chapter, a non-preemptive priority queueing model for NAN in smart grid is developed for a two-class traffic system. Closed-form expressions for average delay of packets are derived. It is shown that this delay is a function of: i) critical packet arrival rate  $\lambda_{HP}$ ; ii) service rate; iii) utilization factor; and iv) rate of arrival of non-critical packets,  $\lambda_{PB}$ . The proposed model serves a 2-class traffic typically found in smart grids. The implementation of the system is relatively simple and requires minimal overhead for HP class of packets. In a nutshell, the jumping mechanism from the PB class queue to the HP class queue provides better results when the arrival rate of the HP class is low. The results indicate that the delay for both classes of traffic is between 0.2m sec and 2 sec, which meets the requirements outlined for smart grids. The proposed model is well suited for access network in smart grid.

# Chapter 4

## Modelling and Delay Analysis of Wireless HAN<sup>3,4,5</sup>

### 4.1 Introduction

In the previous chapter, a non-preemptive queueing model is suggested for delay analysis of traffic generated by EDs that are located distributively in HAN of smart grid. The delay analysis did not particularly reveal the influence of channel characteristics, transmitted powers from EDs and received power at MC, interference etc. In this chapter, therefore, practical models of wireless HAN are presented and their delay analysis are carried out, as they are important in understanding the time critical communication within HAN. The goal is to establish delay bounds that can help in the design of satisfactory smart grids [48, 49, 50]. The most widely used IEEE 802.11 standard requires the use of advanced control access mechanisms to perform a successful transmission operation. Therefore, a wireless HAN model is considered to achieve a minimum communication delay for two real scenarios: i) overlapped and ii) non-overlapped channels. The objective is

- 
3. A. Noorwali, R. Rao and A. Shami, "Modelling and Delay Analysis of Wireless Home Area Networks in a Smart Grid," Proceedings of 2015 IEEE International Conference on Smart Grid Communications (SmartGridComm), Miami, FL, USA pp. 569-574, November 2015.
  4. A. Noorwali, A. Hamed, R. Rao and A. Shami, "Modeling and delay analysis of wireless HANs in smart grids over fading channels subjected to multiple access schemes and interference," Proceedings of 2016 IEEE Canadian Conference on Electrical and Computer Engineering (CCECE), Vancouver, BC, Canada, pp. 1-6, May 2016.
  5. A. Noorwali, R. Rao and A. Shami, "Wireless Home Area Networks in Smart Grids: Modelling and Delay Analysis," Proceedings of IEEE International Conference on Saudi Arabia Smart Grid (SASG), Jeddah, Saudi Arabia, pp. 1-7, December 2016.

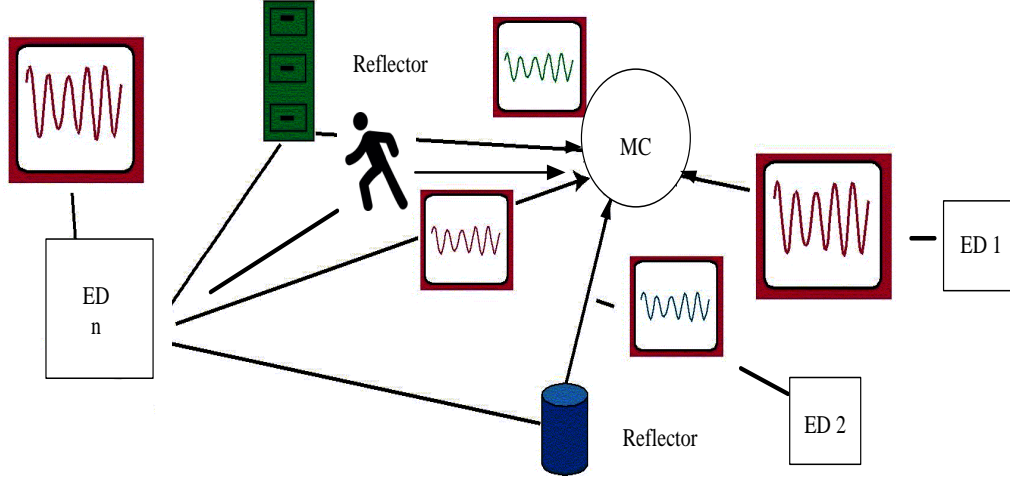


Figure 4.1: Model of typical wireless HAN and its multipath environment.

to develop a network model that allows the EDs to share the transmission resource. The delay performances of models using i) Frequency Division Multiple Access (FDMA) and ii) Time Division Multiple Access (TDMA) are presented. In the analysis, multi-path reception issues in typical HAN also are considered. The signal received by MC in wireless HAN is not only a LoS radio wave, but also is a reflected radio wave caused by obstacles in the environment as shown in Fig 4.1. Therefore, wireless HAN is modeled as a multi path fading environment. In this study, Rayleigh and Nakagami models [52] are used to portray the channel fading in HAN. The path loss exponent factor is considered also for communication between EDs and MC. The path loss exponent impacts the quality of the links. The achievable delay bounds between EDs and MC are derived as a function of Signal-to-Interference-Plus-Noise Ratio  $\gamma$ , interferences  $I$ , number of critical packets  $n$ , size of packet  $L$  in bits, number of scheduled channels  $S$ , channel interference range  $CIR$ , and power transmitted  $P_t$ .

## 4.2 Model of Wireless HAN

In a wireless HAN, a set of EDs is distributed throughout and connected wirelessly to an MC, as shown in Fig. 4.1. The MC is responsible for coordinating transmissions from EDs using the common channel resource. Thus, one MC is sufficient to serve each site. To minimize the interference occurring between sites, it is assumed that MCs of

different sites are far apart from one another. Shadowing effects in HAN are neglected and environmental noise and inter-channel interference are accounted in the model. In Fig. 4.2 is shown the IEEE 802.11 overlapping spectrum. It is noted that for every transmission period, there are only a limited number of channels that do not overlap.

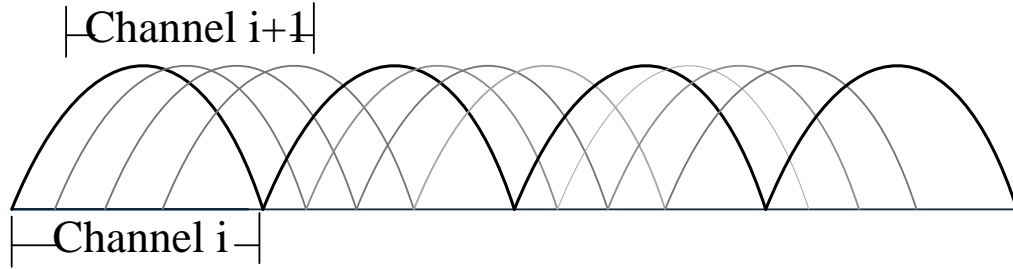


Figure 4.2: Spectrum allocation in IEEE 802.11 networks

A set of  $n$  EDs is connected through wireless links to an MC. The MC coordinates access to EDs and is responsible for collecting critical packets from them. One MC is sufficient to serve each site. To minimize interference, mesh clients are placed far apart, and the communication range between a mesh client and its EDs is set at the minimum necessary level. Fig. 4.3 shows the model of HAN consisting of several sites.

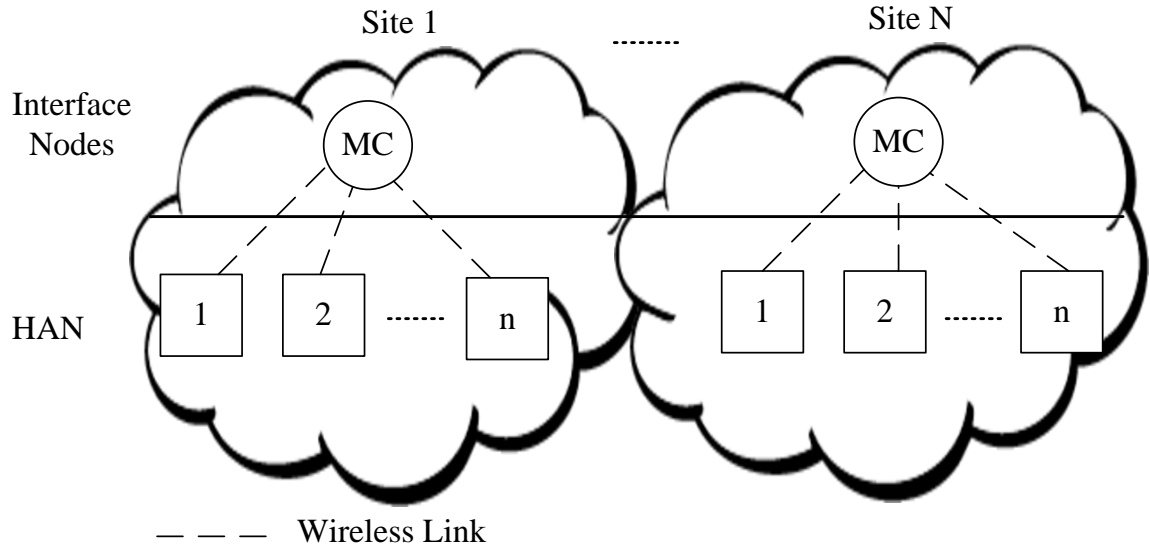


Figure 4.3: General view of wireless HAN communication network.

It is assumed that the IEEE 802.11 technology is used in HAN and the EDs in the system transmit constant power  $P_t$ . This means that the received power  $P_r$  varies with the channel conditions. Small-scale fading is considered, as the locations of EDs

are not completely random. Also, environmental noise and Inter-Channel-Interference Range (ICR) are considered in the HAN model. As shown in Fig. 4.2, the IEEE 802.11 networks have overlapping radio spectrum. There are a limited number of channels that do not overlap every time transmission occurs. Thus,  $I_{u,i,j}$  refers to the interference caused by the simultaneous transmission of  $j$  on channel  $i$  at node  $u$ , and is given by:

$$I_{u,i,j} = \frac{\max\{CIR - |d|, 0\}}{CIR} P_r, \quad (4.1)$$

where  $d$  is the distance between two active channels ( $i-j$ ),  $CIR$  is the channel interference range, and  $P_r$  is the received signal strength from node  $u$  on channel  $j$ , which is equal to  $\Omega P_t$ ,  $\Omega = E[\alpha^2]$ , where  $\alpha$  is the random channel scale and the transmitted power is  $P_t = [s^2]$ , and  $s$  is the transmitted signal. Also, we model  $P_r$  as:

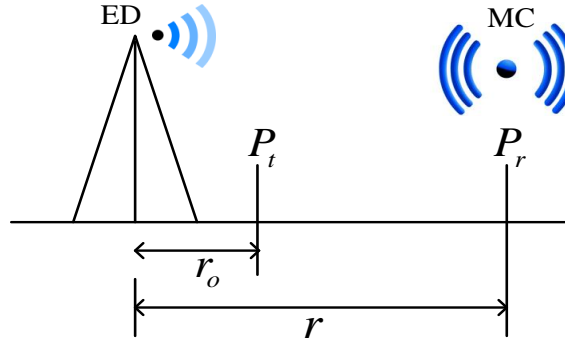


Figure 4.4: Path loss model for transmission between ED and MC.

$$P_r = \Omega P_t \left(\frac{r}{r_o}\right)^{-\varphi}, \quad (4.2)$$

where  $\varphi$  is the path loss exponent,  $\Omega$  is the strength of power that is equal to  $E[\alpha^2]$ ,  $\alpha$  is the random channel scale,  $r$  is the distance between an ED and MC, and  $r_o$  is the reference distance. This is illustrated in Fig. 4.4. Practically, it is presumed that the MC uses node  $u$  to estimate the number of channels that have not interfered with the current active channels and which experienced less impairment. It is assumed that all  $n$  packets are generated at  $t = 0$  with size  $L$  bits for each packet. The arrival time then, depends on the channel quality and the access scheme being used.

### 4.2.1 Channel Models and Fading Statistics

The noise and interference in the system and the wireless signal received by MC is susceptible to multi-path fading effect. These effects cause degradation in Signal-to-Noise Ratio (SNR), which leads to poor performance. In this study, slow and flat fading channels are considered, where the symbol duration is assumed to be smaller than the channel coherence time. Additionally, it is assumed that all spectral components of signals of EDs and MC are affected in the same manner by the fading. There are several statistical models available to describe fading effects; however, Rayleigh and Nakagami models [51] are used in this study. The received signal thus can be modeled as:

$$r = \alpha \cdot s + N_o, \quad (4.3)$$

where  $N_o$  is the Additive and White Gaussian Noise AWGN. The instantaneous SNR and average SNR based on (4.2) can be described as  $\gamma = \frac{\alpha^2 P_t}{N_0} (\frac{r}{r_o})^{-\varphi}$  and  $\bar{\gamma} = \frac{\Omega P_t}{N_0} (\frac{r}{r_o})^{-\varphi}$ , respectively. For Rayleigh Fading Channel, the probability density function is given by [54]:

$$P_R(\gamma) = \frac{1}{\bar{\gamma}} \exp\left(-\frac{\gamma}{\bar{\gamma}}\right), \quad \gamma \geq 0. \quad (4.4)$$

For the Nakagami Fading Channel, the probability density function of  $\gamma$  is given as [54]:

$$P_N(\gamma) = \left(\frac{k}{\bar{\gamma}}\right)^k \frac{\gamma^{k-1}}{\Gamma(k)} \exp\left(-k\frac{\gamma}{\bar{\gamma}}\right), \quad \gamma \geq 0. \quad (4.5)$$

### 4.2.2 Centralized Multiple-Access Schemes for Scheduling Transmissions

Typically MC covers hundreds or even thousands of EDs that periodically transmit short packets. In this study, modified FDMA and modified TDMA schemes are used in Point Coordination Function (PCF) mode for communication between EDs and MC. The MC polls EDs for allocating channels. The access schemes are considered next.

#### 4.2.2.1 Modified FDMA Scheme

The MC allocates a maximum of  $S$  disjoint channels, within  $W$  Hz to accommodate a maximum number of  $S$  of  $n$  critical packets as shown in Fig. 4.5. Each block of  $S$  critical packets are transmitted in  $\tau$  sec. During the next  $\tau$  sec, the second block of  $S$  critical packets is transmitted using the same bandwidth of  $W$  Hz. The process is continued until all the  $n$  critical packets are transmitted. It is noted that for transmission of all  $n$  critical packets the bandwidth  $W$  Hz is used for  $A = \lceil \frac{n}{S} \rceil$  number of times; each time a block of  $S$  critical packets is transmitted. For example, if  $n = 105$  and  $S = 25$ ,  $A = \lceil \frac{105}{25} \rceil = 5$ . The number of critical packets in each of the first four blocks will be 25 and in the 5<sup>th</sup> block there are 5 critical packets. It is noted that the number of critical packets in the last block is given by:

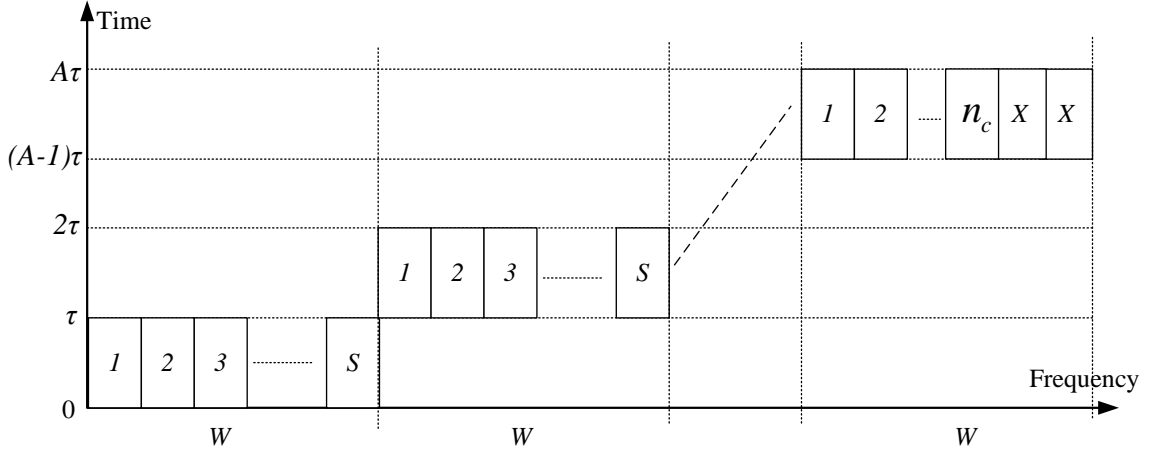


Figure 4.5: Time-frequency plot for modified FDMA.

$$n_c = n - S \text{ int} \left( \frac{n}{S} \right) \quad (4.6)$$

It is noted that  $n \gg S$ . The average critical packet delay in modified FDMA is given by:

$$\Delta_{FD} = \tau + \omega_{FD}. \quad (4.7)$$

where  $\tau$  is the average time required for transmission of each critical packet and  $\omega_{FD}$  is the average critical packet waiting time. This waiting time is given by:



$$\omega_{FD} = \frac{1}{n} \left[ \sum_{a=1}^{\text{int}\left(\frac{n}{S}\right)} S(a-1)\tau + n_c(A-1)\tau \right]. \quad (4.8)$$

Thus, the average critical packet delay is given by:

$$\Delta_{FD} = \tau + \frac{\tau}{n} \left[ \sum_{a=1}^{\text{int}\left(\frac{n}{S}\right)} S(a-1) + n_c(A-1) \right]. \quad (4.9)$$

#### 4.2.2.2 Modified TDMA Scheme

In TDMA, the entire bandwidth  $W$  is allocated for each user for a short duration of time [55]. In modified TDMA, the MC allocates the entire bandwidth  $W$  Hz to each of  $S$  critical packets for a duration of  $\frac{T}{S}$  sec. Once all the  $S$  critical packets are transmitted, the next block of  $S$  critical packets are transmitted in a similar manner. The process is continued until all the  $n$  critical packets are transmitted. The time-frequency plot for modified TDMA is shown in Fig. 4.6.

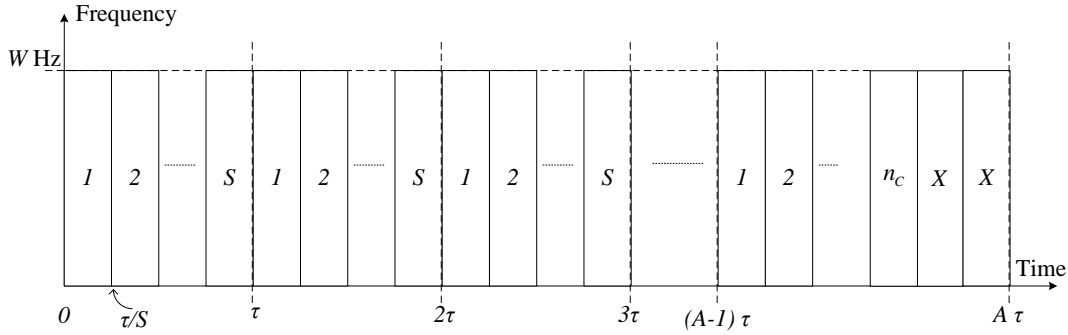


Figure 4.6: Time-frequency plot for modified TDMA.

By noting that  $n \gg S$ , the average critical packet delay for modified TDMA is given by:

$$\Delta_{TD} = \frac{\tau}{S} + \omega_{TD}. \quad (4.10)$$

where  $\frac{\tau}{S}$  is the time required for transmission of each critical packet and  $\omega_{TD}$  is the

average packet waiting time and is given by:

$$\omega_{TD} = \frac{1}{n} \left[ \sum_{a=1}^n (a-1) \frac{\tau}{S} + n_c(A-1)\tau \right] = \frac{(n-1)\tau}{2S}. \quad (4.11)$$

Thus, the average critical packet delay in modified TDMA is given by:

$$\Delta_{TD} = \frac{\tau}{S} \left[ 1 + \frac{(n-1)}{2} \right] = \frac{\tau}{S}(n+1). \quad (4.12)$$

### 4.3 Delay Analysis

Unlike the typical access point, which uses IEEE 802.11 technology with only one channel assigned to all users [32], the proposed scheme allocates maximum number of available channels based on the quality of channels. The MC then polls the EDs to schedule their transmissions simultaneously. Consequently, the MC uses SINR threshold given by:

$$SINR = \frac{P_r}{N_0 + \sum_{\{j\}} I_{u,i,j}}. \quad (4.13)$$

where  $i$  is the current channel used for transmission to determine the maximum number of channels for scheduling simultaneous transmissions.

#### 4.3.1 Lower Bound on the Delay

A lower bound on delay can be determined by first finding the maximum number of transmissions. As shown in Fig. 4.7, the total number of simultaneous transmissions occurring on both sides of the block must not exceed the channel interference range  $CIR$ . This block is limited to  $(CIR - 1)$  from each side. Therefore, the MC (using channel  $i$  in the middle of the block) uses node  $u$  in the site to assign additional channels on either side of channel  $i$ . It then schedules simultaneous transmissions on either sides of  $i$ , such as  $i - (CIR - 1), i + (CIR - 1), i - (CIR - 2), i + (CIR - 2)$ , and so on, until the threshold of the interference on channel  $i$  is reached. The interference on node  $u$  can be calculated as:

$$I = \frac{P_r}{\beta} - N_0. \quad (4.14)$$

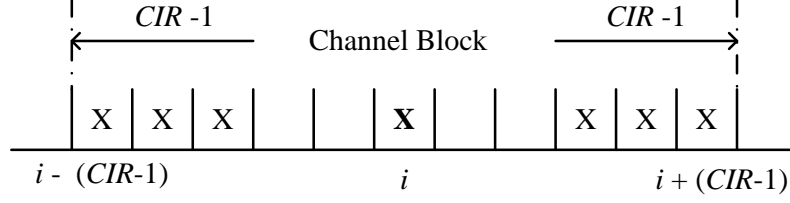


Figure 4.7: Channel block showing interference from each active channel.

Each newly scheduled channel in the given block is then labelled as  $k$ . These allocations clearly cause the  $CIR$  to decrease and increase the chances of interference. Hence, the aggregate interference is given by:

$$\sum_{k=1}^K \frac{k}{CIR}. \quad (4.15)$$

For instance, the interference will increase or decrease by  $\frac{k}{CIR}$  as the scheduled channel moves closer to or farther from the currently active channel.

The power transmitted by each ED,  $P_t$ , affects the interference  $I$ ; therefore, the ratio of the interference  $I$  to the received signal strength is equal to the sum of the quantity  $\frac{k}{CIR}$  from both sides of the block. That is,

$$2 \sum_{k=1}^K \frac{k}{CIR} = \frac{I}{P_r}. \quad (4.16)$$

Using (4.14) and (4.15), the number of scheduled channels  $K$  in the block can be shown to be given by:

$$K = \sqrt{CIR \left( \frac{1}{\beta} - \frac{1}{\gamma} \right) + \frac{1}{4}} - \frac{1}{2}. \quad (4.17)$$

The maximum number of scheduled channels on the block cannot exceed  $2K + 1$  and hence the maximum number of simultaneous transmissions within any channel block of size  $2CIR - 1$  can be written as:

$$\frac{2K + 1}{2CIR - 1}. \quad (4.18)$$

The maximum number of channels  $S$  available for simultaneous transmissions can thus be written as:

$$S_l = \left\lceil \frac{2K+1}{2CIR-1} Q_{HAN} \right\rceil, \quad (4.19)$$

where  $Q_{HAN}$  denotes the total number of channels.

### 4.3.2 Upper Bound on the Delay

For the case of maximum number of busy channels, the minimum distance  $d$  between two active channels has to be determined to schedule simultaneous transmission. At least two available channels have to be identified to attempt transmissions. The value of  $d$  can be determined from (3.13) and (3.14) based on the interference modelling (4.1) using the relationship given by:

$$\frac{2(CIR - |d|)}{CIR} = \frac{1}{\beta} - \frac{1}{\bar{\gamma}}. \quad (4.20)$$

Thus, the value  $d$  is given by:

$$d = CIR \left( 1 - \frac{1}{2} \left( \frac{1}{\beta} - \frac{1}{\bar{\gamma}} \right) \right). \quad (4.21)$$

Using this, the MC schedules a total of  $S_u = \left\lceil \frac{C_{HAN}}{d} \right\rceil$  simultaneous transmissions.

### 4.3.3 Capacity Estimation over Wireless Fading Channels

The capacity of wireless link between access point and ED can be determined using Shannon's capacity theorem. For the AWGN channel [55], this capacity is given by

$$C_{AWGN} = W \log_2 (1 + \gamma), \quad \left\lceil \frac{bits}{s} \right\rceil, \quad (4.22)$$

where  $W$  is the channel bandwidth. Channel capacity is an important parameter for estimating the transmission time ( $\tau$ ) required to complete a successful transmission. For example, the following parameters can be used to calculate the capacity: channel bandwidth  $W$  MHz, packet size  $L$  bits, and average SNR. The transmission time can then be directly estimated using the ratio of packet size to capacity. For a fading channel, the channel capacity needs to be estimated to determine  $\tau$ . The fading channel capacity

can be obtained by averaging the conditional AWGN capacity [54], using:

$$C_{AWGN} = \int_0^{\infty} C_{AWGN|\gamma} P_{\gamma}(\gamma) d\gamma. \quad (4.23)$$

where  $\gamma$  denotes the signal-to-noise ratio over the fading channel.

#### 4.3.3.1 Rayleigh Fading Channel

The capacity for Rayleigh channel can be derived by substituting (4.4) and (4.22) into (4.23) is given by:

$$C_R = \frac{W}{\log_2} e^{\frac{-1}{\gamma}} E_i\left(\frac{1}{\gamma}\right), \quad (4.24)$$

where  $(E_i(.))$  is the exponential integral function [52].

#### 4.3.3.2 Nakagami Fading Channel

The capacity for Nakagami channel can be derived using (4.5), (4.22) and (4.23) and is given by:

$$C_N = W \left(\frac{k}{\gamma}\right)^k \frac{e^{\frac{k}{\gamma}}}{\log_2} \sum_{l=1}^k \frac{\Gamma\left(l - k, \frac{k}{\gamma}\right)}{\left(\frac{k}{\gamma}\right)^k}, \quad (4.25)$$

where  $\Gamma(.,.)$  is the complementary incomplete gamma function [52]. To illustrate the effect of fading on channel capacity, the capacities for AWGN, Rayleigh, and Nakagami channel are plotted in Fig. 4.8 as functions of the average SNR. It shows that upper and lower bounds on channel capacities are plotted when AWGN and Rayleigh fading are employed respectively. Also, capacity under Nakagami fading in (4.25) is decreasing as parameter  $k$  decreases. When  $k = 1$ , the performance of the system matched very well with the worse impacted channel caused by Rayleigh fading in (4.24). Therefore, the upper and lower bounds on transmission of critical packet wirelessly  $\tau$  is calculated as:

$$\tau = \frac{L}{C_{\text{fading}}} \quad (4.26)$$

where  $L$  is the critical packet size in bits, and  $C_{\text{fading}}$  is the capacity under AWGN, Rayleighm and Nakagami.

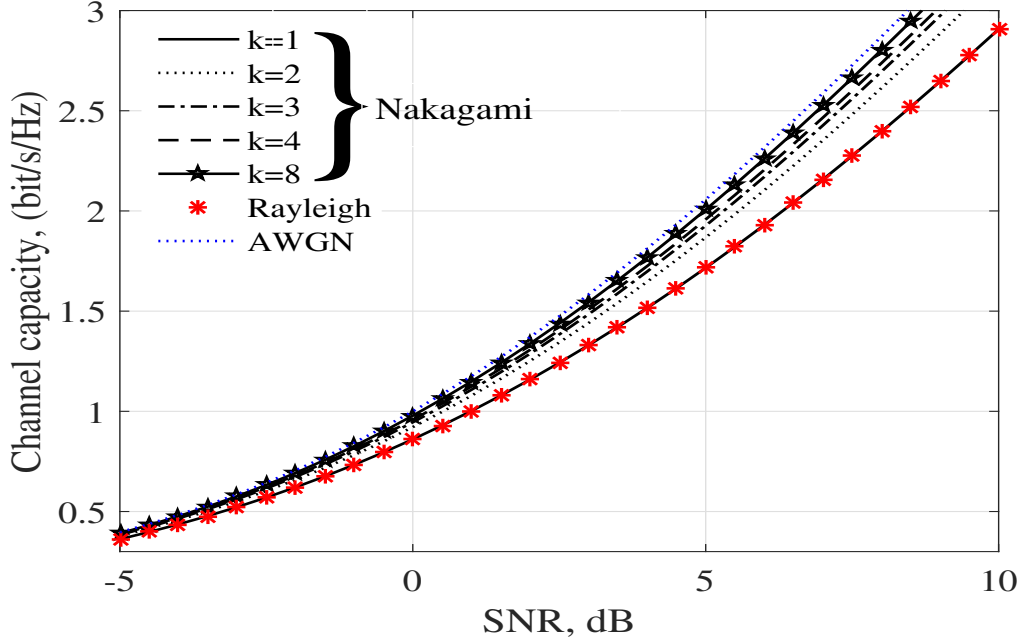


Figure 4.8: Channel capacity as a function of SNR for Nakagami, Rayleigh, and Gaussian channels.

#### 4.3.4 Delay Analysis for Multiple Access Schemes

1) In modified FDMA, transmissions are scheduled such that each packet fits into just one frequency band,  $s$ . Using the assumption that  $n$  packets are generated at time  $t = 0$ , a group of  $S$  EDs begin their transmissions using the available channels. The remaining EDs have to wait  $\omega_{FD}$  on the average before their critical packets are transmitted. Substituting (3.6), (3.17), (3.19), and (3.26) into (3.9), a lower bound on the critical packet delay can be determined and is given by:

$$\Delta_{HAN} \geq \tau \left[ 1 + n \left( \frac{2(CIR - 1)}{4Q_{HAN} \sqrt{CIR(\frac{1}{\beta} - \frac{1}{\bar{\gamma}}) + \frac{1}{4}} + 2(2CIR - 1)} + 1 \right) - S_{l\text{int}} \left( \frac{n}{S_l} \right) \right] \quad (4.27)$$

Similarly, an upper bound on the delay can be determined by substituting (4.21), and (3.26) into (4.9), and is given by:

$$\Delta_{HAN} \leq \left[ 1 + n \left( \frac{CIR \left( 1 - \frac{1}{2} \left( \frac{1}{\beta} - \frac{1}{\gamma} - 1 \right) \right) + \frac{Q_{HAN}}{n}}{2Q_{HAN}} + 1 \right) - S_{u\text{int}} \left( \frac{n}{S_u} \right) \right] \tau \quad (4.28)$$

2) In modified TDMA, the scheduler is able to schedule  $S$  EDs to  $S$  number of slots repeatedly until all  $n$  EDs transmit their critical packets. It is assumed that each critical packet fits into one time slot of duration  $\tau_{TD}$ .

To determine lower bound on the delay, (4.17), (3.19), and (3.26) are substituted into (4.12). The lower bound is given by:

$$\Delta_{HAN} \geq \frac{(2CIR - 1)(n + 1)}{\left( 2Q_{HAN} \sqrt{CIR \left( \frac{1}{\beta} - \frac{1}{\gamma} \right) + \frac{1}{4}} + 2CIR - 1 \right)} \tau. \quad (4.29)$$

The upper bound can be shown to be given by:

$$\Delta_{HAN} \leq \frac{(n + 1)(CIR(1 - \frac{1}{2}(\frac{1}{\beta} - \frac{1}{\gamma})) + Q_{HAN})}{Q_{HAN}} \tau. \quad (4.30)$$

## 4.4 Numerical Results and Discussions

Analytical expressions given by (4.27), (4.28), (4.29), and (4.30), can be used to determine upper and lower bounds on critical packet delay for modified FDMA and modified TDMA. Also, scenarios of HAN with modified FDMA and modified TDMA for transmission of critical packets from EDs to MC were simulated for different network settings. The simulation results show that they always lie in between analytically derived upper and lower bounds. To analyze the upper and lower bounds on the delay over the fading channel, AWGN, Rayleigh and Nakagami capacities given by (4.23, 4.24, and 4.25) were used. For instance,  $k$  in Nakagami density was varied from 1 to 8. It is observed that lower the value of  $k$ , higher is the capacity; except when  $k = 8$ . As discussed in Chapter 1, FCC allows the use of various distinct frequency ranges under IEEE 802.11 standard [2]. Each range is divided into a multitude of channels up to a maximum of 25 overlapped/non-overlapped channels. To avoid these channels from interfering, allocation of additional channels should be avoided when using the current channel  $i$ , based on  $CIR > 1$ . These

channels will be allocated by MC for  $n$  EDs. Accordingly, for channel interference range,  $CIR = 2$ ; number of critical packets,  $n = 200$ ; and number of channels in wireless HAN,  $Q_{HAN} = 25$ , the bounds on critical packet delay for modified FDMA and modified TDMA systems, as function of SNR, are shown in Figs. 4.9 and 4.10, respectively. It is observed that when packet size  $L = 1000$  bits and  $W = 22$  MHz, modified TDMA performs better than modified FDMA from the view point of critical packet delay.

To verify the analytical bounds, system simulation was carried out as well. Results show that the actual value of the critical packet delay is always in between the upper and lower bounds as shown in Figures 4.9, 4.10, 4.11, 4.12, and 4.13. For instance, the delay was examined as a function of channel interference range,  $CIR$ ; SNR threshold,  $\beta$ ; and number of critical packets,  $n$ . In particular, it was observed that the MC allowed the EDs to transmit all critical packets between  $0.1m$  s and  $0.9$  s. Under modified TDMA, the EDs were able to transmit all critical packets within the range of  $0.1ms - 5ms$  and for the modified FDMA, in the range of  $5ms - 0.9s$ .

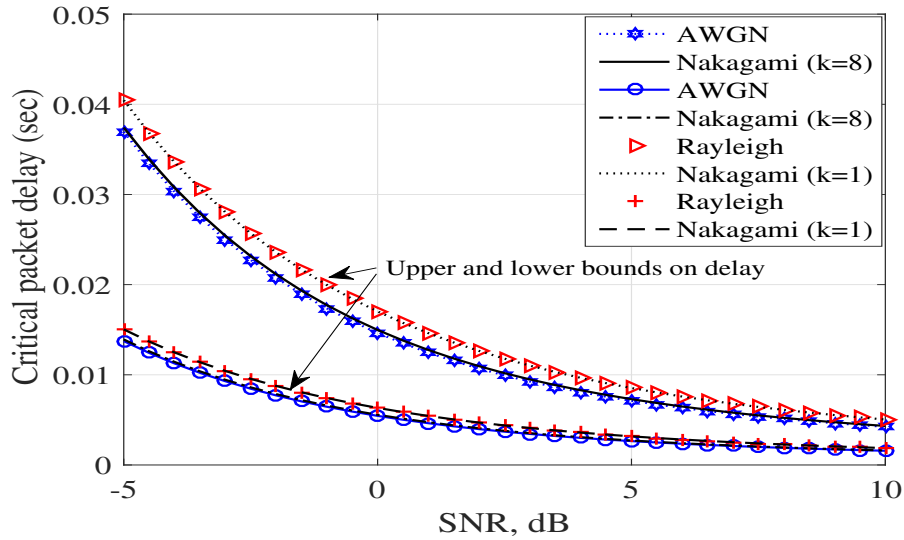


Figure 4.9: Critical delay bounds for HAN with modified FDMA as a function of SNR ( $\bar{\gamma}$ ) for  $CIR = 2$ ,  $Q_{HAN} = 25$ ,  $n = 200$ ,  $\beta = 2$ .



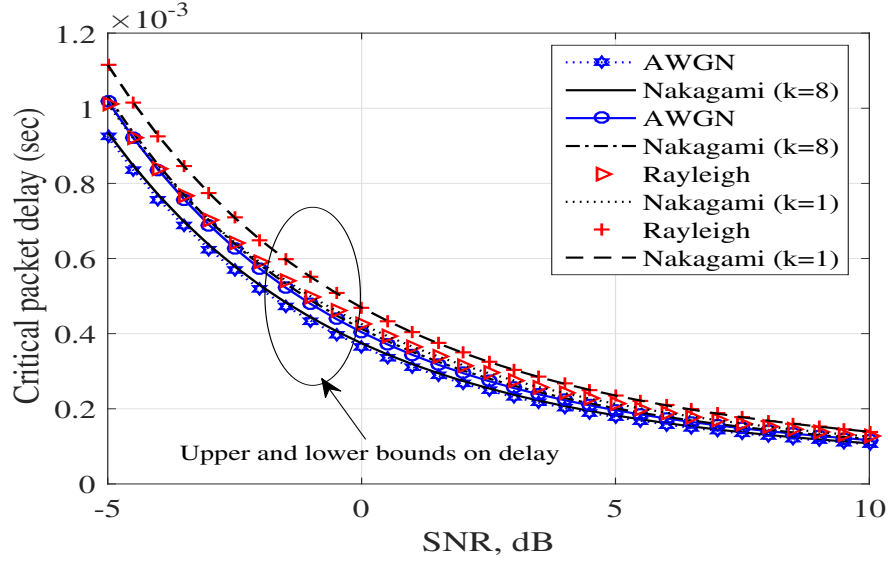


Figure 4.10: Critical delay bounds for HAN with modified TDMA as a function of SNR ( $\bar{\gamma}$ ) for  $CIR = 2$ ,  $Q_{HAN} = 25$ ,  $n = 200$ ,  $\beta = 2$ .

In Fig. 4.11, for:  $Q_{HAN} = 25$ ,  $n = 200$ ,  $\beta = 3$ ,  $\bar{\gamma} = 5$  dB, simulation results are shown for critical packet delay as a function of  $CIR$ . The delay was found to increase as  $CIR$  increased, and fewer simultaneous transmissions occurred per time slot. The value of  $CIR$  imposes stronger ICR, resulting in more space between the channels. This consequently reduces the number of available channels for simultaneous transmissions to occur. By using parameters:  $Q_{HAN} = 25$ ,  $n = 200$ ,  $CIR = 8$ , the simulation results of delay as a function of SNR threshold,  $\beta$ , is shown in Fig. 4.12. It is observed that an increase in the number of successful transmissions occurred as  $\beta$  was increased. When  $\beta$  became larger, an insufficient number of available channels occurred. The lower bound exhibited an increasing trend toward a higher delay. As the number of critical packets increased (for the set of parameters:  $Q_{HAN} = 25$ ,  $\beta = 3$ ,  $CIR = 8$ ,  $\bar{\gamma} = 5$  dB,) a linear increase occurred in the delay (Fig. 4.13).

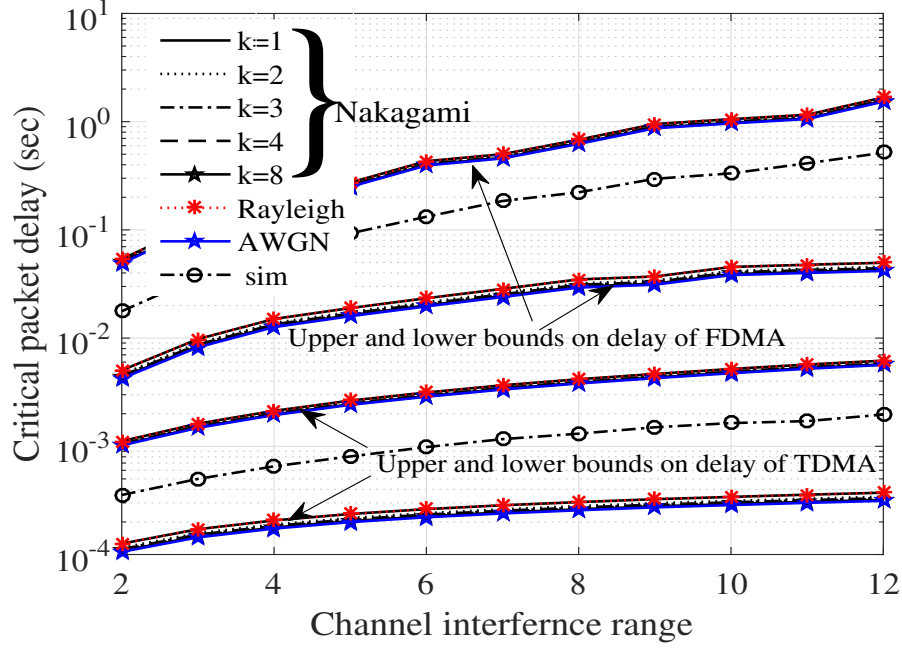


Figure 4.11: Critical delay bounds for HAN as a function of  $CIR$  for:  $Q_{HAN} = 25$ ,  $n = 200, \beta = 3$ , and  $\bar{\gamma} = 5\text{dB}$ .

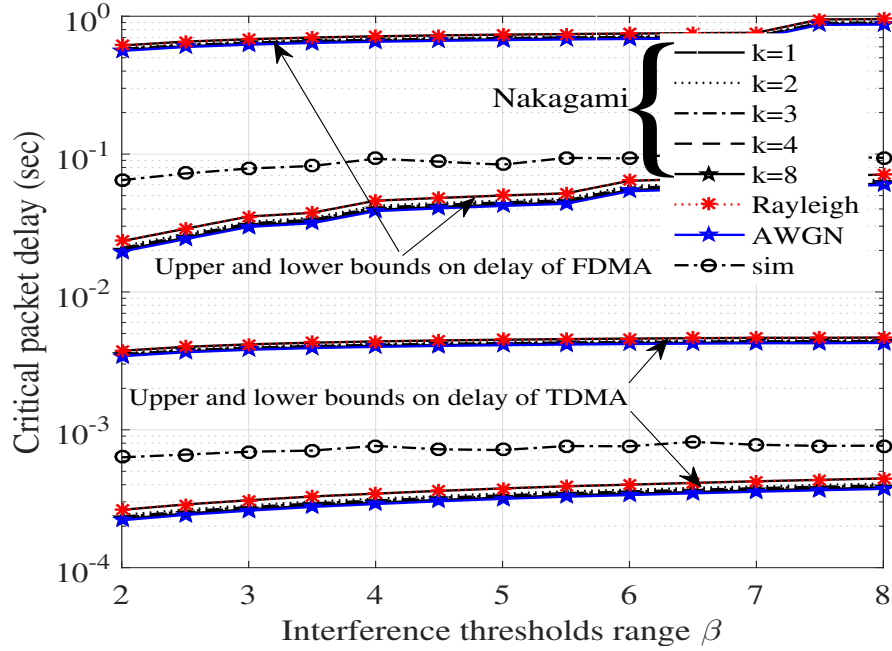


Figure 4.12: Critical delay bounds for HAN as a function of  $\beta$  for  $Q_{HAN} = 25$ ,  $n = 200, CIR = 8$ , and  $\bar{\gamma} = 5\text{dB}$ .

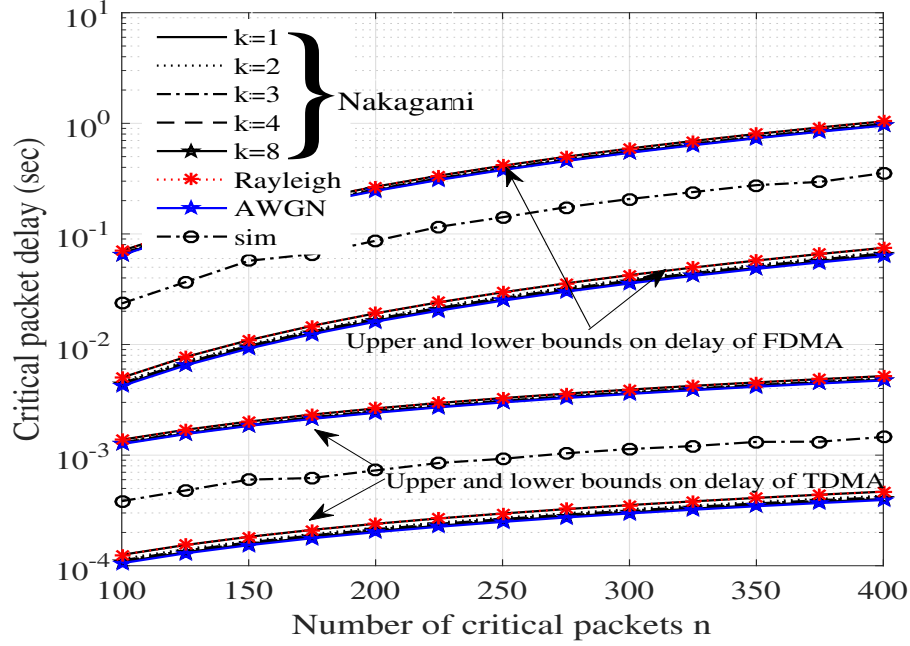


Figure 4.13: Critical delay bounds for HAN as a function of  $n$  for  $Q_{HAN} = 25$ ,  $\beta = 3$ ,  $CIR = 8$ , and  $\bar{\gamma} = 5$  dB.

Closed form expressions for critical packet delay bounds are derived in [53] ignoring multiple access schemes and fading over wireless channel. The analytical bounds derived in this chapter reduces to these derived in [53] if channel fading is ignored and  $A = 1$ . For example, in Figs. 4.14, 4.15, and 4.16, critical packet delay bounds are plotted using bounds derived in this chapter ignoring the channel impairments as a function of  $CIR$ ,  $\beta$ , and  $n$  for  $A = 1$ ,  $\bar{\gamma} = 100$ , and  $Q_{HAN} = 25$ . The results are in close agreement with the results presented in [53].

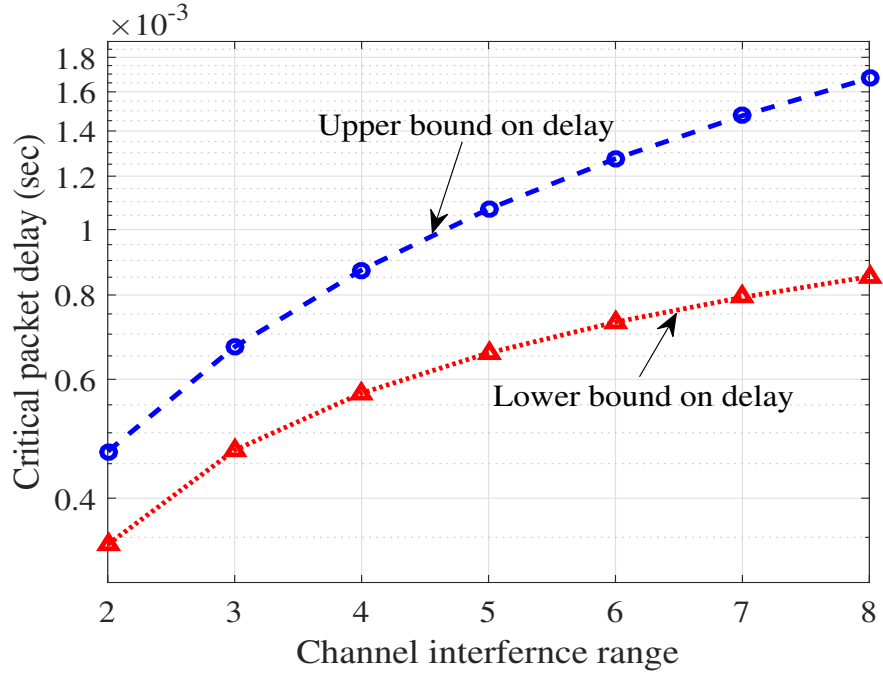


Figure 4.14: Critical delay bounds for HAN ( $A = 1$ ) as a function of  $CIR$  for:  $Q_{HAN} = 25$ ,  $n = 200$ ,  $\beta = 3$ , and  $\bar{\gamma} = 100$ .

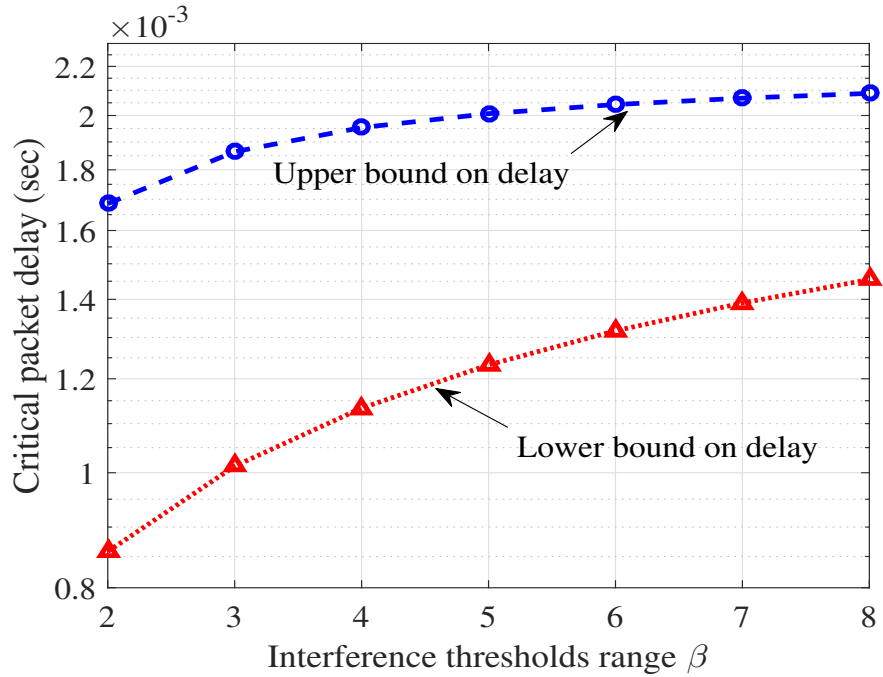


Figure 4.15: Critical delay bounds for HAN ( $A = 1$ ) as a function of  $\beta$  for  $Q_{HAN} = 25$ ,  $n = 200$ ,  $CIR = 8$ , and  $\bar{\gamma} = 100$ .

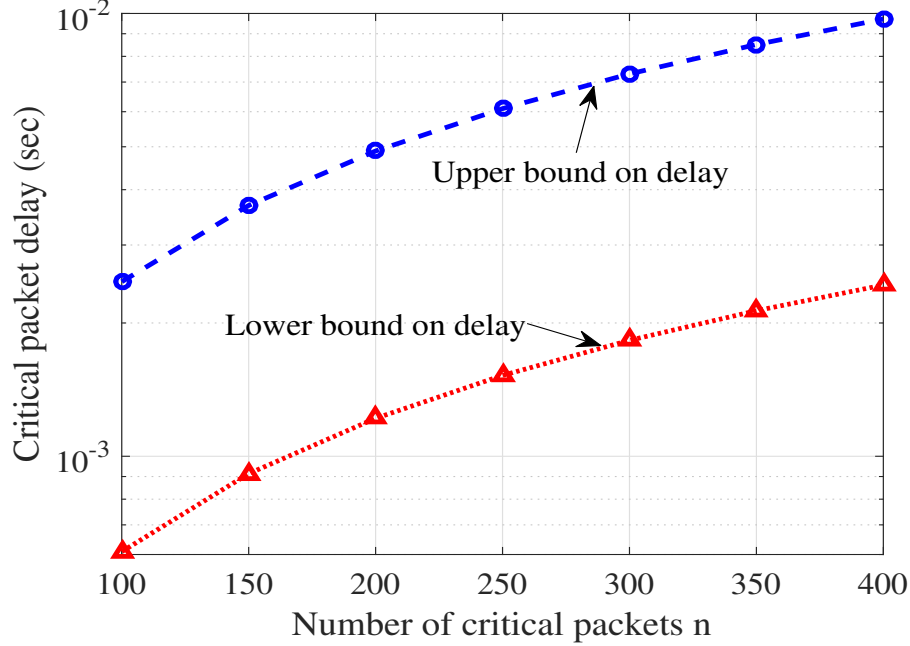


Figure 4.16: Critical delay bounds for HAN ( $A = 1$ ) as a function of  $n$  for  $Q_{HAN} = 25$ ,  $\beta = 3$ ,  $CIR = 8$ , and  $\bar{\gamma} = 100$ .

## 4.5 Summary and Conclusions

In this chapter, a model of wireless HAN using modified FDMA and modified TDMA is presented to facilitate communication between the EDs and their respective MC. The model takes into account the nature of fading over the wireless channel between EDs and MC using Rayleigh and Nakagami distributions. Upper and lower bound expressions for critical packet delay are derived in closed-form, and are functions of i) average of signal-to-interference-plus-noise ratio, ii) random channel scale, iii) transmitted power strength, iv) received power strength, v) number of EDs, vi) critical packet size, vii) number of channels, viii) path loss component, ix) distances between electrical devices and mesh client, x) channel interference range, xi) channel capacity, xii) bandwidth of the channel, and xiii) number of time slots/frequency bands. Analytical and simulation results are presented as a function of channel interference range,  $CIR$ ; SNR threshold,  $\beta$ ; and number of critical packets,  $n$ . Analytical results are in agreement with the simulation results. The simulation results lie in between analytical upper and lower bounds on critical packet delay. Results show that as  $CIR$ , and  $\beta$  increase in value, fewer number

of channels met the requirements and resulted in higher delay. Both simulation and analytical results show that critical packet transmission to MC from EDs using modified TDMA met the critical delay requirement compared to modified FDMA.

# Chapter 5

## Intelligent Distributed Channel-Aware MAC Protocol for HAN<sup>6,7</sup>

### 5.1 Introduction

The HAN in smart grid if equipped with Multiple Input Multiple Output (MIMO) communication infrastructure with directional antennas, the critical delay and throughput performance of the network can be enhanced. In [57], Fang has discussed relevant technologies for smart grids and conditions required for their use. Among the conditions is that any model should minimally satisfy reliability criterion and provide high coverage. Based on this, an effective model has been built for HAN in [58] and it uses IEEE 802.11 standard. The standard however requires advanced channel control access mechanisms for completing more than one successful transmission operation. Recently, in order to enable successful utilization of the channel, researchers [59, 60, 61, 62, 63, 64, 65, 59] have investigated the overall throughput of transmission by exploiting the advantages of MIMO systems, which are capable of providing higher data rates. Nevertheless, the vast number of EDs in HAN makes the job of exchanging critical packets more difficult. Since IEEE 802.11 endorses the use of beamforming to enable any particular station to selectivity tune-in and tune-out, it allows for simultaneous transmissions.

- 
6. A. Noorwali, *Performance Analysis of Channel-Aware Media Access Control Schemes*, M.S.C dissertation, Western University, Available: <http://ir.lib.uwo.ca/etd/727>, August 2012.
  7. A. Noorwali, R. Rao and A. Shami, "Performance Evaluation of Channel-Aware MAC protocol in Smart Grid," Proceedings of 2015 IEEE Conference on Electrical Power and Energy Conference (EPEC), London, ON, pp. 429-435, October 2015.

This chapter focuses on modelling real scenarios of reporting critical data in HAN. The objective is to propose a scheme that allows simultaneous transmission of multiple packets at a (higher/lower) rate depending on conditions of wireless channel between EDs and MC. Thus, an Intelligent Distributed Channel-Aware MAC (IDCA-MAC) protocol for HAN that uses MIMO technology is proposed, evaluated, and compared with the MA-Aware scheme described in [62]. This IDCA-MAC protocol and the model of the entire system for HAN are explained in detail and simulated using NS-2 simulator [66] and MATLAB.

### 5.1.1 Background

Many researchers have recently paid attention to re-designing MAC layers for industrial applications to allow more than one transmission at the same time for enhanced throughput and delay performance. However, the major challenge is that collisions are increased for the hidden ED terminals that are unaware of each other. In order to overcome this challenge, in IEEE 802.11 standard, any ED wanting to share a particular channel should make a Request to Send (RTS) for transmission. However, this allows for only a single transmission at a time. To overcome this issue, Thapa [60] has proposed modified distributed coordination functions (M-DCF) that permit two simultaneous transmissions. In this algorithm, each function is modified to hold an extended blank in its frame to carry extra information for the receiver side. The extended frame contains addresses of the multiple antenna receivers'. During the transmission, each antenna would reply with necessary permissions. Thus, data streams can be sent in parallel over the channel, and collisions can be avoided. In the system, the number of simultaneous transmissions is equal to the number of antennas on the senders' side. In the reverse scheme, transmissions are assumed to be error-free over the channel. There is no interference cancellation, and each of the senders' antenna sends one packet to a different receiver. Barghi [61] suggested that major modifications to the PHY layer in the system through interference cancellations to preserve collision of packets by sending multiple packets through the channel to enhance QoS. Space-Time Codes (STCs) based on Zig-Zag decoding are used in this system instead of Code Division Multiple Access (CDMA) to enhance the link quality and to increase the data transmission rate. Also, PHY layer functions are used to detect the number of simultaneous transmissions by using a synchronous Multiple-Packet



Reception (MPR) scheme and a Shuffle algorithm for scheduling transmissions. On the other hand, Duchene [62] has made significant modifications to 802.11 MAC protocol to make it more suitable for sending simultaneous transmissions through the wireless channel. Modifications to 802.11 frame of Distributed Coordination Function (DCF), the exchange timer, and the weighted gain have been used. The Media Access Aware (MA-Aware) protocol is proposed in [62] to allow wireless stations to be connected through the MAC layer within a single collision domain without interference. This makes it possible for all of the stations to share the same channel.

In this study, Intelligent Distributed Channel-Aware MAC (IDCA-MAC) algorithm is proposed that uses the weighted nulling technique [62] and the Zig-Zag decoding technique [64]. These are used to recover the packets after a collision. In order to achieve this, the operation library of 802.11 has been modified for timing of protocol operations. Moreover, the RTS and Clear to Send (CTS) control frames have also been extended with antenna weights. Specific changes in the Carrier Sense Multiple Access/Collision Avoidance (CSMA/CA) scheme are needed and consequently, antennas at both sides are adjusted so that they work for both sending and receiving data. The new mechanism sends data using 802.11 MAC layer and is still based on handshaking process; RTS, and CTS. The RTS and the CTS will complete their exchange process after a Short Inter Frame Space (SIFS) time period, and then all nodes will update their Network Allocation Vector (NAV). The technique accounts for a large number of EDs in HAN, and makes the network more reliable.

## 5.2 HAN Environment Description

### 5.2.1 CSMA/CA Scheme

DCF is used for synchronous data transmission over the channel using CSMA/CA protocol which is responsible for monitoring the channel. For the protocol to work, Short Inter-frame Space (SIFS) is used; frames such as ACK frame, CTS frame, and any frame exchanges. For completing one transmission, handshaking frames RTS and CTS are required in conjunction with CSMA/CA. If the data arrived without any error, the receiver will reply back with ACK packet. The length of RTS frame is 20 bytes, which is much

Table 5.1: Extended RTS frame structure for IDCA-MAC protocol

Frame Control	Duration	Receiver Address	Transmitter Address	Antenna Weights	Frame Check
2 byte	2 byte	2 byte	6 byte	12 byte	4 byte

Table 5.2: Extended CTS frame structure for IDCA-MAC protocol

Frame Control	Duration	Receiver Address	Antenna Weights	Frame Check
2 byte	2 byte	6 byte	12 byte	4 byte

shorter than data frame, while the length of data frame is 2300 bytes long. Moreover, CTS has only 14 bytes length. For avoiding collision, CSMA/CA senses the channel in order to perform a transmission while the backoff counter is random. The duration required to complete one successful transmission is incorporated in the duration field with adjusted value of NAV. The Slot Time used in 802.11 defines Inter-frame Space period (IFS) to determine the backoff time in the range 0 to 7. When the backoff counter becomes zero, CSMA/CA will sense the channel for transmission.

### 5.2.2 MAC System Description

A beamforming technique is used to avoid any interference with the signal transmission. Thus, the entire signal spectrum can be used efficiently. The availability of this technology will eventually cause all wireless stations to elect to transfer data to a specific station. The range of transmissions is improved as the transmitter signal is focused in the direction of the target receiver. Indeed, this will enhance the SNR and hence can be used to increase the range of transmission.

In order to simulate practical beamforming for IDCA-MAC protocol, IEEE 802.11 standards library has been adopted with modifications to frame structure, as shown in Tables 5.1 and 5.2 for the RTS and CTS packets, respectively. The timing of protocol operations permits all possible scenarios.

The RTS and CTS handshaking has been augmented with MA-Aware through antenna weights and each requires 4 bytes [62]. In this chapter, three antennas are considered in all scenarios.

### 5.2.3 Tuning In/Tuning Out Specifications

By using adjusted antenna weights [62], the ability to control tuning in / tuning out of the channel for different transmission stations can be enhanced. Consequently, it will be possible to control all stations, and they will share a single collision domain.

MIMO plays an important role in organizing the transmission and generates an overall received signal given by:

$$y(t) = x(t)w_nH_{nm}w_m, \quad (5.1)$$

where  $y(t)$  is the signal at the input of the receiver,  $w_n$  is the weight of transmitting station,  $w_m$  is the weight of receiving station,  $x(t)$  is the transmitted signal, and  $H_{nm}$  is the MIMO channel matrix between the transmitting station  $n$  and the receiving station  $m$ . The weight adjustments for both idle and busy states that have been designed to either tune in or tune out for a particular transmission is given by (5.1). These weights are normalized to unity. It is noted that no additional power is introduced into the system. An analogy of the weighting technique used here can be found in an air traffic control system in which the landing and taking off of aircrafts are controlled. The receiving stations in the wireless HAN can choose weights to tune out transmissions.

## 5.3 Intelligent Distributed Channel-Aware MAC Protocol

The IDCA-MAC protocol is designed to increase the efficiency of simultaneously data transmissions. The proposed protocol to make it compatible with the protocol given in [58]. Fig. 5.1 provides an illustration of multiple packet transmissions in a single domain. To control ED transmissions in HAN, Duchene [62] explained the approach of tuning in and tuning out for these transmissions. For simplicity, suppose that HAN network has five EDs. When the channel is idle and ED 1 wants to transmit on the channel to MC, it adjusts its antenna array element weights using normalization to maximize the SINR and replies to the transmitter to allow the transmission to proceed. The rest of the EDs will tune out transmissions from both ED 1 and the MC.

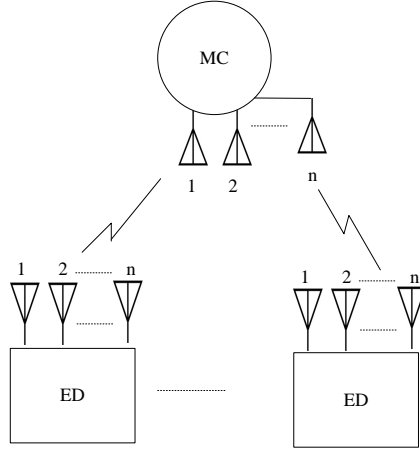


Figure 5.1: Structure of HAN with EDs and MC equipped with multiple antennas.

Since each ED carries a specific address direction of MC antenna, instead of sending one packet of information per transmission, multiple packets in each beam direction can be sent. Based on [62], the weighted gain and IEEE 802.11 features are modified so that they can transmit more than one packet. Consequently, modifications were done to the timing as well to handle any arbitrary scenario.

### 5.3.1 Interference Cancellation

To limit the interference in IDCA-MAC protocol, Zig-Zag decoding can be used for a limited number of antennas. However, increasing the number of antennas leads to data collisions. Thus, in HAN a limited number of antennas, such as those used in mobile phones and laptops are used. The Zig-Zag decoding is also considered to achieve reconstruction of Zig-Zag coded data which is explained next.

### 5.3.2 Zig-Zag Decoding

The 802.11 networks suffer from collisions and hidden node problems. CSMA can be used to mitigate these problems to some extent. In [60] [61] [62], a modified systems are suggested to overcome the problems of 802.11 networks. For example, in [60] and [62] limited number of antennas are used with CSMA to avoid collisions. In, [61] the level of interference is reduced by using a polling scheme. These enhancements; however, reduce the overall throughput and relieve from saturation.

Zig-Zag decoding is needed to detect multiple users through hidden terminals in wireless networks. In [64], Rahman has discussed many collision scenarios and how Zig-Zag decoding can be used to resolve collision problems. The Zig-Zag decoding works well when two EDs are sending data simultaneously to MC over the same channel resource as shown in Fig. 5.2.

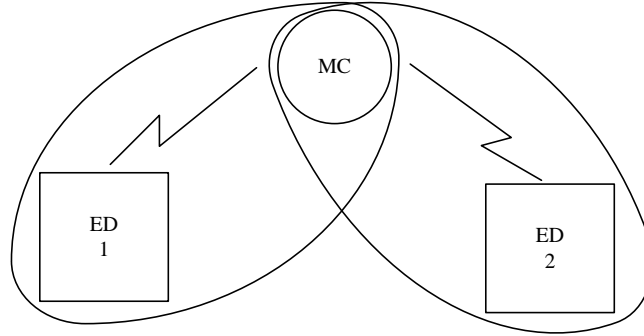


Figure 5.2: Collision scenario of transmitting more than one packet over the channel.

As shown in Fig. 5.2, data collision takes place when two EDs transmit simultaneously and therefore interference cancellation using Zig-Zag decoding can be used. The technique decodes the packets at MC assuming that there is no data collision. However, if it fails, the decoding will check if the packets are experiencing collisions. If so, MC will request retransmissions from EDs if again a collision is experienced, the MC will request transmissions with necessary preamble. As shown in Fig. 5.2, the four packets received from two transmissions have different offsets. It is impossible to have two transmissions exactly at  $t = 0$ . Therefore, Zig-Zag decoding will then decode chunk 1 in packet 1 in the collision 1 so that there is no collision. Then, it will subtract chunk 1 from collision 2 received via a second antenna to decode chunk 2 in packet 2. Meanwhile, Zig-Zag decoding will subtract from the first collision to detect chunk 3 from packet 1, and so on.

Because it is impossible to have exactly matching transmission packets, there is always an offset or a phase difference between them, expressed as:  $\delta f$ . The frequency offset causes a linear displacement in the phase of the received signal that increases over time. The ZigZag correlation technique is used to detect collisions of the known preamble at MC. When collisions are recognized, the MC will compute the correlation

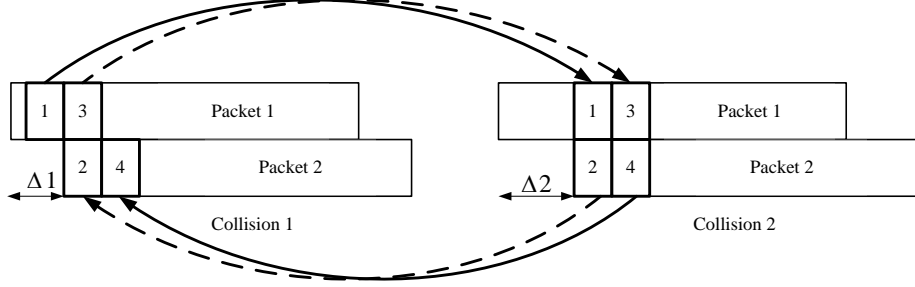


Figure 5.3: Two transmitted packets with collision.

Table 5.3: ICDA-MAC protocol parameters used in the simulation [62]

Parameter	Value
SIFS	$10 \mu s$
SlotTime( $\phi$ )	$20 \mu s$
DIFS	$n \times (SIFS + 2SlotTime)$
Data Frag2 PHY header	72 bits
WSP Partial	$194 \mu s$
WSP	$250 \mu s$
RTS	$n \times 56$ bytes
CTS	$n \times 50$ bytes
Propagation Delay	$6 \mu s$
Data Rate	2Mbps
Minimum Contention Window ( $W$ )	32
Maximum Contention Window ( $W$ )	1024
EIFS	SIFS+CTS+DIFS
Data ( $L$ )	$\varepsilon\{512, 1024\}$

between received samples, shifts and re-computes correlation until the end of the packet. Thus, to detect the collision, the receiver side will compensate for the current offset of ED and itself.

### 5.3.3 Simulation Results and Analysis

The parameters used for simulation are shown in Table 5.3 and these have been chosen to increase the efficacy of data rate. The packets are divided and each portion is sent independently to the MC. This technique is similar to MPR, discussed in [61]. MPR has two senders and each directs its signal to one receiver at MC.

A simulation of the system using IDCA-MAC protocol has been developed using the NS-2 networking platform, and the results are described in the following sections.

The total throughput of the system compared to the payload size is given by:

$$\text{Total Throughput} = \frac{L}{T_s} \text{bps} \quad (5.2)$$

where,  $T_s$  is the time of a successful transmission,  $L$  is the payload size. The time of maximum throughput is given by:

$$T_{\text{sth}} = \bar{W} \times \sigma + T_{\text{DIFS}} + T_{\text{RTS}} + 2T_{\text{SIFS}} + T_{\text{M-CTS}} + T_{\text{HDR}} + T_{ps} + T_{\text{ACK}}, \quad (5.3)$$

where,  $T_{\text{sth}}$  is the time of maximum throughput,  $\bar{W}$  is the average backoff value,  $\sigma$  is the slot time,  $T_{ps}$  is the time of partial sensing,  $T_{\text{ACK}}$  is the time of Acknowledgement, and  $T_{\text{HDR}}$  is the time of a header containing both physical and MAC address.

### 5.3.4 IDCA-MAC Protocol Operation

The IDCA-MAC protocol is designed to allow simultaneous transmissions to take place within a single collision domain. Based on previous discussions, Algorithm 1 provides details for implementing the protocol operation for smart grids. In Algorithm 1, an initialization of EDs is performed to prepare them for simultaneous transmission. The MC adjusts antenna weights when it receives an RTS embedded with antenna weights, to avoid interference. The MC will reply with CTS to ED that requested for transmission using the steps 17-19. It shows also the MAC decision steps (21-26) required throughput when a collision occurs. Finally, when a collision occurs, Zig-Zag decoding is used using steps 27-33.

These algorithms are evaluated in the following scenarios. Let A, B, C, and E are the EDs in the network, and D is the MC. In the first scenario, depicted in Fig. 5.4, the time for completing full transmission in the primary connection is more than that for the secondary transmission. When ED C sends the RTS to the channel, if the condition time is accepted, MC D will update the weight of the reception and will apply it within CTS. This procedure will notify the other nodes to update their NAVs.

In the scenario shown in Fig. 5.5, the transmission has started but the secondary connection has determined that the primary station activity will end soon. In this case,

---

**Algorithm 1** RECEIVE<sub>RTS</sub> (Beamforming) (channel)

---

**Require:** If the aimed MC receives RTS request

```
1: IF channel is idle THEN
2:   IF MC is the destination THEN
3:     Design Weights for best SNR;
4:     Send CTS;
5:   ELSE
6:     Design Weights to NULL transmission
7:     Store Transmission Duration in NAV1;
8:   ELSE
9:     IF station is the destination THEN
10:      Send CTS (designed with Antennas weights to not interfere);
11:    ELSE
12:      Store the Weights of Antennas;
13:      Store the Durations in NAV2;
14:      SET the General NAV to min (NAV1,NAV2);
15:      FREEZE backoff counter;
16:    END if
```

**Require:** Backoff MC if reached zero

```
17: IF channel is idle THEN
18:   Send CTS (designed with Antennas weights);
19: ELSE
20:   MAC DECISION (NAV1 expire time);
```

**Require:** Collision will occur

```
21: ELSE IF
22:   RTS/CTS exchange: SET NAV to NAV1
23:   Increment contention window;
24:   Send RTS has (Offset and phase tracking for chunk (1));
25: ELSE
26:   Send RTS (designed with antennas weights to not interfere);
```

**Require:** If first transmission line is considered as a primary transmission

```
27: Listen to Channel for WSPpartial time;
28: IF RTS received THEN
29:   Listen for received chunk1;
30:   Store Antenna and channel information;
31:   Store Transmission Duration in NAV1;
32: END IF
33: END IF
34: Defer DIFS;
35: Backoff stage starts decrementing its counter;
```

---



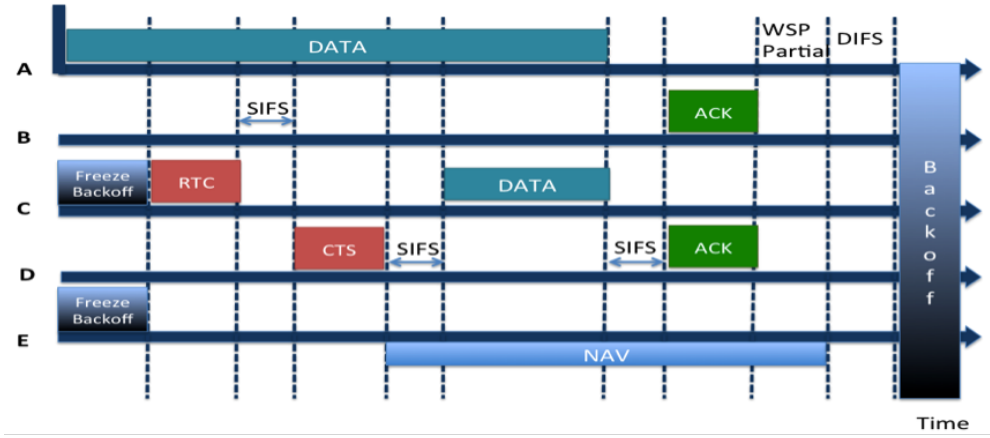


Figure 5.4: Timing diagram of MAC decision process when secondary transmission time is less than the primary [62].

new parameters will be introduced. This step is called Partial Weight Sensing (PWS). This parameter is used to identify any ongoing transmission. Therefore, it will refer to the ACK packet until the transmission is complete, and then it will notify all of the stations to update their NAVs so that their primary connections will be extended, along with the new  $ACK_{Defer}$  time.

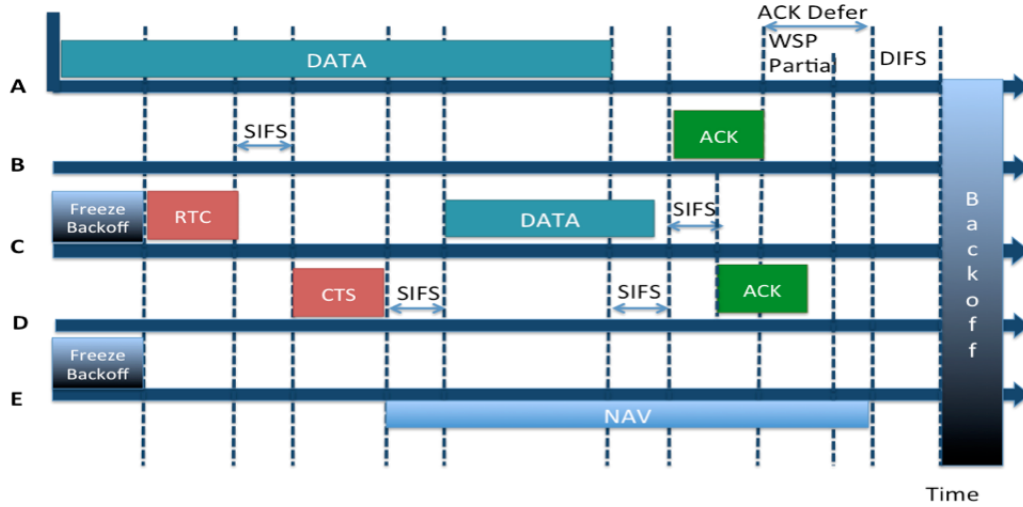


Figure 5.5: Timing diagram of MAC decision process for the case of partial weight sensing [62].

Splitting the secondary data packet and using new handshaking is shown in Fig. 5.6. This behaviour takes place when the primary transmission has been completed but the MC is not aware of other ongoing transmission, since the nodes do not sense secondary transmission. Partial Sensing ( $SP_{src}$ ) contains the antenna weights, the transmission du-

ration, and the pilot symbols for the next estimate of channel. After calculating the propagation delay, D will respond with a  $SP_{dst}$  that contains the same information as the  $SP_{src}$  except for the transmission duration, as shown in Fig. 5.7. After proceeding with the transmission and attaching the necessary short PHY header, the secondary transmission will be converted to primary. The worst-case scenario is when the handshaking process is insufficient. This happens when the request does not take place until the primary connection is complete. This situation is illustrated in Fig. 5.7.

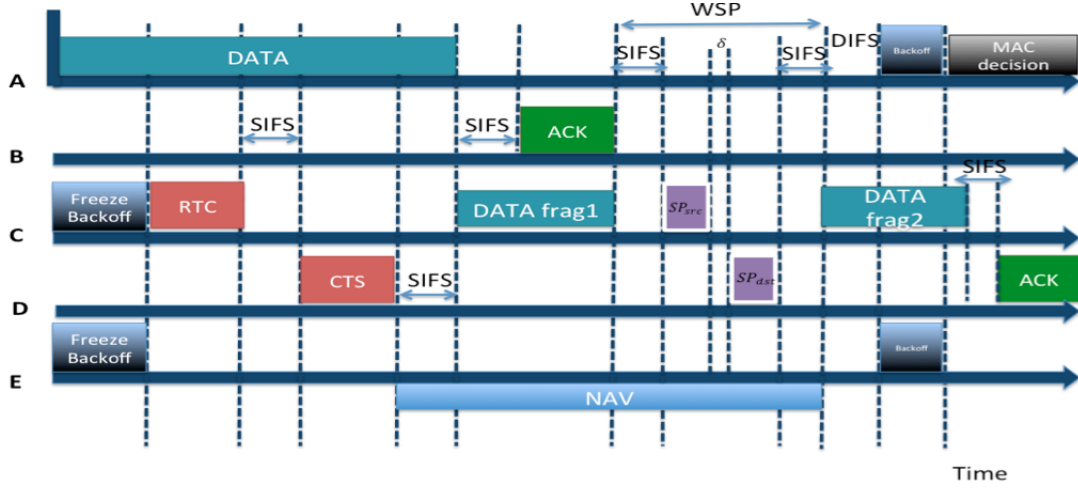


Figure 5.6: Timing diagram of MAC decision process for the case of splitting data through transmission [62].

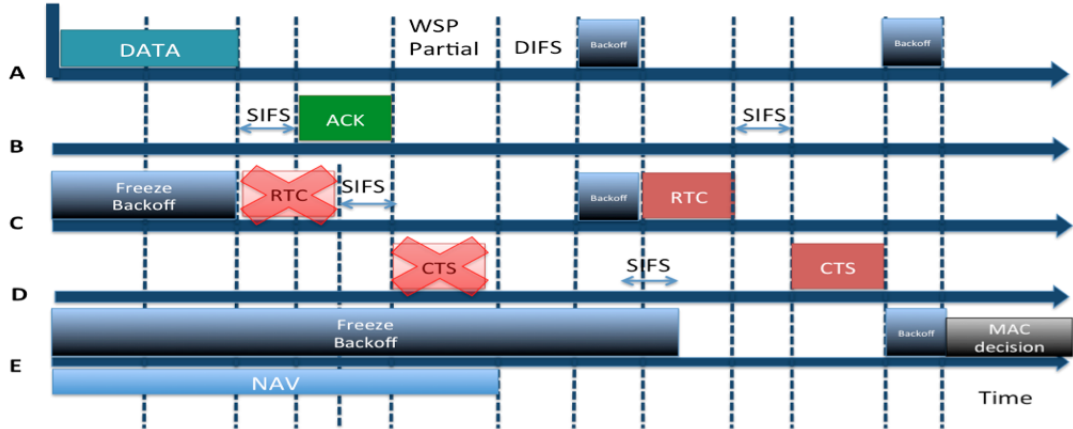


Figure 5.7: Timing diagram of MAC decision process for the case of collision [62].

## 5.4 Overall Evaluation

In order to evaluate the performance of the overall system with IDCA-MAC and MA-Aware protocols, various scenarios were created so that all stations in both systems send fixed-size packets that have maximum data rate.

The stations are assumed to be located within the transmitting range. The maximum number of stations is set to be 50. Fig. 5.8 shows the throughput performance for this system and it can be observed that for number of stations less than 50, a reduction in throughput is observed due to wasted idle channels. Also, it can be seen that the IDCA-MAC shows a 29% improvement in throughput compared to MA-Aware protocol. Approximately 2.1 bits per second (bps) improvement in throughput performance is observed for number of EDs greater than 20. Nevertheless, while IDCA-MAC provides a higher throughput compared to MA-Aware protocol, it introduces an additional delay. This delay is introduced by the Zig-Zag decoding.

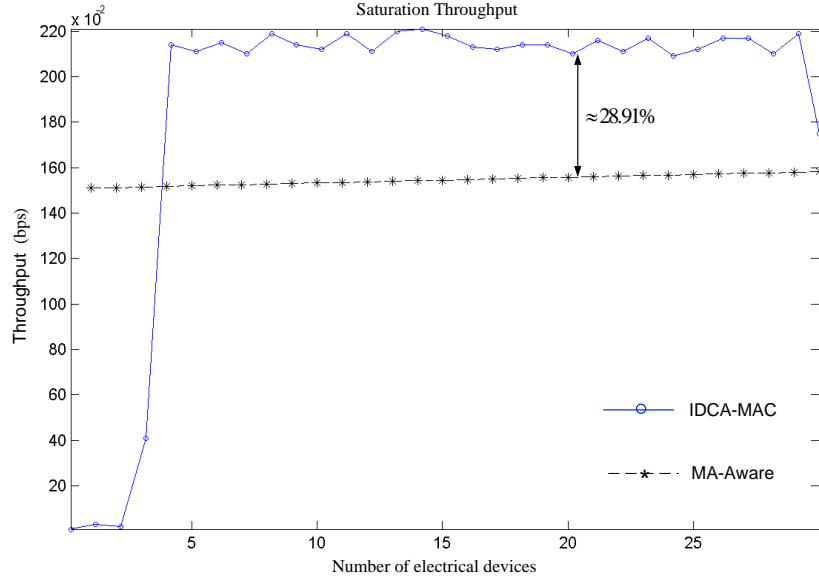


Figure 5.8: Throughput of the system as a function of number of electrical devices [62].

Fig. 5.9 shows that IDCA-MAC introduces an additional 2 ms delay as compared to MA-Aware protocol. The proposed IDCA-MAC method introduces more delay because of the reconstruction collision technique using Zig-Zag decoding. Furthermore, IDCA-MAC provides a higher data transmission rate as shown in Fig. 5.9.

Fig. 5.10 shows that best throughput for IDCA-MAC is achieved when the window

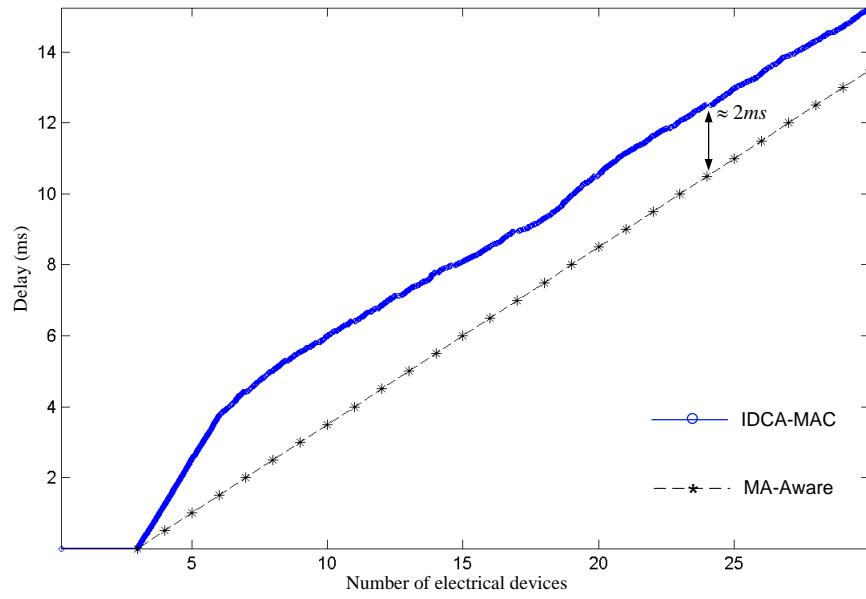


Figure 5.9: Critical packet delay of the system using IDCA-MAC protocol as a function of number of electrical devices [62].

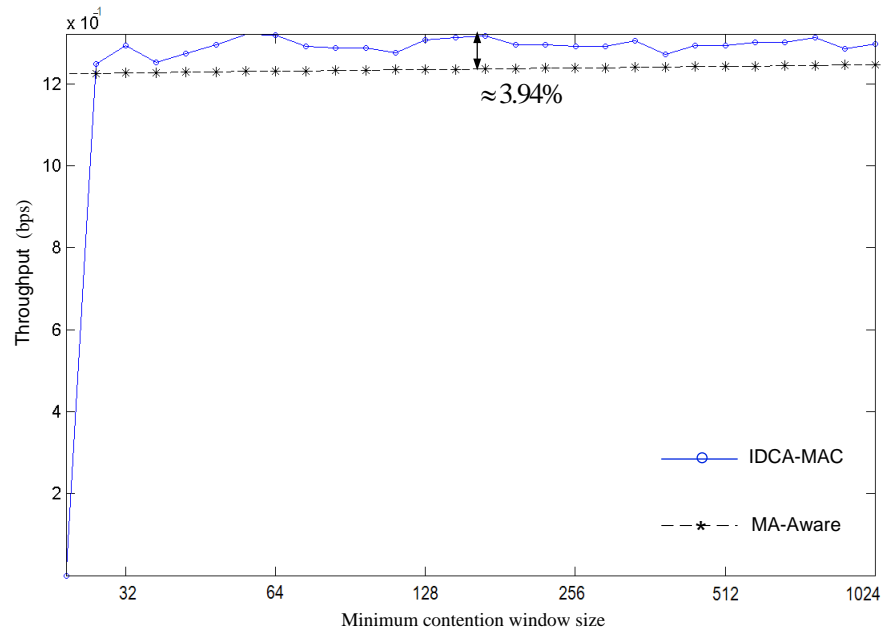


Figure 5.10: Throughput of the system as a function of CW size [62].

size is set to 64. There is approximately a 4% enhancement in throughput with IDCA-MAC compared to MA-Aware protocol, necessary to avoid collisions.

## 5.5 Summary and Conclusions

In this chapter, an IDCA-MAC protocol for wireless HAN using Distributed Coordination Function (DCF) is presented. The protocol eliminates collision and employs MIMO system to enhance system performance. Simulation results show that critical packet delay can be reduced by nearly 20% using MA-Aware protocol compared to IDCA-MAC protocol; however, the latter offers better throughput.

# Chapter 6

## Modelling and Delay Analysis of NAN <sup>8</sup>

### 6.1 Introduction

As discussed in the previous chapters, EDs generate packets in HAN and are collected by mesh clients. The packets generated are often classified as either periodic or critical. The critical packets received at MCs are required to be transported to identified gateway nodes with minimal delay. The gateway nodes in NAN serve as interface points to WAN. In this chapter, a wireless mesh network is deployed for NAN and it serves as the distribution layer that receives data from HAN and forwards it to the upper core layer. In the mesh backbone subnetwork, each mesh router will have one or more mesh clients that are connected directly by a wireline. The mesh routers are wirelessly interconnected and the main objective is to move the packet from router to router until it reaches identified gateway.

#### 6.1.1 Background

Researchers have investigated performance of wireless mesh networks for various types of network traffic and routing. For instance, Bisnik et al [67] have examined delay and capacity of a wireless mesh network with the objective of maintaining capacity for a G/G/1 network. Cost minimization is considered in [68], where authors have developed a routing metric to achieve minimum delay as a function of level of interference. Jiazhen

---

8. A. Noorwali, R. Rao and A. Shami, "End-to-End delay Analysis of Wireless Mesh Backbone Network in a Smart Grid," Proceedings of 2016 IEEE Canadian Conference on Electrical and Computer Engineering (CCECE), Vancouver, BC, pp. 1-6, May 2016.

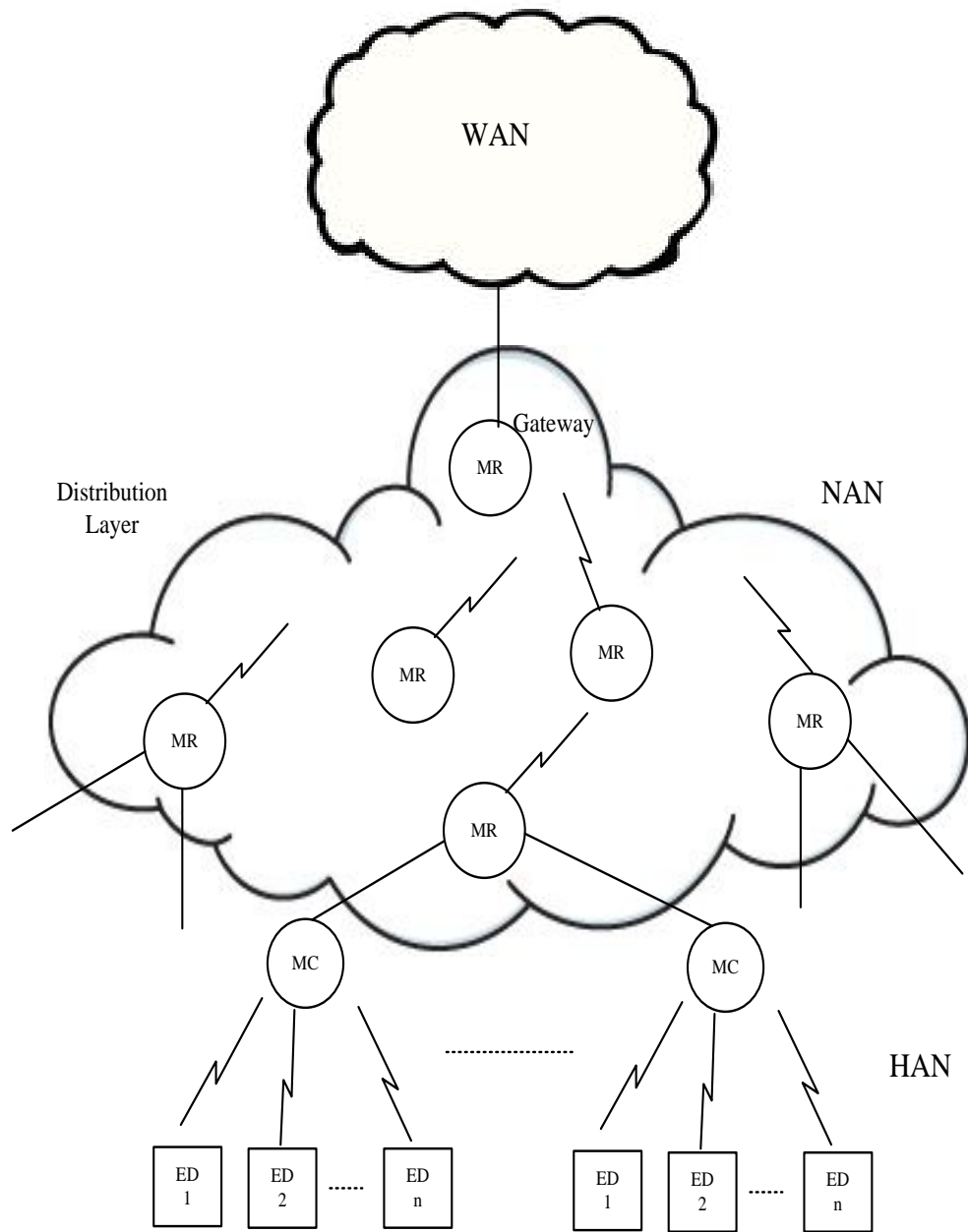


Figure 6.1: Structure and location of NAN in smart grid.

et al in [69] have considered scalability in the modeling of wireless mesh networks by taking into account multi-path effects to optimize large-scale deployment. In [70] a wireless mesh network is considered to evaluate routing overhead as a function of delay. Stanislav et al in [71] studied hidden paths and developed a mechanism to discover as many hidden paths in wireless network as possible by maintaining delay. In [72] more than one channel is considered between a pair of nodes in wireless mesh network in order to reduce delay. Bipul et al [73] have employed cooperative retransmission in wireless mesh networks to reduce delay by taking into account only queuing and backoff delays. Delay sensitive traffic is studied in [74] for an IEEE 802.11 mesh network. Assigning multiple channels to maintain delays in a wireless mesh network is examined in [75]. Xiaobing et al [76] studied the trade off between cost and scalability of wireless networks. All these can be employed for designing an efficient smart grid. Nevertheless, applying available networking technologies to smart grid is challenging particularly to meet the delay requirements. Communication architectures employed in smart grids should be able to meet promptness, reliability and security expectations.

To meet the delay requirements, which is the major concern in smart grid, network must be modeled and examined for worst-case time-critical behaviour [77]. In this chapter, a Wireless Mesh Backbone Network (WMBN) is considered for NAN and its structure is shown in Fig.6.2. The Mesh Routers (MRs) are the wireless nodes that provide connectivity. The critical packets received at MR is forwarded over a series of MRs until it reaches an identified gateway node. The analysis of such a WMBN is presented to understand whether the desired goal of critical packet delay can be met in smart grids or not. The  $n$  critical packets collected by each mesh client, with each packet of length  $L$  bits are forwarded to the mesh router in NAN. Mesh routers are assumed to be distributed among Voronoi cells. The links between mesh routers are subject to communication challenges. In this chapter, the transportation delay of critical packets to an identified gateway is addressed. The location of mesh routers in NAN is shown in Fig. 6.2, and is assumed to be well thought out topology. Placing the mesh routers in this way will permit critical packet collection from EDs easily. A realistic example, using Voronoi tessellation for location and distribution for MRs is given next.

Voronoi cell partition is a suitable choice, as it has the advantage of identifying the shortest path to gateway. Figure 6.3 illustrates an example of Voronoi diagram showing



irregularly shaped cells, each of which contains a point that denotes the location of the mesh router in the cell. It is noted that both mesh routers and mesh clients are co-located. Because mesh routers are widely distributed over the mesh backbone network, distance information will be considered for routing packets to gateway.

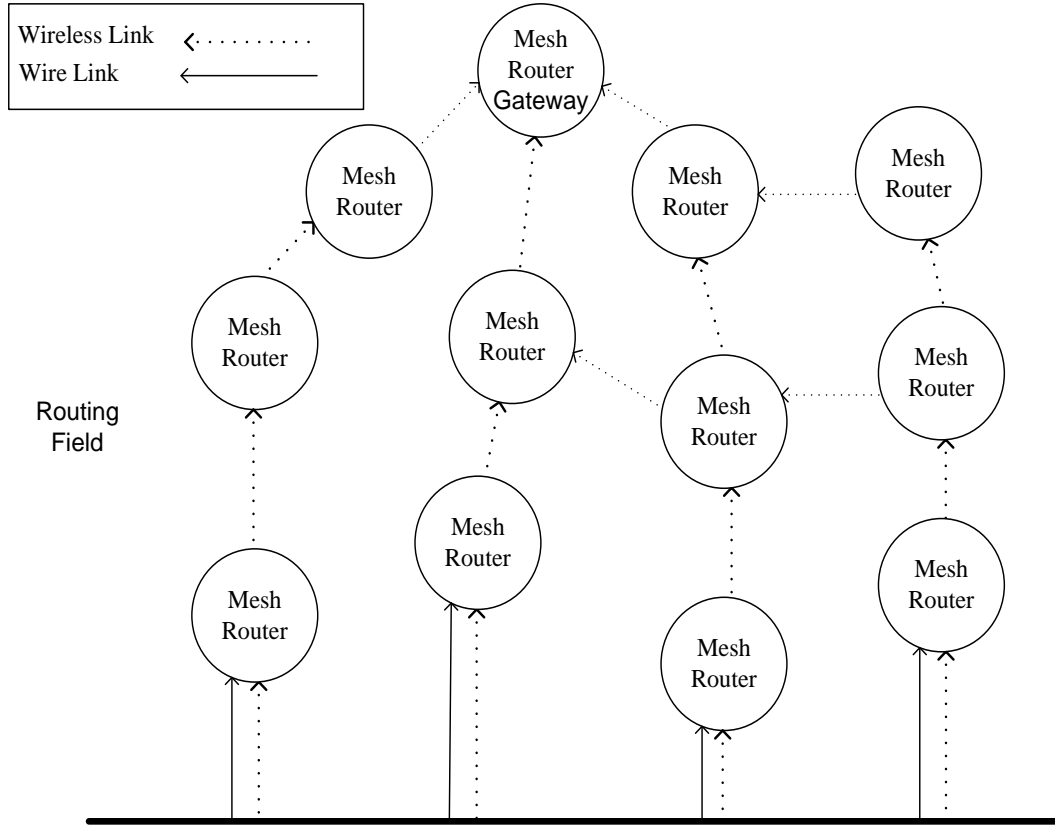


Figure 6.2: Conceptual model of Wireless Mesh Backbone network.

The contributions in this chapter include identifying packets that influence critical packet delay as a function of network architecture, scheduling of traffic, node transmission power, bandwidth of channels, and channel interference. As a first step, a Voronoi tessellation [78] is described for location of MRs, where the distance to the edge of the cell  $d^{(\text{edge})}$  is smaller than the distance to the vertex of the cell  $d^{(\text{vertex})}$ . This is done for selecting the shortest path in the network. A straight-line path is considered for routing in WMBN. The Straight-Line Path Routing (SLPR) Algorithm [79] connects the source MR to the gateway. A conservative communication strategy [48], [49] is developed for forwarding critical packets from MR to gateway using maximal and minimal amount of interference. The lower and upper bounds on the delay are derived first using per-hop

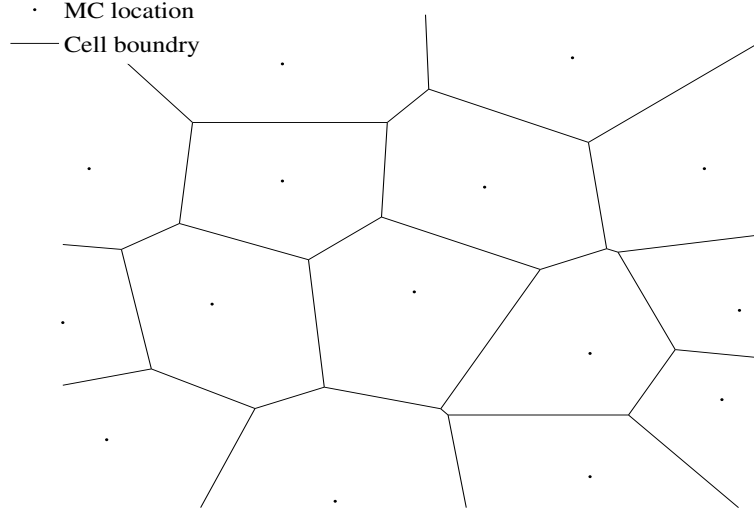


Figure 6.3: Example of Voronoi structure.

basis, and then for multiple hops. Closed-form expressions for bounds for minimal delay between MRs are derived for Distributed Coordination Function (DCF). It is shown that delay is a function of the Signal-to-Noise Ratio  $\gamma$ , signal interference  $I$ , number of channels  $Q_{NAN}$ , channel interference range  $CIR$ , path loss  $\varphi$ , and power of node transmission  $P_t$ .

## 6.2 Model of WMBN

A set of MRs is distributed throughout and MRs are connected wirelessly to form WMBN, as shown in Fig. 6.4. MRs are located sufficiently apart to minimize interference, and the spaces between them are according to a Voronoi definition. Each MR in the network is responsible for checking channel availability prior to the transmissions. In WMBN, it is assumed that all MRs transmit at constant power  $P_t$  and the network is assumed to be IEEE 802.11. The shadowing effect is neglected as the MRs are not randomly located in the Voronoi tessellation.

### 6.2.1 Voronoi Tessellation Definition

The Voronoi tessellation diagram shown in Fig. 6.4 consists of a set of cells. Each irregular cell consists of one MR. Hence, two measurements for the location of an MR in each cell can be identified using: i) the edge; and ii) vertex of the cell. Thus, the location distribution for each MR in the plane can be used for selecting the shortest path between any pair of MRs. The distance to the edge of the cell and the distance to the vertex of the cell are denoted as  $d^{(\text{edge})}$ , and  $d^{(\text{vertex})}$ , respectively. Corresponding to these distances, the distance from each MR to the edge of cell is planned to be minimum and the distance to the vertex of the cell is planned to be maximum. Therefore, the minimum distance between two MRs cannot be smaller than  $2d^{(\text{edge})}$ , and the maximum distance between two MRs cannot be more than  $2d^{(\text{vertex})}$ .

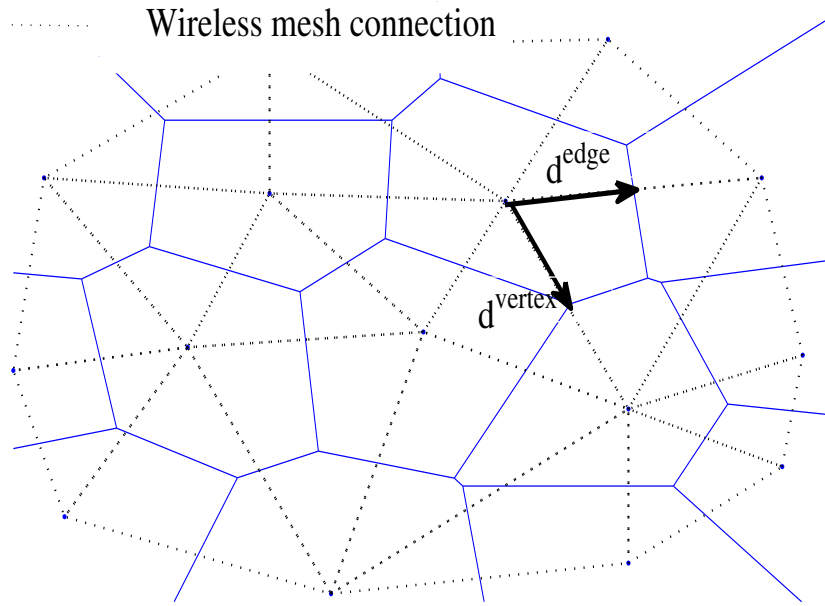


Figure 6.4: Wireless mesh backbone network in the Voronoi diagram.

### 6.2.2 Inter-Channel Interference Model

In the modelling of WMBN, environmental noise, interference  $I$ , and Inter-Channel-Interference Range (ICR) are considered. The IEEE 802.11 networks have overlapping

radio spectrum, and there exist a limited number of channels that do not overlap. Thus,  $I_{(u,i,j)}$  refers to the interference caused by simultaneous transmission  $j$  on channel  $i$  at node  $u$ , as given by:

$$I_{(u,i,j)} = \rho P_{t,(u,j)} \quad (6.1)$$

where  $\rho = \frac{\max(CIR-|d|,0)}{CIR}$  is the interference threshold,  $d$  is the distance between two active channels ( $i - j$ ),  $CIR$  is the channel interference range, and  $P_{t,(u,j)}$  is the signal strength received from node  $u$  on channel  $j$ .

### 6.2.3 Wireless Interference

As the packet moves away from an MR, as shown in Fig. 6.5, interferences from other MRs in the plane are affected. To represent the maximum number of MRs that are affected by the current transmission, the WMBN is divided into a ring area as shown in Fig.6.6. Using the Voronoi definition, for the best communication case, the minimum distance between two MRs is set for the case of interference at minimal level. Therefore the radius in each ring cannot exceed  $2d^{(\text{edge})}$ , where there is no interference. Each Voronoi cell is assumed to covers an area equal to  $\pi(d^{(\text{edge})})^2$ . Hence, the difference between two arbitrary rings gives the number of MRs as:

$$\pi(2(k-1)d^{(\text{edge})})^2 - \pi(2kd^{(\text{edge})})^2 = 4\pi(2k-1)(d^{(\text{edge})})^2$$

And:

$$X(k) = 4(2k-1), \quad (6.2)$$

where  $k$  is the number of the ring. Once  $X$  is known, an upper bound on the amount of interference,  $I$ , can be derived.

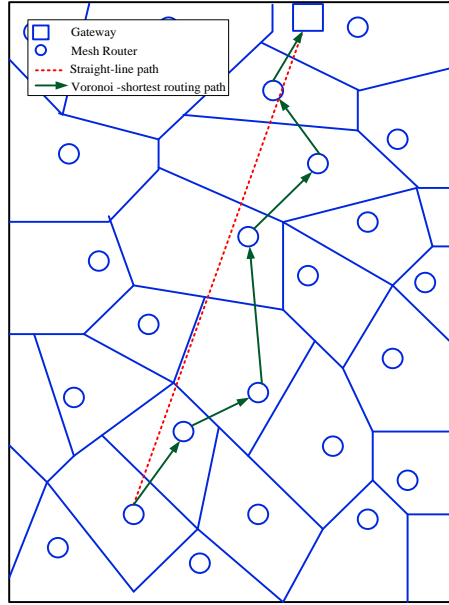


Figure 6.5: Straight-line path in Voronoi diagram.

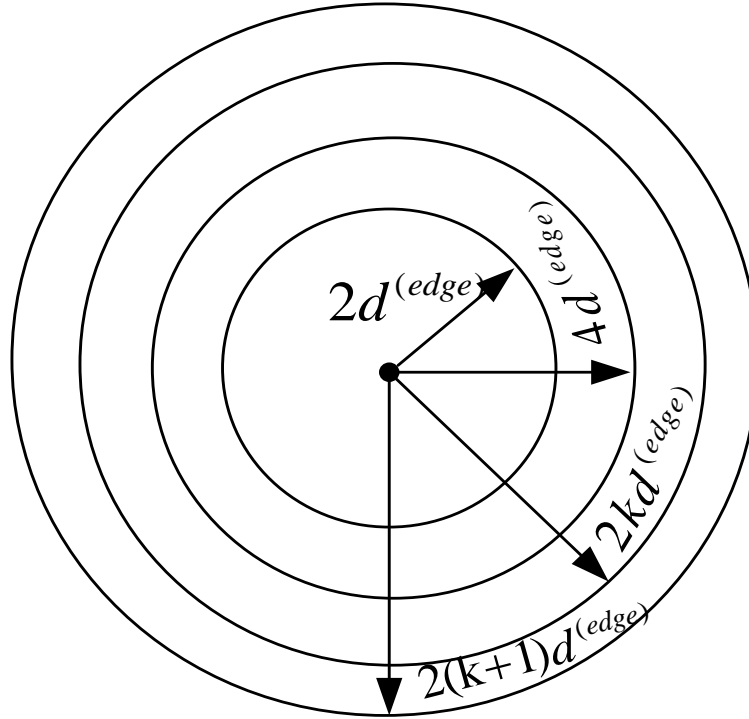


Figure 6.6: Division of ring area for WMBN.

The received signal strength from each MR is given by:

$$P_r = P_t \left( \frac{2d^{(\text{edge})}}{r^{(\text{ref})}} \right)^{-\varphi}. \quad (6.3)$$

where  $r^{(\text{ref})}$  is the reference unit distance in which the transmitted power is no loss, and  $\varphi > 2$  is the path-loss exponent. Consequently, the total interference in the WMBN can be determined by substituting (6.2), and (6.3) in the summation  $\sum_{k=1}^{\infty} P_r Q(k)$ , and is given by:

$$I = \frac{4P_r(3\varphi^2 - 6\varphi + 2)}{\left( \frac{2d^{(\text{edge})}}{r^{(\text{ref})}} \right)^{-\varphi} (\varphi^2 - 3\varphi + 2)}. \quad (6.4)$$

### 6.2.4 Scheduling Transmissions

Unlike in a HAN [48, 49], the DCF mode is preferred in NAN because there is no need for an access point to manage transmissions between the MRs. Hence, each MR senses the channel using the Carrier Sense Multiple Access with Collision-Avoidance (CSMA/CA) protocol to determine channel availability. However, this process leads to unwanted delay because if this assigned single channel is busy, the MR will remain silent for an exponential random period of time called backoff time [80], which will affect the quickness of the decision required. Therefore, a modified DCF protocol is used to maximize the network transmission capacity. After this, the delay associated with the proposed conservative communication strategy is compared by using CSMA/CA with Code Division Multiple Access (CDMA) protocol. Each MR is responsible for scheduling transmissions using modified CSMA/CA or CDMA protocol. It is assumed that all  $n$  critical packets are generated at  $t = 0$ , and the arrival time depends on the channel access protocol used.

#### 6.2.4.1 Parallel Transmission in CSMA/CA

Each MR in NAN listens and senses the channel for a short, random period of time in order to announce simultaneous transmission. It collects channel occupancy information from the previous announcements from other MRs to determine which channel can be used for the next transmission without collision with existing transmissions. Once MR

has successfully determined number of the channels (as shown in Fig. 6.7) to be used for an interval of time  $\tau$ , the rest of the MRs will wait for the next interval of time  $\tau$ . Note that, in WMBN there is no hidden terminal problem because all MRs have been located strategically. The number of simultaneous transmissions must not exceed the Channel Interference Range ( $CIR$ ). The MR, therefore, locates channel  $i$  in the middle of the block of channels, and places additional channels from both sides. It will start allocation from the low points of the two side boundaries for simultaneous transmission, such as  $i - (CIR - 1)$ ,  $i + (CIR - 1)$ , and so on, until the threshold of interference on channel  $i$  is reached. The interference at MR can be calculated using (6.4) and is given by:

$$I_{th} = \frac{P_r}{\beta} - N_o. \quad (6.5)$$

where  $\beta$  is the threshold of  $\gamma$ , the signal to noise ratio, and  $N_o$  is the receiver noise. The maximum number of scheduled channels in the block of channels represents the lower delay scenario and cannot exceed  $(2CIR - 1)$ ; thus, the maximum number of channels is given by:

$$Z_{CSMA/CA}^l = \left\lceil \frac{Q_{NAN}}{2CIR - 1} \right\rceil. \quad (6.6)$$

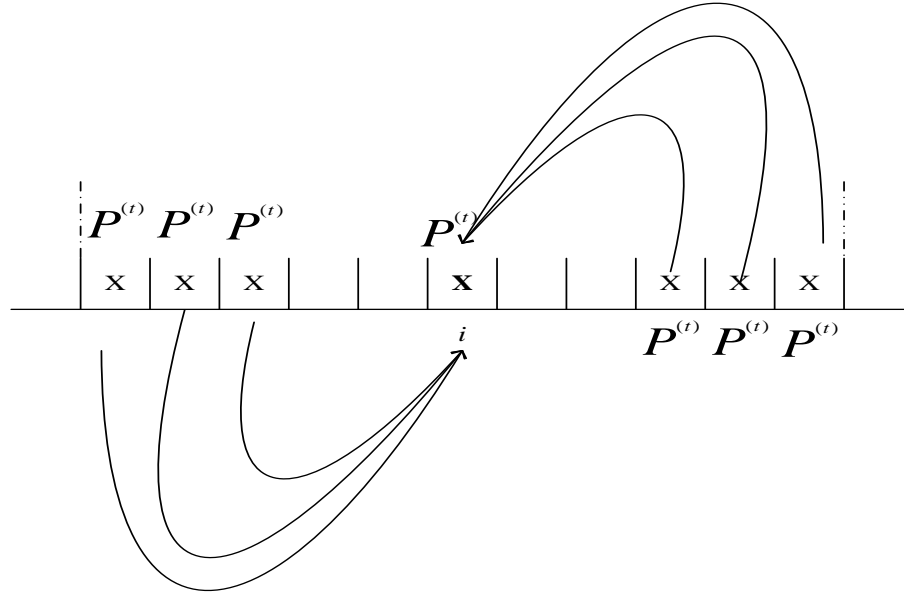


Figure 6.7: Channel block showing interference from each active channel.

On the other hand, in an overlapping situation, the deferral of transmissions occurs

with extra channels. Thus, the modified CSMA/CA is used to locate additional channels such that they do not interfere with other transmissions in the network. Using (6.5), the spectrum distance between two channels must be at least  $CIR\left(\frac{\beta-1}{\beta}\right)$ . Therefore, the maximum number of channels can be shown to be given by:

$$Z_{\text{CSMA/CA}}^u = \left\lceil \frac{Q_{NAN}}{CIR\left(\frac{\beta-1}{\beta}\right)} \right\rceil \quad (6.7)$$

To validate this enhancement, the delay in transmitting of different numbers of packets is compared between two hops. As shown in Fig. 6.8, the modified CSMA/CA provides better delay performance than the regular CSMA, for the worst case scenario of limited number of channels. Modified CSMA/CA protocol can transmit 1 to 40 packets to the next hop in 14  $\mu\text{s}$  in the worst case, while using regular CSMA/CA it takes 40  $\mu\text{s}$ . In the next step, a re-defined CDMA scheme for a fair comparison is proposed.

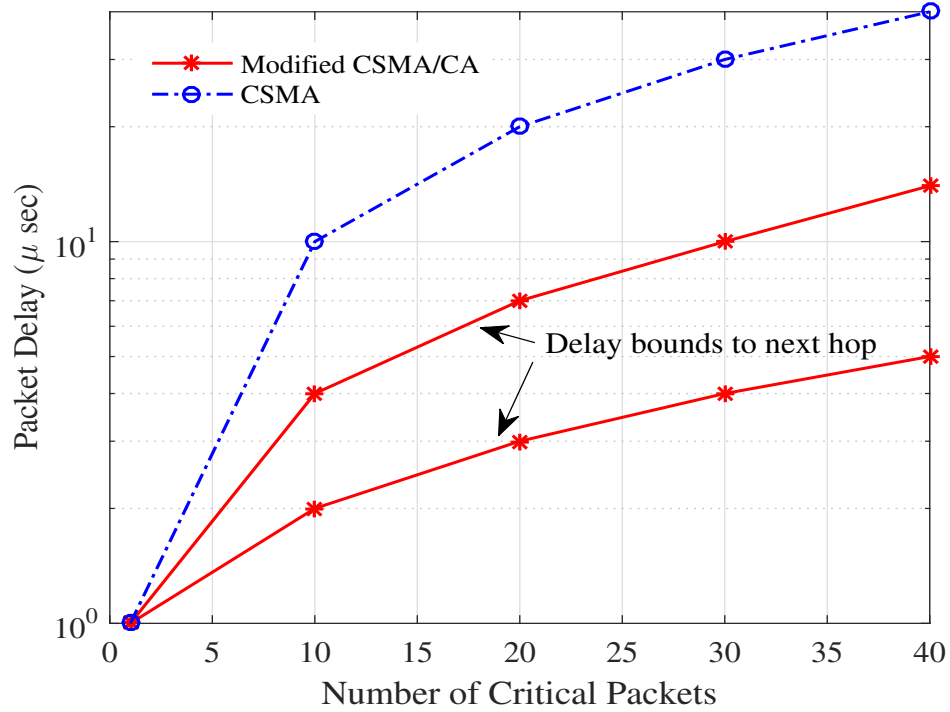


Figure 6.8: Packet delay bounds as a function of number of critical packets.



### 6.2.4.2 CDMA Scheme

In CDMA, the signal is spread over a wider frequency band, as shown in Fig. 6.9 and the technique widely used in a variety of wireless networks. In CDMA, Multi User Detection (MUD) technique is used as the protocol allows several transmitters to send information simultaneously over the same bandwidth.

Each newly scheduled channel in a given block as shown in Fig.6.7 is denoted as  $s$ . The channel allocations will cause the  $CIR$  to decrease which increases the chance of interference. The aggregate interference can be written as:

$$\sum_{s=1}^S \frac{s}{CIR} \quad (6.8)$$

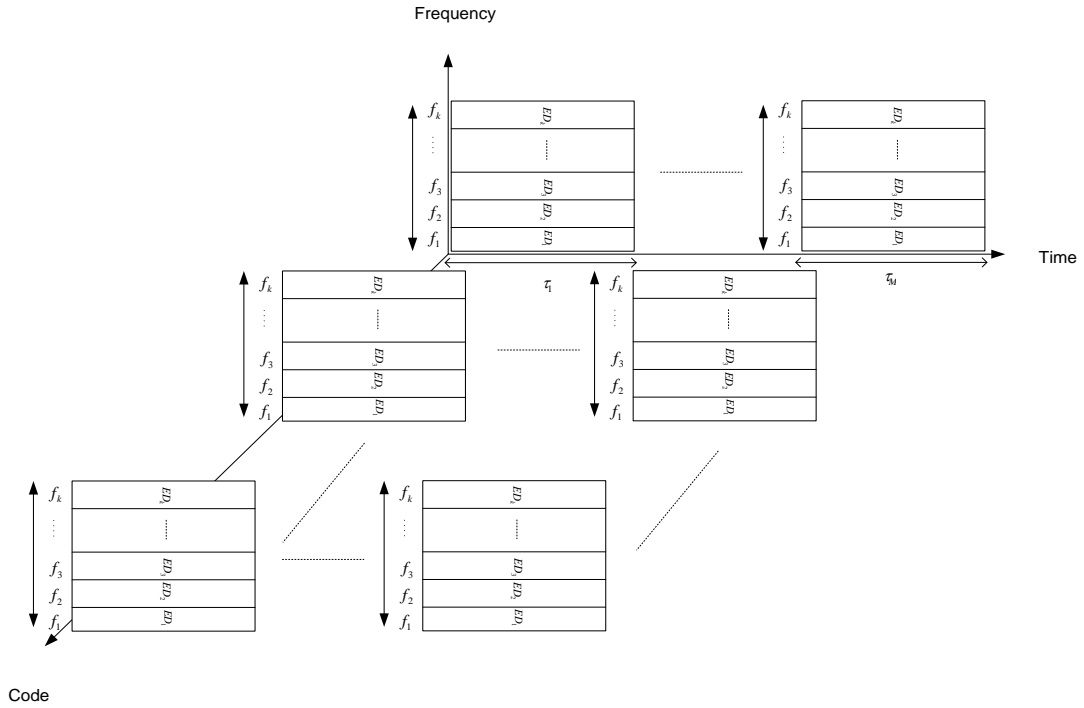


Figure 6.9: CDMA: Time, frequency and code slots.

For instance, the interference will increase or decrease by  $\frac{s}{CIR}$  as the scheduled channel moves closer to or farther from the currently active channel. Because each MR is transmitting  $P_t$ , which affects the interference,  $I_{th}$ , the ratio of the interference  $I_{(th)}$

to the received signal strength  $P_r$  is equal to the sum of the quantity  $\frac{s}{CIR}$  from both sides of the block. Once this relationship is known, number of scheduled channels  $S$  in the block can be determined from (6.4) and (6.5), and is given by:

$$\sum_{s=1}^S \frac{s}{CIR} = \frac{I_{th}}{P_r}. \quad (6.9)$$

$$S = \sqrt{CIR \left( \frac{1}{\beta} - \frac{N}{P_r} + \frac{1}{4} \right)} - \frac{1}{2}. \quad (6.10)$$

The maximum number of scheduled channels in a block cannot exceed  $2S + 1$ . Therefore, based on this necessity and using (6.9), the maximum number of simultaneous transmissions within any channel block of a size of  $2CIR - 1$  can be written as:

$$\frac{2K + 1}{2CIR - 1}. \quad (6.11)$$

To generalize the results for the case of total number of channels  $Q_{HAN}$ , the maximum number of channels  $S$  for simultaneous transmission can be written as:

$$Z_{CDMA}^l = \left\lceil \frac{2S + 1}{2CIR - 1} Q_{HAN} \right\rceil. \quad (6.12)$$

It is noted that the minimum distance  $d$  between two active channels required for scheduling maximum number of simultaneous transmissions can be determined using (6.4) and (6.5) as follows:

$$\frac{2(CIR - |d|)}{CIR} = \frac{1}{\beta} - \frac{N_o}{P_r}. \quad (6.13)$$

That is:

$$d = CIR \left( 1 - \frac{1}{2} \left( \frac{1}{\beta} - \frac{N_o}{P_r} \right) \right). \quad (6.14)$$

Thus, total number of simultaneous transmissions scheduled by MR is given by:

$$Z_{CDMA}^u = \left\lceil \frac{Q_{HAN}}{d} \right\rceil. \quad (6.15)$$

Thus, CDMA allows for twice the amount of simultaneous transmissions of critical packets by using coding theory in transmission time. CDMA divides the available bandwidth into sub-channels depending on the given spreading factor. This division enables the time of

transmission to overlap and thin out the set of interfering transmitters. CDMA allows packets to be transmitted to the available channels, but only extracts the desired signal; the rest is considered noise.

### 6.2.5 Straight-Line Path Routing (SLPR) Algorithm

SLPR [79] is defined as a straight-line path that cuts a sequence of nodes between a source and a destination, as shown in Fig. 6.5 and the path is hop-by-hop type. Each MR maintains the distance values to the next hop recorded the distance  $r$  in the direction of destination or gateway node. If an MR has a choice of two next nodes that have identical distance metric, either can be arbitrarily selected. To prevent backward-direction routing, each MR records the list of visited and then chooses a neighbour node with minimum distance that has not yet received the packet. To transport the packet in WMBN from source to destination, the minimum and the maximum numbers of hops are required to be derived.

#### 6.2.5.1 Number of Hops between Source and Destination

Once the distance between source to the identified and destination (gateway) is determined to be equal to  $r$ , the packet can be forwarded gateway hop-by-hop. The minimum number of hops between source and destination can be shown to be given by:

$$h^l = \frac{r}{2d^{(\text{vertex})}}, \quad (6.16)$$

where  $2d^{(\text{vertex})}$  is the metric associated with the Voronoi cell in which source MR is located and  $r$  is the distance between source MR and the gateway MR.

In the worst case, a packet moves to gateway within the rectangular area in a straight-line path. Moreover, each MR covers an area equal to  $\pi(d^{(\text{edge})})^2$  as shown in Figs. 6.4, and 6.5. Therefore, from every MR (vertically and horizontally), the maximum distance to the next hop is equal to  $2 \times 2d^{(\text{vertex})} = 4d^{(\text{vertex})}$  which represents the rectangular width. The length of the rectangular can be determined by the knowledge of distance  $r$  from source MR to the gateway and is equal to  $r$  plus  $4d^{(\text{vertex})}$ . Consequently,

the maximum number of hops between source MR to destination MR is given by:

$$h^u = \frac{(4d^{(\text{vertex})})(r + 4d^{(\text{vertex})})}{\pi(d^{(\text{edge})})^2}. \quad (6.17)$$

## 6.3 Delay Analysis

The overall delay in transporting  $n$  packets from the source MR to gateway MR can be determined using the knowledge of number of hops in the path and is given by:

$$\Delta_{\text{end-to-end}} = h \frac{n}{Z} \tau. \quad (6.18)$$

where  $h$  is the number of hops,  $n$  is the number of packets,  $Z$  is the number of available channels, and  $\tau$  is the time required to complete one successful transmission.

Using Shannon's relation formula [55], the channel capacity is given by:

$$R = W \log_2(1 + \gamma) \text{ (bits/s)}. \quad (6.19)$$

where  $W$  is bandwidth and  $\gamma$  is the signal-to-noise ratio. Using the knowledge of  $R$ , the time required to transmit each packet is given by:

$$\tau = \frac{L}{R} \text{ sec.} \quad (6.20)$$

where  $L$  is the size of the packet in bits. The expressions for bounds on delay by examining the maximum number of transmissions. The total number of simultaneous transmissions cannot exceed the channel interference range  $CIR$  and each side of the block of channels is limited by  $(CIR - 1)$ . Thus, there are  $2^{(2CIR-1)}$  possible patterns for assigning channel transmissions. MR can employ either CSMA/CA, or CDMA protocol to schedule transmission to the next hop.

### 6.3.1 Parallel Transmission in CSMA/CA

Unlike in conventional access point using IEEE 802.11 technology, in which only one channel is assigned to all users [80], the proposed scheme would allocate the maximum

number of available channels to schedule wireless transmissions simultaneously, accommodating one packet per channel.

### 6.3.1.1 Lower Bound on Delay

A lower bound on delay for the case of parallel transmission using CSMA/CA protocol can be obtained by finding the maximum number of transmissions that can be accommodated with no overlapping condition. The interference from other MRs are excluded in this case, because each MR is transmitting to a closer MR within the ring range of  $2d^{(\text{edge})}$ . Only  $N_o$  is considered in the system. Thus, the lower bound on delay for simultaneous transmissions can be determined by substituting (6.3), (6.12), (6.16), (6.19) and (6.20) into (6.18) and is given by:

$$\Delta_{\text{end-to-end}}^l \geq \lceil h^l \rceil \times \left\lceil \frac{n}{Z_{\text{CSMA/CA}}^l} \right\rceil \times \frac{L}{W \log_2 \left( 1 + \frac{Pr \left( \frac{2d^{(\text{edge})}}{r^{(\text{ref})}} \right)^{-\varphi}}{N_o} \right)}. \quad (6.21)$$

### 6.3.1.2 Upper Bound on Delay

An upper bound on the delay for the case of parallel transmission using CSMA/CA protocol can be determined by considering threshold-separated condition with overlapping channels. In order to find an unassigned channel, the protocol must detect channels that are not overlapped with the current active channel. Based on the relationship between  $\rho$  and  $\beta$ , the distance  $d$  between channels must be at least  $CIR^{\frac{\beta-1}{\beta}}$ . Moreover, the received signal strength must have a maximum distance to the next MR equal to  $2d^{(\text{vertex})}$ , in which channel interference  $I$  occurs. Thus, the upper bound on delay can be found by substituting (6.3), (6.4), (6.7) (6.17), (6.19) and (6.19) into (6.18) and is given by:

$$\Delta_{\text{end-to-end}}^u \leq \lceil h^u \rceil \times \left\lceil \frac{n}{Z_{\text{CSMA/CA}}^u} \right\rceil \times \frac{L}{W \log_2 \left( 1 + \frac{Pr \left( \frac{2d^{(\text{vertex})}}{r^{(\text{ref})}} \right)^{-\varphi}}{N_o + I} \right)}. \quad (6.22)$$

### 6.3.2 Transmission using CDMA Protocol

The CDMA protocol does not require synchronization between the MRs from delay perspective. It is noted that in CDMA, while few packets have been transmitted, the others must wait for some time equal to  $\omega_{CD}$ . This waiting time for an  $M$  slot system is equal to  $\lceil \frac{n}{S^2} \rceil$ . Consequently, the expression for delay is given by:

$$\Delta_{CD} = \tau + \omega_{CD}. \quad (6.23)$$

#### 6.3.2.1 Lower Bound on Delay

In CDMA,  $Z^2$  packets can be assigned to available channels, and the remaining must wait for  $\omega_{CD} = \frac{\tau}{2}(1 - \frac{\tau}{2})$ . Therefore, a lower bound can be determined by substituting, (6.3), (6.12), (6.16), (6.19), (6.20) and (6.23) into (6.18) and is given by:

$$\begin{aligned} \Delta_{\text{end-to-end}}^l &\geq \left\lceil \frac{r}{2d(\text{edge})} \right\rceil \\ &\times \frac{(M+1)(2CIR-1)^2 n}{2M \left( 2Q_{NAN} \sqrt{CIR \left( \frac{1}{\beta} - \frac{N_o}{P_r} \right) + \frac{1}{4} + 2CIR - 1} \right)^2} \\ &\times \frac{L}{W \log_2 \left( 1 + \frac{P_r \left( \frac{2d(\text{edge})}{r(\text{ref})} \right)^{-\varphi}}{N_o} \right)}. \end{aligned} \quad (6.24)$$

#### 6.3.2.2 Upper Bound on Delay

An upper bound on the delay can be determined and for a total of  $n$  critical packets is given by:

$$\begin{aligned} \Delta_{\text{end-to-end}}^u &\leq \lceil h^u \rceil \times \frac{(M+1) \left( \frac{1}{2} n CIR \left( \frac{1}{\beta} - \frac{N_o}{P_r} \right) + Q_{NAN} \right)^2}{2M Q_{NAN}^2} \\ &\times \frac{L}{W \log_2 \left( 1 + \frac{P_r \left( \frac{2d(\text{vertex})}{r(\text{ref})} \right)^{-\varphi}}{N_o + I} \right)}. \end{aligned} \quad (6.25)$$

## 6.4 Numerical Results and Discussions

Parameters used for simulation of HAN are listed in Tables 6.1, 6.2, 6.3 and 6.4. The simulation results are compared with the theoretical upper and lower bounds on critical packet delay given by (6.21), (6.22), (6.24) and (6.25). The results are shown for  $d^{(\text{edge})} = 100\text{m}$ ,  $d^{(\text{vertex})} = 200\text{m}$ ,  $r^{(\text{ref})} = 5\text{m}$ ,  $\varphi = 3$ ,  $r = 8\text{km}$ , and  $W = 22\text{M Hz}$ . For a wireless network using the IEEE 802.11 standard with the parameters given in Table 6.1 and Table 6.2, the critical packet delay is examined as a function of channel interference range  $CIR$ , the  $SNR$  threshold  $\beta$ , and the number of critical packets  $n$ .

Table 6.1: Model parameters used in simulation of WMBN

Parameter	Value
$d^{(\text{edge})}$	100 meter
$d^{(\text{vertex})}$	200 meter
$r^{(\text{ref})}$	5 meter
$\varphi$	3
Maximum straight distance to gateway	800 meter
$W$	22 MHz

Table 6.2: Parameters used for plotting critical delay as a function of  $CIR$  (Fig. 5.10)

Parameter	Value
$Q_{NAN}$	25
SNR threshold $\beta$	3
Number of critical packets $n$	200
$N_o/P_r$	1/200

Table 6.3: Parameters used for plotting critical delay as a function of  $\beta$  (Fig. 5.11)

Parameter	Value
$Q_{NAN}$	25
Number of critical packets $n$	200
Channel Interference Range $CIR$	8
$N_o/P_r$	1/200

It is noted that critical packets were delivered successfully to identified gateway within 0.85 to 9.8 ms. As shown in Figs. 6.10, 6.11 and 6.12, the modified CDMA protocol exhibits superior delay performance compared to modified CSMA/CA protocol

Table 6.4: Parameters used for plotting of critical packet delay as a function of number of critical packets  $n$  (Fig. 5.11)

Parameter	Value
$Q_{NAN}$	25
SNR threshold $\beta$	3
Channel Interference Range $CIR$	8
$N_o/P_r$	1/200

in DCF mode. The MRs were able to transmit all critical packets to identified gateway within 0.85–1 ms in the case of CDMA and within 4.4–9.8 ms for modified CSMA/CA. In Fig. 6.10, critical packet in NAN delay is examined as a function  $CIR$  for parameters given in Table 6.2. It is observed that, as  $CIR$  increases, the delay increases and fewer simultaneous transmissions occur per time slot. The increase in  $CIR$  imposes stricter condition on inter-channel interference, resulting in wider space between channels. This extra space lowers the number of available channels; consequently allowing fewer simultaneous transmissions per time slot. Using the parameters given in Table 6.3, the critical packet delay performance is examined as a function of  $SNR$  threshold  $\beta$  and the results are shown in Fig. 6.11. The results indicate an increase in the number of successful transmissions as  $\beta$  increases. This finding suggests that there is an insufficient number of available channels when  $\beta$  becomes large in the case of CDMA scheme, while it is not a factor in the case of modified CSMA/CA protocol. The critical packet delay bounds as a function of number of critical packets is plotted in Fig. 5.12 for set of parameters given in Table 5.4. It is noted that the delay increases linearly as a function of  $n$ .



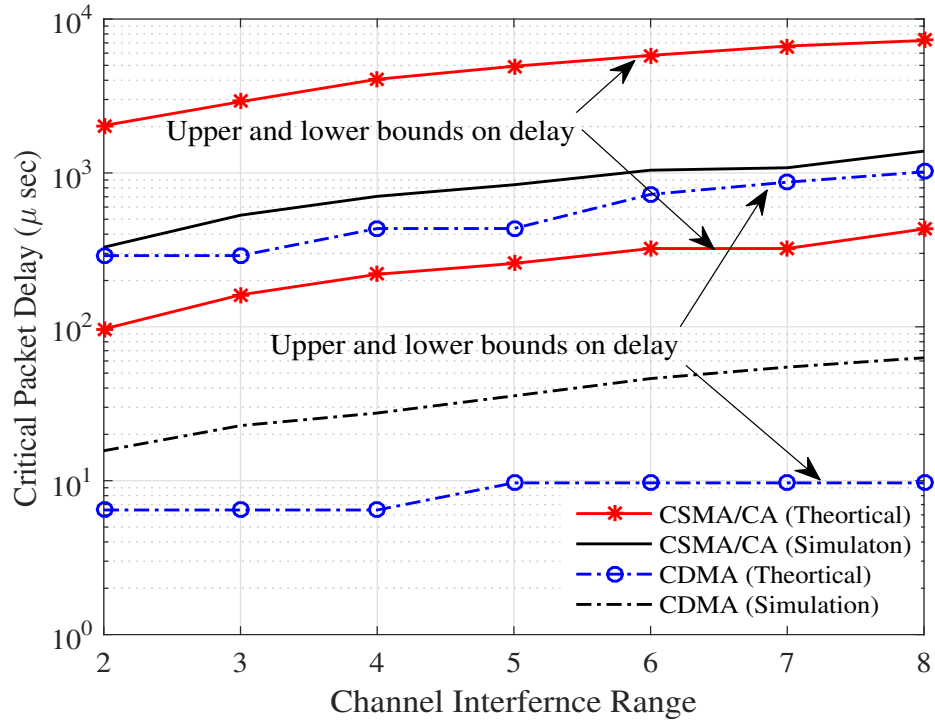


Figure 6.10: Delay bounds as a function of the  $CIR$ .

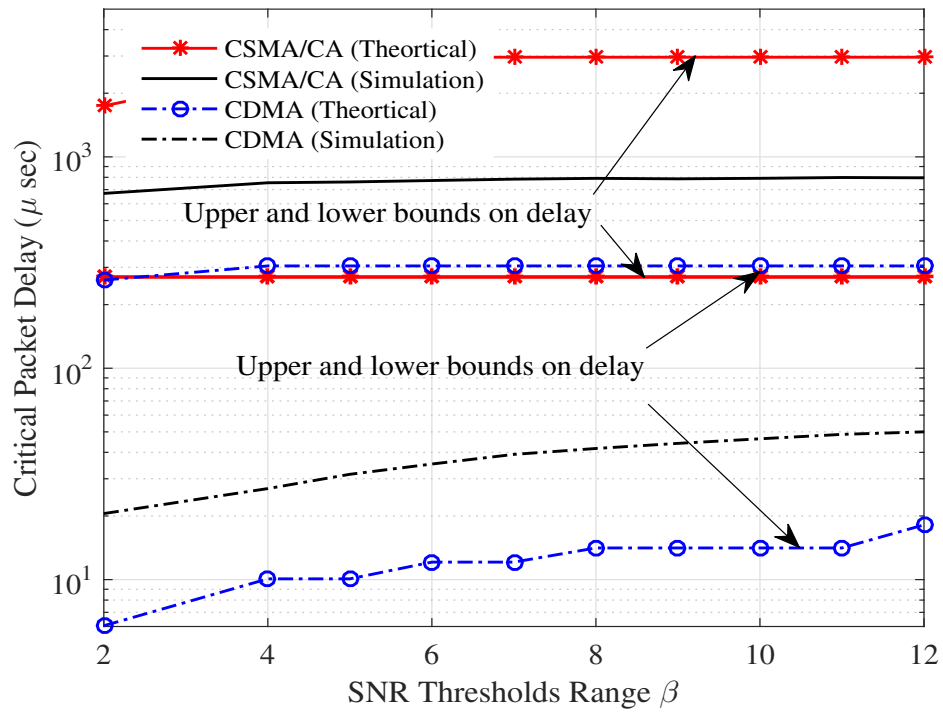


Figure 6.11: Delay bounds as a function of the  $SNR$ .

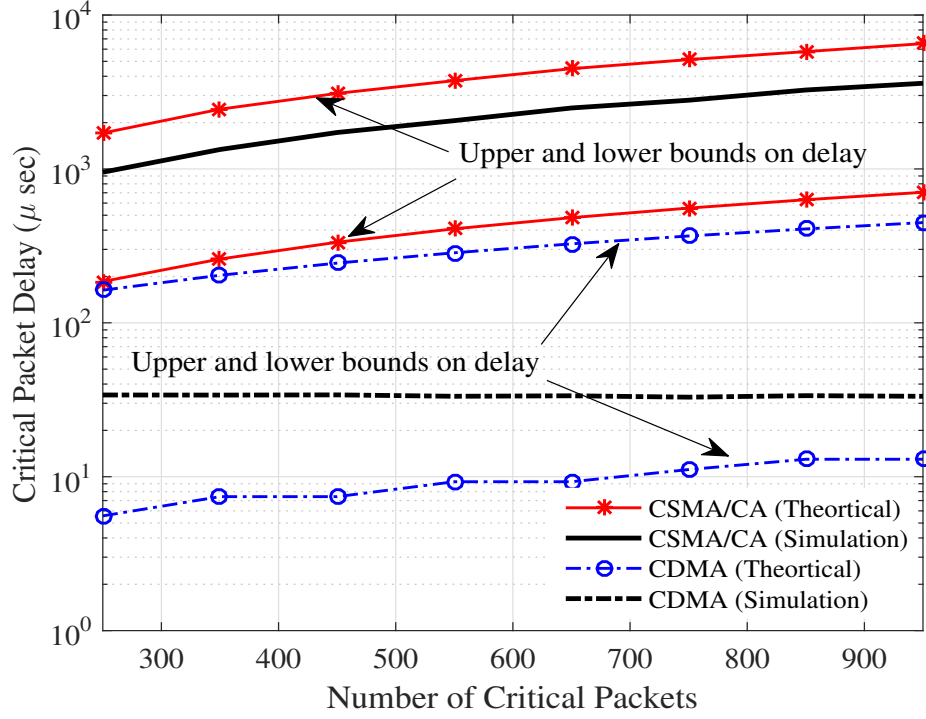


Figure 6.12: Delay bounds as a function of number of critical packets  $n$ .

## 6.5 Conclusions and Summary

In this chapter, a wireless mesh backbone network model for NAN is presented for forwarding critical packets received from HAN to an identified gateway. The routing suggested is based on shortest path using Voronoi tessellation. CSMA/CA and CDMA protocols are considered and closed-form expressions for upper and lower bounds on critical packet delay have been derived and illustrated as functions of i) signal-to-noise ratio, ii) signal interference, iii) critical packet size, iv) number of channels, v) channel interference range, vi) path loss components, vii) channel bandwidth, and viii) distance between MRs. The results show that critical packet delay to gateway using CDMA is lower compared to CSMA/CA protocol.

# Chapter 7

## Modelling and Delay Analysis of WAN <sup>9</sup>

### 7.1 Introduction

It is important to choose an appropriate WAN model for transporting critical packets received at gateway nodes in NAN to a control station in smart grid. For this purpose, a high-speed fiber-optic WAN [81, 82, 83] is considered. The gateway nodes of NAN can be thought of as inputting traffic (periodic + critical) to WAN. The purpose then is to transport this traffic with minimum delay to a control station. In this chapter, therefore, the problem of minimizing critical packet delay is addressed. Also, parameters that affect this delay such as topological structure of WAN, nature of traffic and scheduling, bandwidth, congestion, routing, etc are determined.

The communication between nodes of WAN is assumed to be using TDMA. A Dynamic Fastest Routing Strategy (DFRS) is presented for WAN consisting of  $n$  number of nodes and  $m$  number of links for routing packets from source to destination. This method takes into account the level of clogging over each link based on three principles: i) the average threshold time to transmit a packet over a link, ii) the Quality of Service (QoS) expected, and iii) the level of performance for forwarding packets over sprightly routes. Expressions for overall delay are derived as a function of number of packets, traffic intensity, death rate, capacity, and latency of links. It is noted that the model of WAN is easy-to-implement, and minimizes the average packet delay that meets smart grid standards.

---

9. A. Noorwali, R. Rao, and A. Shami, “Modeling and Delay Analysis of Wide Area Network in Smart Grid Communications,” Proceedings of 2016 IEEE Smart Energy Grid Engineering (SEGE), pp. 347-352, Aug 2016.

## 7.2 Expression for Delay in WAN

The structure of WAN in smart grid is shown in Fig. 1.6 and is responsible for providing communication between a set of nodes of NAN to control stations. It is assumed that the  $n$  nodes are connected through high-speed fiber-optic links. Each node may be a source or a destination of a packet. Therefore, the network contains  $n_{sd} = n(n-1)/2$  possible links. In the WAN, the identified gateway provides wireline access from the nodes to the control station. It is assumed that the traffic in each link is M/M/1 queuing system. The  $k$  packets of size  $B_k$  bits generated at each node follows Poisson distribution. The packets can be either in transit over the link, or waiting for an available link. The traffic  $y_{i,j}$  between a pair of nodes  $(i, j)$  over a link represents the number of packets per second from node  $i$  to node  $j$ . This leads to the total load on the network given by:

$$y = \sum_{i=1}^n \sum_{j=1}^n y_{i,j}, \quad i \neq j \quad (7.1)$$

Each node in WAN is a router and it is assumed that each node transmits  $k$  packets over  $L_l$  (in km) with a capacity of  $C_l$  Mbps. In this system, optical communication is considered in which pulses of light are sent over fiber optic line. The nodes in WAN and the control station are equipped with transmitter and receiver that convert the information signal into a light signal and convert it back to information signal at the destination [84]. The advantage of using optical communication is that it provides up to 15 channels known as “superchannels,” which carry various wavelengths in a single optical fiber link. The propagation delay  $\tau_l$  of each packet depends on the speed of light ( $3 \times 10^8$ ) m/s, and can be expressed as:

$$\tau_l = \frac{10^{-8}}{3} L_l. \quad (7.2)$$

From queuing theory [47], the expected delay  $T_l$  over the link  $L_l$  can be written as:

$$T_l = \frac{1}{\mu C_l - \lambda_l} + \tau_l. \quad (7.3)$$

where  $\mu$  is the service rate, and  $\lambda_l$  is the arrival rate for link  $l$ . Averaging delays of all links of network, the average packet delay can be written as [47]:

$$T_{avg} = \frac{1}{m} \sum_{l=1}^m \lambda_l \left[ \frac{1}{\mu C_l - \lambda_l} + \tau_l \right], \quad (7.4)$$

where  $m$  is the total number of links. Assuming service time is exponentially distributed. The mean service time over link  $l$  is given by:

$$T_s = \frac{1}{\mu C_l} + \tau_l, \quad (7.5)$$

where,  $\tau_l$  denotes the propagation delay. Each high-speed link is capable of transmitting up to  $b_l$  packets simultaneously between a pair of nodes. The delay over links is a function of the routing strategy used in WAN.

## 7.3 Proposed Dynamic Routing Strategy (DFRS)

To find the optimal choice of routes, a dynamic procedure that takes into account the current state of the network is considered. The DFRS routing strategy is proposed to protect the networks from congestion. This leads to minimization of average packet delay from source nodes to control stations, as shown in Fig. 7.1. It is noted that a packet takes  $d_1 + d_2 + d_3$  sec before reaching the control station. In [48],[49],[77], expressions for delay bounds have been presented, where  $d_1 = d_{HAN}$  [48] +  $d_{NAN}$  [77]  $\approx 120$ m sec. Once the packet arrives at the source gateway, it has to be routed quickly in the WAN to achieve a minimum delay  $d_2$  using the fastest path to the control station. It is noted that the notation  $d_2$  refers to  $d_{WAN}$ . In order to find this, it is assumed that there are  $n$  number of nodes and  $m$  number of links in the WAN and each queue is analyzed independently in the network.

### 7.3.1 Problem Formulation to Determine Optimal Path

In the proposed DFRS the objective is to find the shortest path from the origin source node to the gateway (control station) node based on the load at each link. For example, in the scenario presented in Fig. 7.2,  $r_{i,j}$  represents the path between nodes  $i$  and  $j$ . Assigning  $r_{i,j}$  binary value, it is noted that it is equal to 1 if the nearest available link is the shortest, otherwise it is equal to 0.

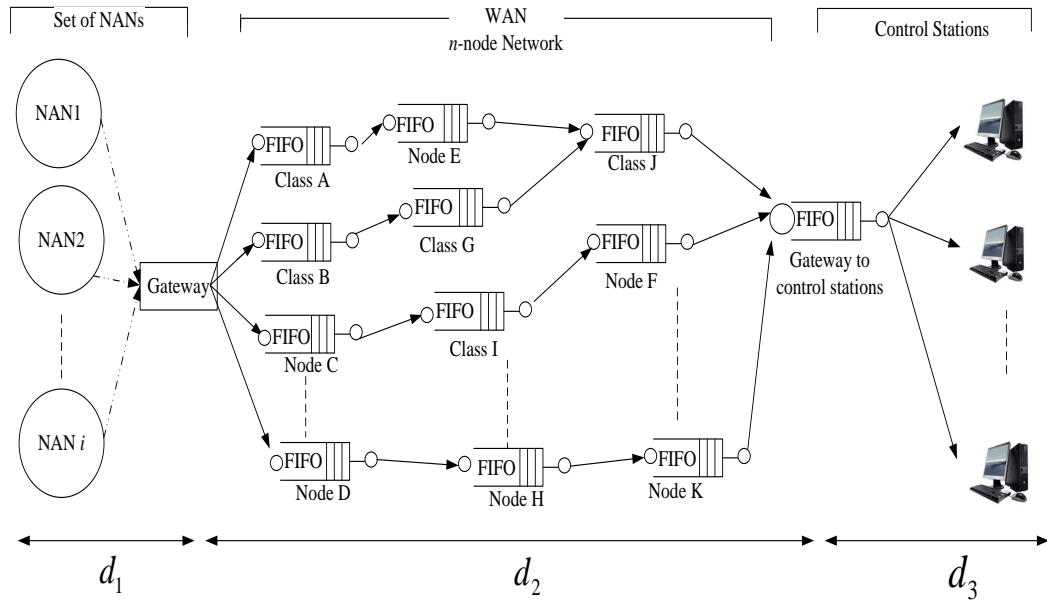


Figure 7.1: Structure of high-speed WAN.

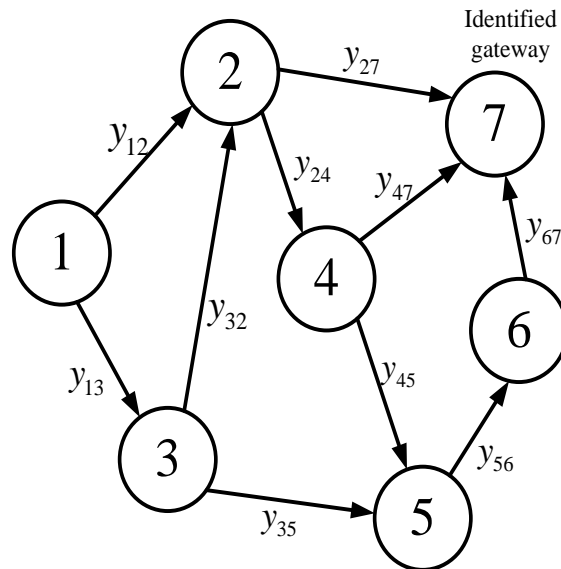


Figure 7.2: Network model scenario.

The minimum end-to-end path can be written as:

$$m = \min \sum \sum y_{i,j} r_{i,j}. \quad (7.6)$$

Considering the scenario in Fig. 7.2, where node 1 forwards packets until they eventually reach the gateway (node 7), the optimal path from source to destination is given by:

$$\begin{aligned} m = \min & (y_{1,2}r_{1,2} + y_{1,3}r_{1,3} + y_{3,2}r_{3,2} \\ & + y_{2,4}r_{2,4} + y_{2,7}r_{2,7} + y_{4,7}r_{4,7} + y_{3,5} \\ & r_{3,5} + y_{4,5}r_{4,5} + y_{5,6}r_{5,6} + y_{6,7}r_{6,7}), \end{aligned} \quad (7.7)$$

where  $y_{i,j}$  is the current load (bits/sec). For the case of randomly generated value given by:  $y_{1,2} = 10$ ,  $y_{1,3} = 15$ ,  $y_{3,2} = 4$ ,  $y_{2,4} = 3$ ,  $y_{2,7} = 6$ ,  $y_{4,7} = 5$ ,  $y_{3,5} = 8$ ,  $y_{4,5} = 2$ ,  $y_{5,6} = 7$ , and  $y_{6,7} = 6$ , and subject to:

$$r_{1,3} + r_{1,2} = 1, \quad (7.8)$$

and at intermediate nodes 3,5, and 6,

$$r_{3,5} + r_{3,2} - r_{1,3} = 0, \quad (7.9)$$

$$r_{5,6} - r_{3,5} - r_{4,5} = 0, \quad (7.10)$$

$$r_{6,7} - r_{5,6} = 0, \quad (7.11)$$

For a gateway node  $r_{6,7}$ , the shortest path is determined by:

$$r_{2,7} + r_{4,7} + r_{6,7} = 1. \quad (7.12)$$

After solving the optimization problem in MATLAB, it is found that packets should follow the path:  $1 \mapsto 2 \mapsto 4 \mapsto 7$ . Accordingly, two specific steps are required in modelling the DFRS routing in WAN.

1. Select each  $y_{i,j}$  between each pair, such that node  $i$  is adjacent to node  $j$ .

In this step, we determine the delay of each link based on the initial flow of each link  $(i, j)$  and the capacity of the link  $C_l$ . For each of these selected  $y_{i,j}$ , where node  $i$  is adjacent to node  $j$ , by setting the average transmission delay as follows: (a) set each load on the link as  $\lambda_l$  and calculate traffic intensity  $\rho_l = y_{i,j} \times T_s$ :

$$\rho_l = \frac{y_{i,j}}{b_l \mu C_l}. \quad (7.13)$$

Based on (7.13), the next step is: (b) find the average transmission delay of each link using:

$$T_{lt} = \frac{1}{\mu [C_l - \rho_l]}. \quad (7.14)$$

2. Determine the fastest route between node  $i$  and  $j$  toward the destination.

In this step, the previous step is repeated, for all links in the network to determine the fastest route. For an  $n$ -node network,  $\sum T_{lt}$  is limited to the threshold time, given by:

$$T_{l,\max} = \frac{QoS}{\bar{y}}, \quad (7.15)$$

where QoS is in bits and  $\bar{y}$  is the average total load in the network and is given by:

$$\bar{y} = \frac{1}{n_{sd}} y. \quad (7.16)$$

Finally, the attribute of each link is updated and stored them in the routing matrix. This process will determine the number of  $m$  links that have the fastest rates with minimum delay all the way upto the control station. The routing algorithm steps are given in Algorithm 2.

## 7.4 End-To-End Delay Analysis in WAN

The objective is to determine the minimum delay  $d_{WAN}$  required to send  $k$  packets from source to destination (control station). Each link allows a node to transmit up to  $b_l$  packets simultaneously, but in most scenarios  $k > b_l$ . Therefore, there is at least one packet waiting in the queue of a node. As a result, the rest of the packets will be deferred to the next state of the queuing system.



---

**Algorithm 2** DFRS algorithm

---

**Require:** All  $y_{i,j}$  from each pair  $(i, j)$  such that node  $i$  is adjacent to node  $j$

- 1: Starting from node  $i = 1$
  - 2: Set initial  $T_{lt}$  to maximum.
  - 3: Set initial  $m$  to zero.
  - 4: **FOR**  $i \leftarrow 1$  to  $n_{sd}$
  - 5: Go over the traffic matrix for nodes  $j$  is adjacent to node  $i$
  - 6:     **FOR**  $j \leftarrow 1$  to  $n_{sd}$
  - 7:     Label the current  $y_{i,j}$
  - 8:     Calculate the transmission time based on 7.14
  - 9:     **IF**  $T_{lt,j} < T_{lt,(j-1)}$
  - 10:     **THEN**
  - 11:     Select link  $l_j$  with minimum  $T_{lt,j}$
  - 12:     **Break;**
  - 13:     **ELSE**
  - 14:     Increment  $j$
  - 15:     **GO** 5
  - 16: **IF**  $\sum T_{lt,(i,j)} < (7.15)$
  - 17: **THEN**
  - 18: Increment  $m$
  - 19: Increment  $i$
  - 20: Update the attribute of each link and store it in the routing matrix table
  - 21: **IF** Packets reach destination
  - 22: **Break;**
  - 23: **ELSE**
  - 24: **END FOR**
  - 25: **return** number of links  $m$
-

### 7.4.1 Transition State

Based on Markov chain characteristics [85], the queueing system can be modeled as M/M/ $b_l$ . The goal here is to derive the steady state probabilities. The utilization  $u_l$  of link  $l$  is given by:

$$u_l = \frac{\lambda_l}{\mu C_l}. \quad (7.17)$$

Consequently, knowing that the traffic intensity is  $\rho_l$  in (7.13),  $u_l$  in (7.17), and based on expressions derived in [85], the probability that there are no packets in the M/M/ $b_l$  system is given by:

$$P_l(0) = \left( \left[ \sum_{k=0}^{b_l-1} \frac{u_l^k}{k!} + \frac{u_l^{b_l}}{b_l!(1-\rho_l)} \right] \right)^{-1}. \quad (7.18)$$

Furthermore, the probability of the packets that have arrived finding all the links busy is given by:

$$E_{lq}^{M/M/b_l} = \frac{\rho_l u_l^{b_l} P_l(0)}{b_l!(1-\rho_l)^2}. \quad (7.19)$$

Because the input of a node in the network is the output of previous nodes, the network follows G/G/ $b_l$  queueing system. Using the Kingman approximation, the number of packets that are waiting in the queue is given by [86]:

$$E_{lq}^{G/G/b_l} = \frac{V_a^2 + V_s^2}{2} \frac{\rho_l u_l^{b_l} P_l(0)}{b_l!(1-\rho_l)^2}, \quad (7.20)$$

where  $V_a^2 = \frac{\sigma_a^2}{(1/\lambda_l)^2}$  is the coefficient of variation of inter-arrival time,  $\sigma_a^2$  denotes the variance of the inter-arrival time,  $V_s^2 = \frac{\sigma_s^2}{(1/\mu)^2}$  is the coefficient of variation of service time, and  $\sigma_s^2$  denotes the variance of the service time.

By applying the Kleinrock independence approximation to the serial path in network, with the assumption that service times are independent from queue to queue [87], the average number of packets in transit is given by:

$$E_{lt} = \lambda_l \left[ \frac{1}{\mu C_l} + \tau_l \right]. \quad (7.21)$$

The total average number of packets in each link can be expressed as  $E_l = E_{lq}^{G/G/b_l} + E_{lt}$ . For  $k$  packets, as shown in Fig. 7.3, the death rate corresponds to  $\lambda_l$ , is given by:

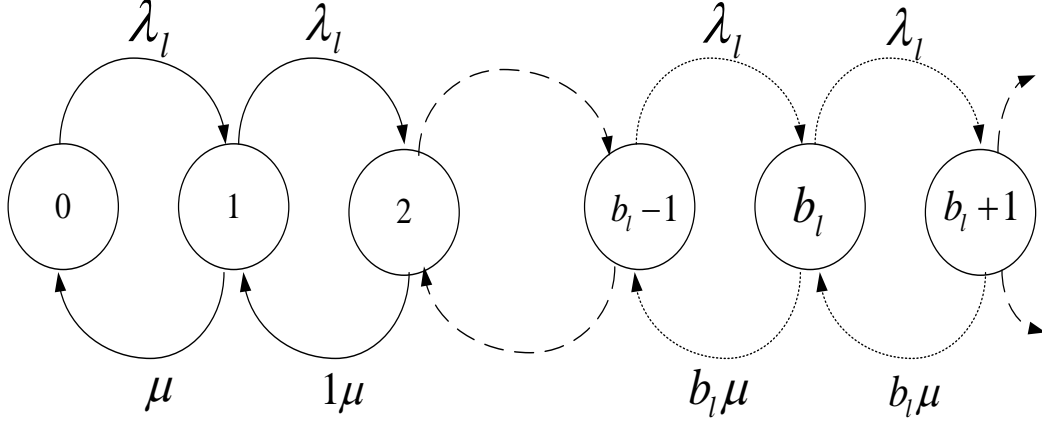


Figure 7.3: Death and birth process of a WAN in a smart grid.

$$\mu_k = \begin{cases} \frac{k}{T_s}, & \text{if } k \leq b_l, \\ \frac{b_l}{T_s}, & \text{if } k > b_l. \end{cases} \quad (7.22)$$

Consequently, substituting (7.5) in (7.22) gives:

$$\mu_k = \begin{cases} \frac{k\mu C_l}{1+\tau_l\mu C_l}, & \text{if } k \leq b_l, \\ \frac{b_l\mu C_l}{1+\tau_l\mu C_l}, & \text{if } k > b_l. \end{cases} \quad (7.23)$$

### 7.4.2 Average Delay Analysis

The end-to-end delay can be defined as the total amount of time that a packet spends in the queue and in transit in the WAN. To find the average delay, the number of packets  $E_t$  in the path and  $m$  links are considered. Noticing that each router has  $E_l$  packets in its queuing system, the sum of packets is expressed as:

$$E = \sum_{l=1}^m E_l. \quad (7.24)$$

According to Little's theorem, the number of packets in each link is expressed as  $E_l = \lambda_l T_l^{(G/G/b_l)}$ . Therefore, the transmission time over link  $l$  is given by:

$$T_l^{(G/G/b_l)} = \frac{E_l}{\lambda_l} = \frac{V_a^2 + V_S^2}{2\lambda_l} \frac{b_l u_l^{b_l} P_l(0)}{\mu_k C_l b_l! (b_l - u_l)^2} + \frac{1}{\mu_k C_l} + \tau_l, \quad b_l \geq 1. \quad (7.25)$$

By substituting (7.2), and (7.18) into (7.25), the mean time delay in WAN can be obtained. The average packet delay is, thus, given by:

$$T_{\text{mean}}^{G/G/b_l} = \frac{1}{\bar{y}} \sum_{l=1}^m T_l^{(G/G/b_l)}. \quad (7.26)$$

### 7.4.3 Multiple Access Scheme for Scheduling Transmissions

In particular, TDMA is used to schedule transmissions between routers [55]. Also, all  $k$  packets are assumed to be ready at  $t = 0$  and the arrival time of packets is denoted as  $d_{WAN}$  depends on the channel access schemes used.

#### 7.4.3.1 TDMA Scheme

In TDMA, the time period is divided into a number of time slots  $Z$  as shown in Fig. 7.4. Thus, the waiting time,  $\omega_{TD}$ , needs to be considered and is given by:

$$\omega_{TD} = \frac{1}{Z} \sum_{z=1}^Z (z-1) \frac{T_{\text{mean}}^{G/G/b_l}}{Z} = \frac{T_{\text{mean}}^{G/G/b_l}}{2} \left(1 - \frac{1}{Z}\right), \quad (7.27)$$

where  $Z$  is the number of time slots.

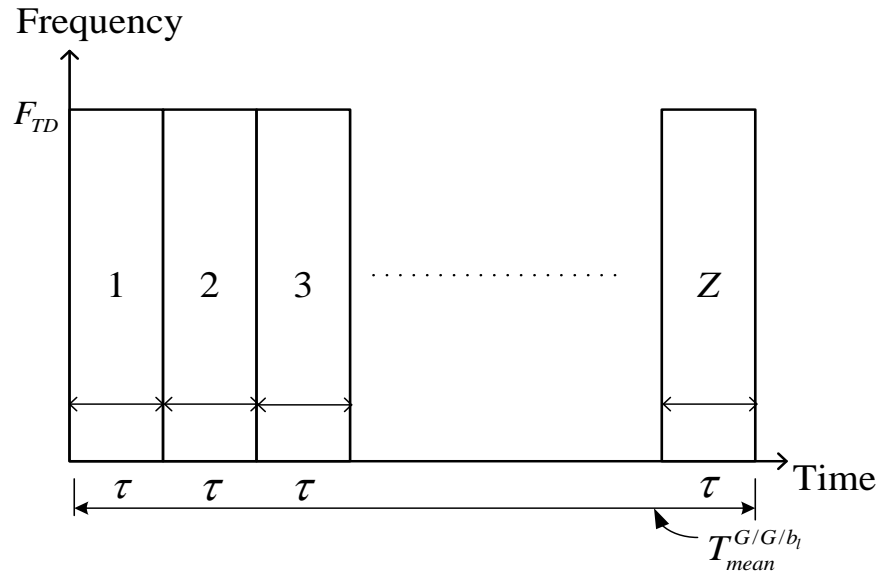


Figure 7.4: TDMA time slots.

The transmission time for packet is given by:

$$\tau_{TD} = \frac{T_{\text{mean}}^{G/G/b_l}}{Z}. \quad (7.28)$$

The average packet delay in TDMA is, thus, given by:

$$d_{TD} = \tau_{TD} + \omega_{TD}, \quad (7.29)$$

By substituting (7.27) and (7.28) in (7.29), The average packet delay for a G/G/ $b_l$  is given by:

$$d_{TD}^{G/G/b_l} = T_{\text{mean}}^{G/G/b_l} \left( \frac{Z+1}{2Z} \right). \quad (7.30)$$

## 7.5 Numerical Results and Discussion

The critical packet delay for WAN can be determined by finding for all nodes, the shortest paths to the destination as described in Section 6.1.3.1. Then, using the Monte Carlo simulation critical packet delay performance is evaluated. Finally, the analytical results are compared with Monte Carlo simulation results. For the G/G/1 system, approximation for the number of packets in the queue derived by Marchal [88] is used and is given by:

$$E_q^{G/G/1} \approx \frac{\rho^2(1 + V_s^2)(V_a^2 + \rho^2 + V_s^2)}{2(1 - \rho)(1 + \rho^2 V_s^2)}. \quad (7.31)$$

The average packet delay over link  $l$  can then be written as:

$$T_l^{(G/G/1)} = \frac{V_a^2 + V_s^2}{2\lambda_l} \frac{u_l P_l(0)}{\mu_k C_l (1 - u_l)^2} + \frac{1}{\mu_k C_l} + \tau_l. \quad (7.32)$$

By replacing  $T_{\text{mean}}^{G/G/b_l}$  with  $T_{\text{mean}}^{G/G/1} = \frac{1}{y} \sum_{l=1}^m T_l^{(G/G/1)}$  in (7.30), an upper bound on delay can be obtained and is given by:

$$d_{TD}^{G/G/1} = T_{\text{mean}}^{G/G/1} \left( \frac{Z+1}{2Z} \right). \quad (7.33)$$

In addition, it is noted that (7.30) itself is the lower bound on delay.

### 7.5.1 Overall Evaluation of Critical Packet Delay

Using the closed-form expression given by (7.30), analytical bounds on delay can be computed. These upper and lower bounds can be plotted as a function of number of channels and the number of paths available in the network. Closed-form solutions for delay for arbitrary composite congestion models are not available. Therefore, simulations were carried out using random traffic models available for Toronto neighbourhoods [89]. Toronto is named as “the city of neighbourhoods” because it has as many as 240 districts. The parameters listed in Table 7.1 have been used in the fiber-optic WAN model used for numerical results. For instance, the inter-arrival time of each single queue process is exponentially distributed with a mean of 2m sec and the service time is also exponentially distributed with a mean of 1.6m sec. Delay analysis is performed as a function of: i) QoS

Table 7.1: Parameters used in the fiber-optic WAN model used for numerical computations

Parameter	Value
Number of nodes $n$	240
Distances $r_{i,j}$	5 - 10 Km
Number of channels $b_l$	1-15
Arrival rate $\lambda$	500 packets/sec
Service rate $\mu$	600 packets/sec
Packet size $B_k$	1000 bits
Capacity of link $C_l$	100–273 Mbs
WAN $QoS$	100k - 10 M bits

in WAN  $QoS$ , ii) capacity of link  $C_l$ , ii) load on adjacent nodes  $y_{i,j}$ , iv) link utilization  $\rho_l$ , and v) number of channels in each link  $b_l$ . In particular, for  $d_{WAN}$  in the range of  $0.37\mu$ – $28\mu s$ , it is observed that the average packet delay from source to control station meets the smart grid standards, as shown in Figs. 7.5, 7.6, 7.7, 7.8, and 7.9.

In Fig. 7.5, it can be observed that, as WAN  $QoS$  increases, the delay also increases. The increase in the threshold value of WAN  $QoS$  results in fewer channels and hence increase the value of delay. In other word, it will lower the number of available channels, and consequently allow fewer transmissions per time slot. As the channel capacity of links are increased, the overall network delay decreases as shown in Fig. 7.6. In Figs. 7.7, 7.8, 7.9, the delay is examined as a function of  $y_{i,j}$ ,  $\rho_l$ , and  $b_l$ . As  $y_{i,j}$ ,  $\rho_l$ , and  $b_l$  increase,

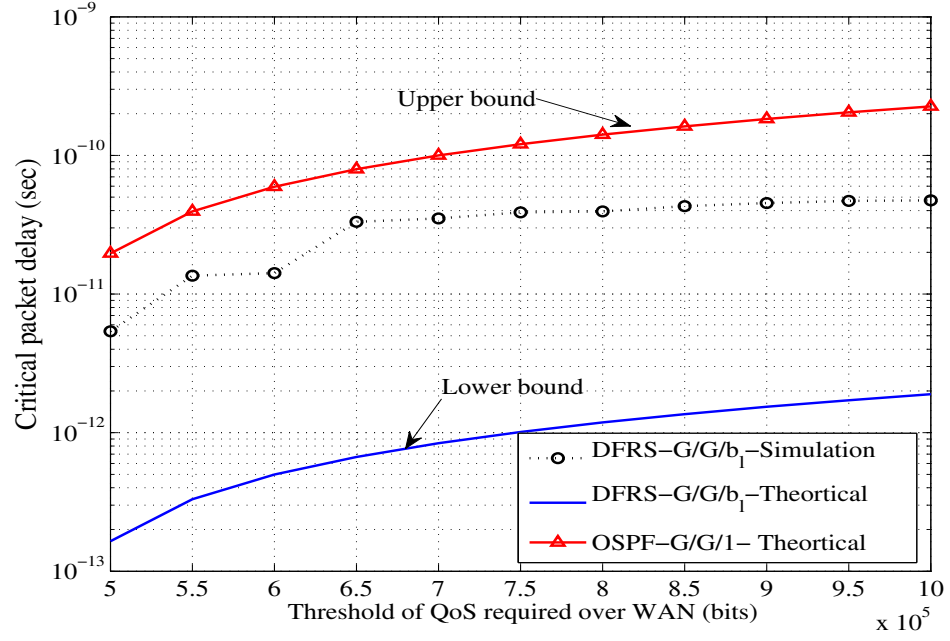


Figure 7.5: Critical packet delay as a function of threshold WAN  $QoS$ .

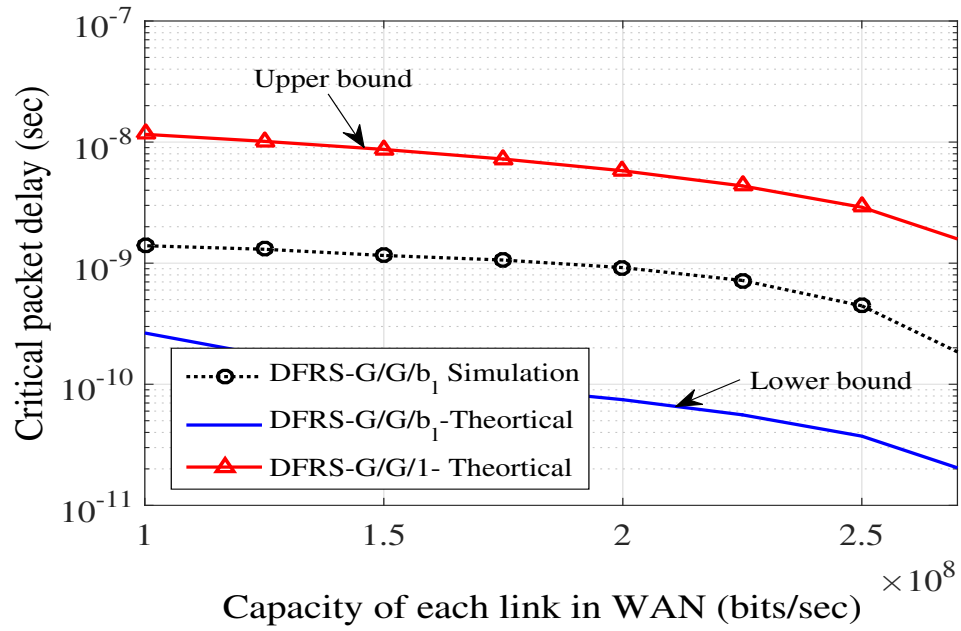


Figure 7.6: Critical packet delay in WAN as a function of capacity of links  $C_l$ .

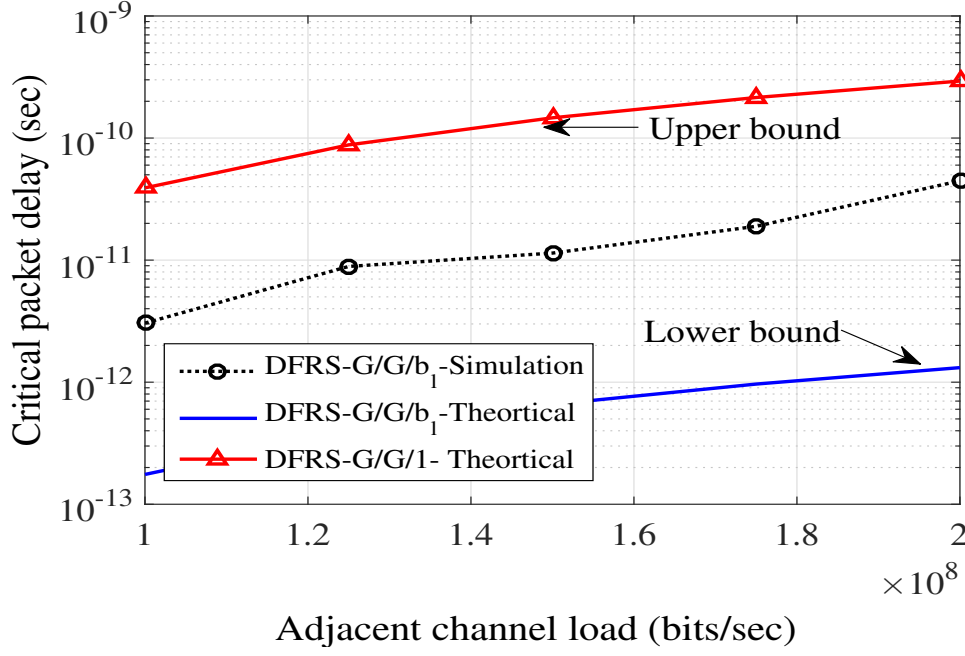


Figure 7.7: Critical packet delay as a function of adjacent channel load  $y_{i,j}$ .

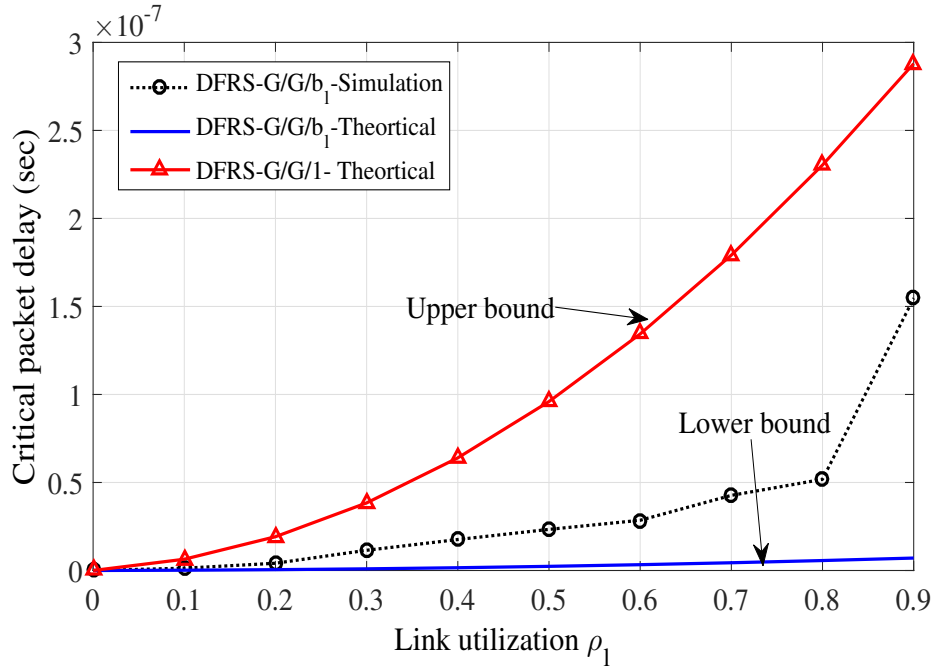


Figure 7.8: Critical packet delay a function of link utilization  $\rho_l$ .



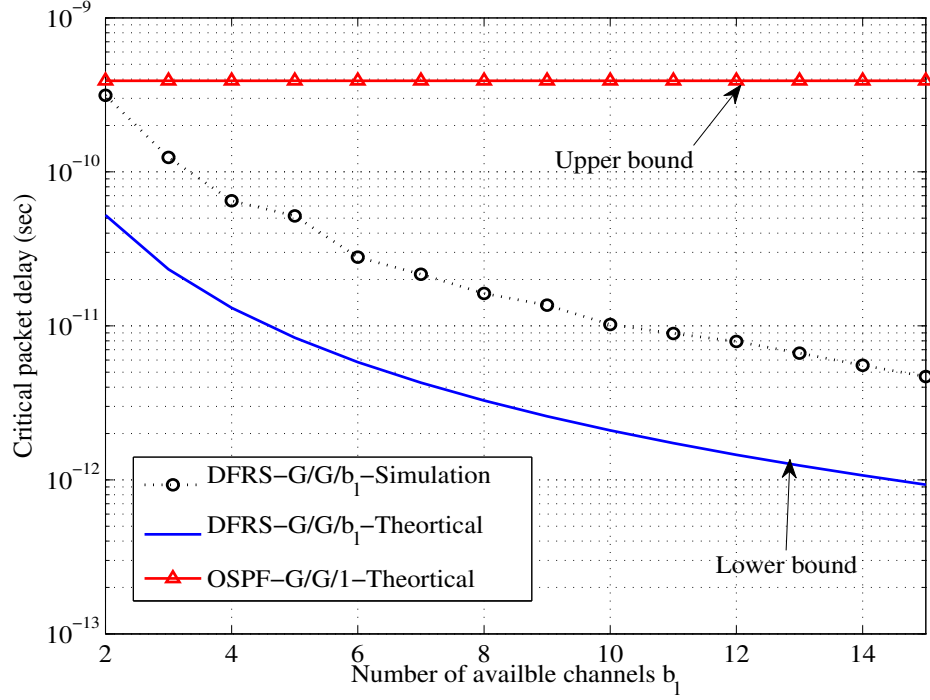


Figure 7.9: Critical packet delay as a function of number of available channels  $b_l$ .

it is observed that delay also increases. This indicates that if there is an increase in the successful transmission time, there exist an insufficient number of available channels.

Finally, the results suggest the need to consider DFRS in WAN in the design of smart grid for achieving minimum delay. As the number of packets increase, it can be observed from Figs. 7.5, 7.6, 7.7, 7.8, 7.9 that the classical G/G/1 network using DFRS algorithm results in a higher delay, causing congestion in WAN.

## 7.6 Conclusions and Summary

In this chapter, a fiber optic WAN is presented for transporting critical packets received from NAN to a control station. A DFRS algorithm is proposed for routing critical packets to control station in WAN. Closed-form expression for mean critical packet delay is derived and is illustrated as a function of: i) traffic intensity, ii) capacity of fiber links, iii) number of links, iv) variance of inter-arrival time, v) variance of service time, and vi) the latency of links. It is shown that delay of critical packets to control station meets acceptable standards set for smart grid.

# Chapter 8

## Conclusions

### 8.1 Introduction

This chapter summarizes the contributions of this thesis and the conclusions drawn from the results obtained. Also, areas for further research in the modelling and delay analysis of smart grid are given. In Section 8.2, summary of contributions is provided, and in Section 8.3, suggestions for future research are sketched.

### 8.2 Summary of Contributions

Data communication network or smart grid will be an integral component of future power grids for effective energy management. In this thesis, a generic model of smart grid consisting of three subnetworks, namely HAN, NAN, and WAN, is presented. While there exist a plethora of issues associated in the design of smart grid, the primary objective in this thesis is to present practical models for each of the three subnetworks of smart grid and subject them to critical packet delay analysis in order to understand the parameters that would influence the end-to-end delay. It is noted that critical packet delay in smart grid plays an important role in the operation of power grid.

In Chapter 3, a model of wireless HAN is presented and consists of a set of  $n$  EDs (or customers) in wireless communication with an MC. The traffic generated by each ED is modeled as either High Priority (HP) or Periodic Base (PB). A single-server non-preemptive queueing model with HOL scheduling strategy is suggested for transmission of packets from EDs to MC. The queueing model is analyzed and closed-form expressions for critical packet delay are derived. It is noted that the delay is a function of: i) critical packet arrival rate; ii) service rate; iii) utilization of server; and iv) rate of arrival of non-critical packets. It is noted that the expressions derived for delay are applicable to

both wired and wireless channels. The queueing model suggested is easy-to-implement and requires minimal overhead. Although, the analysis of delay has been preformed for a two-class priority traffic, it can easily be tented to multi-class priority traffic. Analytical results agree very well with simulation results.

In Chapter 4, a practical model of wireless HAN using modified FDMA and modified TDMA multiple access techniques is presented. The wireless channel between EDs and MC is modeled as Rayleigh and Nakagami. First, closed-form expressions for average packet delay for modified FDMA and TDMA are derived and then used to derive upper and lower bounds on critical packet delay in HAN. It is shown that these bounds are function of: i) SINR; ii) channel fading; iii) strength of transmitted power from EDs; iv) number of EDs; v) critical packet size; vi) number of non-overlapping channels, vii) number of channels, viii) path loss component, ix) distances between electrical devices and mesh client, x) channel interference range, xi) channel capacity, xii) bandwidth of the channel, and xiii) number of time slots/frequency bands. Analytical bounds on critical packet delay are illustrated as a function of a variety of system parameters. It is noted that simulation results always lie in between upper and lower bounds on critical packet delay. An analysis of delay performance as a function of typical system parameters is also provided.

In Chapter 5, an IDCA-MAC protocol for wireless HAN is proposed. The protocol eliminates collision of packets and employs MIMO system to enhance system performance. It is observed that the critical packet delay in such a HAN is poorer by nearly 20% compared to HAN using conventional IDCA-MAC protocol. However, one of the major advantages of using IDCA-MAC protocol in HAN is that throughput can be increased considerably for a given value of delay.

In Chapter 6, a model of NAN referred to as Wireless Mesh Backbone Network (WMBN) is presented along with its critical packet delay analysis. For routing packets in WMBN shortest path using Voronoi tessellation is used. This routing technique is described mathematically and used for deriving closed-form expressions for upper and lower bounds on critical packet delay. Two protocols are considered in WMBN and they are: i) CSMA/CA and ii) CDMA. It is noted that the critical packet delay is a function of i) signal-to-noise ratio, ii) signal interference, iii) critical packet size, iv) number of channels, v) channel interference range, vi) path loss components, vii) channel bandwidth,

and viii) distance between MRs. One of the chief results of this chapter is that CDMA protocol is superior to CSMA/CA from the view point of critical packet delay in WMBN.

In Chapter 7, a fiber-optic WAN model is presented for transporting critical packets received from NAN. A DFRS algorithm is proposed for routing within WAN and closed-form expression for mean critical packet delay is derived and the parameters that influence delay are identified and illustrated.

The end-to-end critical packet delay is the sum of delays in HAN, NAN, and WAN. That is:

$$d_{\text{end-to-end}} = d_{\text{HAN}} + d_{\text{NAN}} + d_{\text{WAN}} \quad (8.1)$$

Thus, the end-to end delay depends on the resources and models used in each of the three subnetworks of smart grid. An experimental scenario with  $n$  EDs that have critical packets ready at  $t = 0$  for transmission to the control station was considered and end-to-end critical packet delay was computed using MATLAB. The delay was examined as a function of  $n$ . If the end-to-end delay,  $d_{\text{end-to-end}}$ , is below 150 ms, it implies that the critical packets reach the control station within the 150 ms, a standard for smart grid. The tolerable delay is between 10 – 150 ms [90].

As shown in Fig. 8.1, it is clear that the end-to-end delay bounds are lower than that specified for smart grid. In both the lower and upper case scenarios, the communication systems in smart grid were able to transmit the given number of critical packets to the control station within 1-150 ms. It is noticed that there is an increasing trend in delay for both upper and lower bounds as the number of critical packets increases. Since the bounds on delay are below of 150 ms, it confirms that the proposed model has the potential to serve as smart grid. However, further analysis is required for large number of EDs and multiple MCs.

### 8.3 Suggestions for Future Work

The major concern in this research was to model and establish theoretical bounds on critical packet delay from EDs to control station. One of the issues with establishing the theoretical bounds on delay of critical packets is the limited resources of smart grid. Therefore, if each mesh router is equipped with  $n$  antennas, a high data rate and minimum delay can be achieved. However, other issues that need to be studied are:

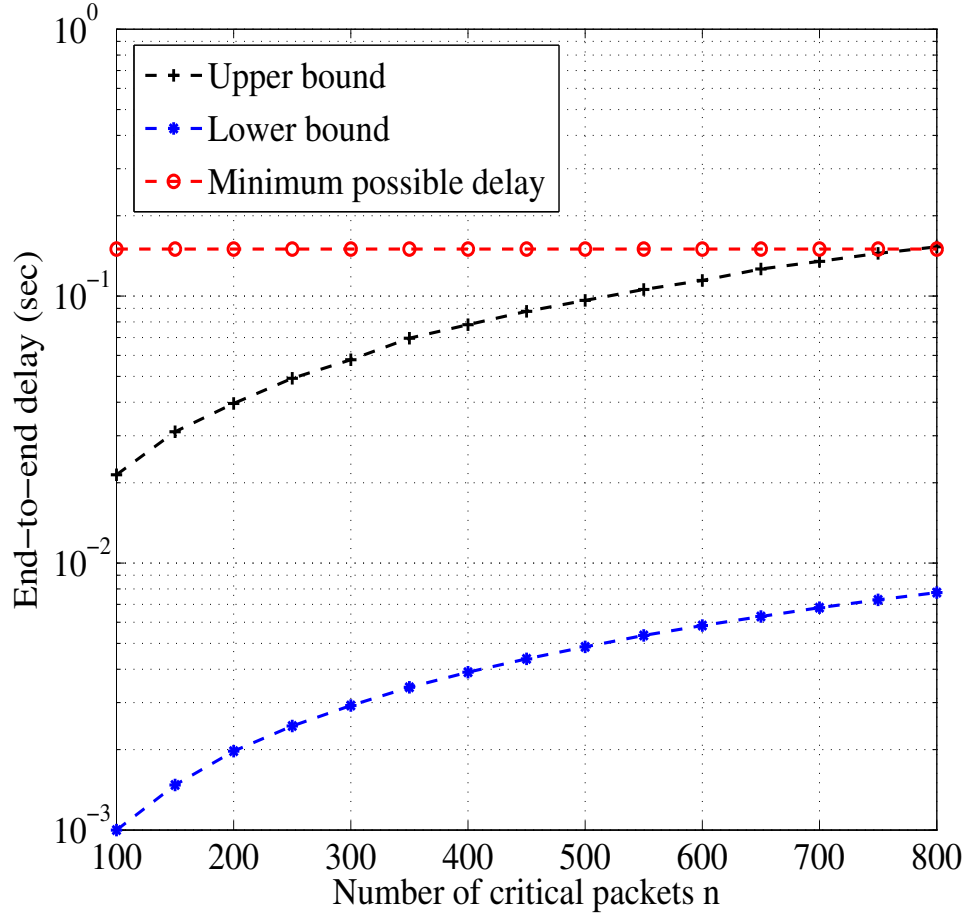


Figure 8.1: End-to-end delay of smart grid as a function of number of EDs for:  
 $Q_{HAN} = 25$ ,  $Q_{NAN} = 25$ ,  $b_l = 1 - 15$ ,  $\beta = 3$ ,  $r = 8000$ ,  $d^{edge} = 100\text{m}$ ,  $d^{vertex} = 200\text{m}$ ,  
 $L = 1000$ ,  $W = 22\text{MHz}$ ,  $r_o = 5\text{m}$ ,  $\varphi = 3$ ,  $\bar{\gamma} = 200$ ,  $\lambda = 500\text{packts/sec}$ ,  
 $\mu = 600\text{packts/sec}$ ,  $C_l = 100\text{Mbs}$ ,  $QoS = 50\text{Mbits}$ , and  $r_{i,j} = 10\text{Km}$ .

1. How to provide fair channel access for all mesh clients in the network?
2. How to optimize power budgeting?
3. How to implement Voronoi routing schemes in the mesh backbone network?

MIMO is a system that is used to increase the efficiency of space utilization with respect to both transmitter and receiver. In the MIMO system [91], data on the transmitter side are de-multiplexed into a specific number of substreams. These numbers match the number of transmitting antennas. The advantage of MIMO is that it increases the capacity without requiring extra bandwidth. Therefore, network MIMO (netMIMO) technology is suggested for WMBN. Huang et al. [92] defined netMIMO as many mesh routers that are very close to each other; these cooperate to send or receive a data stream as shown in Fig. 8.2. Moreover, Goldsmith [56] has identified how constraints such as interferences, signal power, and delay could be reduced when netMIMO is employed. This technology has not been examined in detail for smart grids and is worthwhile for further research work.

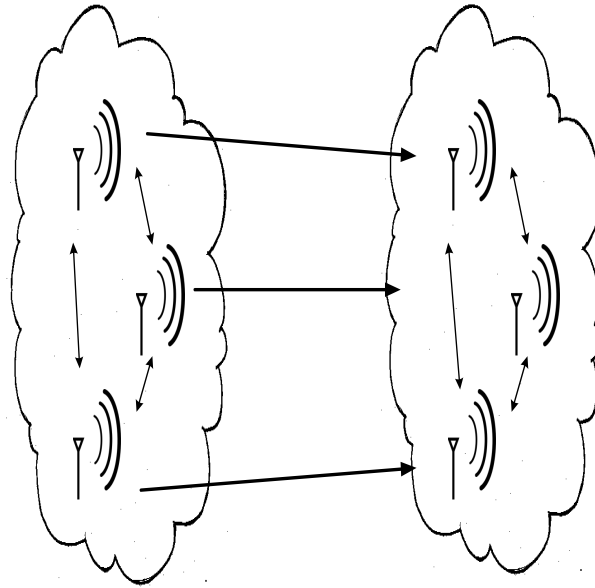


Figure 8.2: NetMIMO

## References

- [1] S. Bush, S. Goel, and G. Simard, “IEEE Vision for Smart Grid Communications: 2030 and Beyond Roadmap,” Proceedings of IEEE Vision for Smart Grid Communications: 2030 and Beyond Roadmap , pp.1-19, September 2013.
- [2] NIST, “NIST Framework and Roadmap for Smart Grid Interoperability Standards, Release 2.0,” Available: <http://www.nist.gov>, 2012.
- [3] H. Louie, M. Burns and C. Lima, “An Introduction and User’s Guide to the IEEE Smart Grid Web Portal,” 2010 IEEE PES Innovative Smart Grid Technologies Conference Europe (ISGT Europe), Gothenburg, pp. 1-5, 2010.
- [4] W. Pentland, “Blackout Risk Tool Puts Price Tag on Power Reliability.” Available: <http://www.virlab.virginia.edu>, 2016.
- [5] V. K. Sood, D. Fischer, J. M. Eklund and T. Brown, “Developing a Communication Infrastructure for the Smart Grid,” Proceedings of Electrical Power and Energy Conference (EPEC), 2009 IEEE Conference on, Montreal, QC, pp. 1-7, 2009.
- [6] A. P. García, J. Oliver and D. Gosch, “An Intelligent Agent-based Distributed Architecture for Smart-Grid Integrated Network Management,” Proceedings of 2010 IEEE 35th Conference on Local Computer Networks (LCN), Denver, CO, pp. 1013-1018, 2010.
- [7] D.J. Dolezilek and S. Schweitzer, “Practical Applications of Smart Grid Technologies,” Schweitzer Engineering Laboratories, Inc, 2009.
- [8] M. Souryal, C. Gentile, D. Griffith, D. Cypher and N. Golmie, “A Methodology to Evaluate Wireless Technologies for the Smart Grid,” Proceedings of 2010 First IEEE International Conference on Smart Grid Communications (SmartGridComm), Gaithersburg, MD, pp. 356-361, 2010.

- [9] M. Rahman and A. Mto, “Technologies Required for Efficient Operation of a Smart Meter Network,” Proceedings of 2011 6th IEEE Conference on Industrial Electronics and Applications (ICIEA), Beijing, pp. 809-814, 2011.
- [10] H. Gharavi and B. Hu, “Multigate Communication Network for Smart Grid,” Proceedings of the IEEE, vol. 99, no. 6, pp. 1028-1045, 2011.
- [11] S. Galli, A. Scaglione and Z. Wang, “For the Grid and Through the Grid: The Role of Power Line Communications in the Smart Grid,” Proceedings of the IEEE, vol. 99, no. 6, pp. 998-1027, June 2011.
- [12] T. Sauter and M. Lobashov, “End-to-End Communication Architecture for Smart Grids,” Industrial Electronics, IEEE Transactions on, vol. 58, no. 4, pp. 1218-1228, April 2011.
- [13] Z. Yang, S. Yu, W. Lou and C. Liu, “ $P^2$  : Privacy-Preserving Communication and Precise Reward Architecture for V2G Networks in Smart Grid,” IEEE Transactions on Smart Grid, vol. 2, no. 4, pp. 697-706, Dec. 2011.
- [14] H. Li, L. Lai, and W. Zhang, “Communication requirement for Reliable and Secure State Estimation and Control in Smart Grid,” Smart Grid, IEEE Transactions on, vol. 2, no. 3, pp. 476–486, September 2011.
- [15] H. Li, S. Gong, L. Lai, Z. Han, R. Qiu, and D. Yang, “Efficient and Secure Wireless Communications for Advanced Metering Infrastructure in Smart Grids,” Smart Grid, IEEE Transactions on, vol. 3, no. 3, pp. 1540–1551, September 2012.
- [16] S. Bu, F. Yu, Y. Cai, and X. Liu, “When the Smart Grid Meets Energy-Efficient Communications: Green Wireless Cellular Networks Powered by the Smart Grid,” Wireless Communications, IEEE Transactions on, vol. 11, no. 8, pp. 3014–3024, August 2012.
- [17] M. H. U. Ahmed, M. G. R. Alam, R. Kamal, C. S. Hong, and S. Lee, “Smart Grid Cooperative Communication with Smart Relay,” Communications and Networks, Journal of, vol. 14, no. 6, pp. 640–652, December 2012.



- [18] J. Zhou, R. Hu, and Y. Qian, "Scalable Distributed Communication Architectures to Support Advanced Metering Infrastructure in Smart Grid," *Parallel and Distributed Systems*, IEEE Transactions on, vol. 23, no. 9, pp. 1632-1642, September 2012.
- [19] H. Sun, A. Nallanathan, B. Tan, J. Thompson, J. Jiang, and H. Poor, "Relaying Technologies for Smart Grid Communications," *Wireless Communications*, IEEE, vol. 19, no. 6, pp. 52-59, December 2012.
- [20] G. López, P. S. Moura, V. Custodio and J. I. Moreno, "Modeling the Neighborhood Area Networks of the Smart Grid," *Proceedings of 2012 IEEE International Conference on Communications (ICC)*, Ottawa, ON, pp. 3357-3361, 2012.
- [21] P. Kulkarni, S. Gormus, Z. Fan, and B. Motz, "A Mesh-Radio-based Solution for Smart Metering Networks," *Communications Magazine*, IEEE, vol. 50, no. 7, pp. 86-95, July 2012.
- [22] B. Fateh, M. Govindarasu, and V. Ajjarapu, "Wireless Network Design for Transmission Line Monitoring in Smart Grid," *Smart Grid*, IEEE Transactions on, vol. 4, no. 2, pp. 1076-1086, June 2013.
- [23] Y. Xu and W. Wang, "Wireless Mesh Network in Smart Grid: Modeling and Analysis for Time Critical Communications," *Wireless Communications*, IEEE Transactions on, vol. 12, no. 7, pp. 3360-3371, July 2013.
- [24] P. Y. Kong, "Wireless Neighborhood Area Networks with QoS Support for Demand Response in Smart Grid," *IEEE Transactions on Smart Grid*, no. 99, 2015.
- [25] G. Gupta and N. Shro, "Delay Analysis for Wireless Networks with Single Hop Traffic and General Interference Constraints," *Networking*, IEEE ACM Transactions on, vol. 18, no. 2, pp. 393-405, April 2010.
- [26] I. Al-Anbagi, M. Erol-Kantarci and H. T. Mouftah, "A Low Latency Data Transmission Scheme for Smart Grid Condition Monitoring Applications," *Proceedings of Electrical Power and Energy Conference (EPEC)*, 2012 IEEE, London, ON, pp. 20-25, 2012.

- [27] I. Al-Anbagi, M. Erol-Kantarci, and H. Mouftah, "Priority- and Delay-Aware Medium Access for Wireless Sensor Networks in the Smart Grid," *IEEE Systems Journal*, vol. 8, no. 2, pp. 608-618, June 2014.
- [28] G. Rajalingham, Q. Ho and T. Le-Ngoc, "Attainable Throughput, Delay and Scalability for Geographic Routing on Smart Grid Neighbor Area Networks," *Proceedings of 2013 IEEE Wireless Communications and Networking Conference (WCNC)*, Shanghai, pp. 1121-1126, 2013.
- [29] Q. D. Ho, Y. Gao, G. Rajalingham and T. Le-Ngoc, "Performance and Applicability of Candidate Routing Protocols for Smart Grid's Wireless Mesh Neighbor Area Networks," *Proceedings of 2014 IEEE International Conference on Communications (ICC)*, Sydney, NSW, pp. 3682-3687, 2014.
- [30] N. Master, J. Mounzer and N. Bambos, "Distributed Smart Grid Architecture for Delay and Price Sensitive Power Management," *Proceedings of 2014 IEEE International Conference on Communications (ICC)*, Sydney, NSW, pp. 3670-3675, 2014.
- [31] I. Al-Anbagi, M. Erol-Kantarci and H. Mouftah, "Time Slot Allocation in WSNs for Differentiated Smart Grid Traffic," *Proceedings of Electrical Power and Energy Conference (EPEC)*, 2013 IEEE, Halifax, NS, pp. 1-6, 2013.
- [32] "IEEE standard for information technology-local and metropolitan area networks specific requirements-part 11: Wireless LAN Medium Access Control (MAC) and physical layer (phy) specifications - amendment 8: mac quality of service enhancements," *IEEE Std 802.11e-2005 (Amendment to IEEE Std 802.11, 1999 Edition)*, pp. 1-212, November 2005.
- [33] G. Upton and I. Cook, *A Dictionary of Statistics (2 rev. ed.)* Oxford University Press, UK: ISBN-13: 9780199541454, 2014.
- [34] MATLAB, "Matrix Labortary, Release 2016b," Available: <https://www.mathworks.com/products/matlab.html>, 2016.
- [35] W. Sun, X. Yuan, J. Wang, D. Han and C. Zhang, "Quality of Service Networking for Smart Grid Distribution Monitoring," *Proceedings of 2010 First IEEE International*

Conference on Smart Grid Communications (SmartGridComm), Gaithersburg, MD, pp. 373-378, 2010.

- [36] C. Ide, B. Dusza, M. Putzke, C. Müller and C. Wietfeld, "Influence of M2M Communication on the Physical Resource Utilization of LTE," Proceedings of Wireless Telecommunications Symposium (WTS), 2012, London, pp. 1-6, 2012.
- [37] M. Levorato and U. Mitra, "Optimal Allocation of Heterogeneous Smart Grid Traffic to Heterogeneous Networks," Proceedings of 2011 IEEE International Conference on Smart Grid Communications (SmartGridComm), Brussels, pp. 132-137, 2011.
- [38] A. Cobham, "Priority Assignment in Waiting Line Problems," Journal of the Operations Research Society of America, vol. 2, no. 1, pp. 70-76, January 1954.
- [39] O. Jouini and A. Roubos, "Multiple Priority Multi-Server Queues," Journal of the Operational Research Society, vol. 65, no. 5, pp. 616-632, May 2014.
- [40] W. Feng, M. Kowada, and K. Adachi, "Analysis of a Multi-Server Queue with Two Priority Classes and  $(m, n)$ -Threshold Service Schedule  $i$ : Non-Preemptive Priority," International Transactions in Operational Research, vol. 7, no. 6, pp. 653-671, 2000.
- [41] T. Maertens, J. Walraevens, and H. Bruneel, "A Modified HOL Priority Scheduling Discipline: Performance Analysis," European Journal of Operational Research, vol. 180, no. 3, pp. 1168 - 1185, 2007.
- [42] H. Bruneel and B. G. Kim, "Discrete-Time Models for Communication Systems Including ATM." New York: Kluwer international series in engineering and computer science, Communication and information theory, p.52, 1993.
- [43] A. Noorwali, R. Rao, and A. Shami, "Wireless EDN in Smart Grids Communication: Modelling, Prioritizing, and Delay Analysis," NNGT International Journal on Networking and Communication, vol. 5, no. 4, pp. 1-12, June 2016.
- [44] A. Noorwali, M. Alsharef, R. Rao, and A. Shami, "Delay Analysis of Discrete-Time Non-Preemptive Priority Queues in EDN of Smart Grids," Proceedings of 2016 International conference on the International Conference on Communications

Computer Science and Information Technology (ICCCSIT), Dubai, pp. 2–7, March 2016.

- [45] M. Levorato and U. Mitra, “Optimal Allocation of Heterogeneous Smart Grid Traffic to Heterogeneous Networks,” Proceedings of 2011 IEEE International Conference on Smart Grid Communications (SmartGridComm), Brussels, pp. 132-137, 2011.
- [46] R. Adams, and C. Essex, *Calculus: A Complete Course Plus MyMathLab with Pearson eText – Access Card Package*. Pearson Education Canada, 2013.
- [47] L. Kleinrock, *Queueing Systems*. Wiley Interscience, I: Theory, 1975.
- [48] A. Noorwali, R. Rao and A. Shami, “Modelling and Delay Analysis of Wireless Home Area Networks in a Smart Grid,” Proceedings of 2015 IEEE International Conference on Smart Grid Communications (SmartGridComm), Miami, FL, pp. 569-574, 2015.
- [49] A. Noorwali, R. Rao and A. Shami, “Wireless Home Area Networks in Smart Grids: Modelling and Delay Analysis,” Proceedings of IEEE International Conference on Smart Grid Conference (SASG), Jeddah, Saudi Arabia, pp. 1-7, December 2016.
- [50] A. Noorwali, A. Hamed, R. Rao and A. Shami, “Modeling and Delay Analysis of Wireless HANs in Smart Grids over Fading Channels Subjected to Multiple Access Schemes and Interference,” Proceedings of 2016 IEEE Canadian Conference on Electrical and Computer Engineering (CCECE), Vancouver, BC, Canada, pp. 1-6, May 2016.
- [51] A. M. Hamed and R. K. Rao, “Bandwidth and power efficiency analysis of fading communication link,” 2016 International Symposium on Performance Evaluation of Computer and Telecommunication Systems (SPECTS), Montreal, QC, pp. 1-7, July 2016.
- [52] I. S. Gradshteyn and I. M. Ryzhik, *Table of Integrals, Series, and Products*. 7th ed. Amsterdam: Elsevier/Academic Press, 2007.

- [53] Y. Xu and W. Wang, "Wireless Mesh Network in Smart Grid: Modeling and Analysis for Time Critical Communications," in *IEEE Transactions on Wireless Communications*, vol. 12, no. 7, pp. 3360-3371, July 2013.
- [54] M. K. Simon and M.-S. Alouini, *Digital Communication Over Fading Channels*. Hoboken, New Jersey: John Wiley & Sons, Inc., p.19, 2005.
- [55] B. Sklar, *Digital Communications: Fundamentals and Applications*. Upper Saddle River, NJ, USA: Prentice-Hall, Inc., 1988.
- [56] A. Goldsmith and A. Nin, *Wireless Communications*. New York: Cambridge University, pp. 27-65, 2005.
- [57] X. Fang, S. Misra, G. Xue and D. Yang, "Smart Grid — The New and Improved Power Grid: A Survey," *IEEE Communications Surveys & Tutorials*, vol. 14, no. 4, pp. 944-980, Fourth Quarter 2012.
- [58] Y. Tsado, D. Lund and K. Gamage, "Resilient Wireless Communication Networking for Smart Grid BAN," *Proceedings of 2014 IEEE International Conference on Energy Conference (ENERGYCON)*, Cavtat, pp. 846-851, 2014.
- [59] A. Noorwali, R. Rao and A. Shami, "Performance Evaluation of Channel-Aware MAC protocol in Smart Grid," *Proceedings of 2015 IEEE Conference on Electrical Power and Energy Conference (EPEC)*, London, ON, pp. 429-435, October 2015.
- [60] A. Thapa, S. Pudasaini, M. Kang and S. Shin, "On Achievable Performance Limits of CSMA/CA Adapted MIMO Aware MAC for WLANs," *Proceedings of 2010 6th International Conference on Networked Computing (INC)*, Gyeongju, Korea (South), pp. 1-6, 2010.
- [61] S. Barghi, H. Jafarkhani, and H. zadeh, "MIMO-Assisted MPR-aware MAC Design for Asynchronous WLANS," *IEEE/ACM Transactions on Networking*, vol. 19, no. 6, pp. 1652-1665, Dec 2011.
- [62] D. J. Dechene, K. A. Meerja, and A. Shami, "Performance Evaluation of MIMO-Aware Media Access Control Protocol," *Physical Communication*, vol. 2, no. 3, pp. 204 -216, 2009.

- [63] J. Park, A. Nandan, M. Gerla and H. Lee, "SPACE-MAC: Enabling Spatial Reuse Using MIMO Channel-Aware MAC," Proceedings of IEEE International Conference on Communications, pp. 3642-3646 Vol. 5, 2005.
- [64] M. S. Rahman, Y. Li, and B. Vucetic, "An Iterative ZigZag Decoding for Combating Collisions in Wireless Networks," IEEE Communications Letters, vol. 14, no.3, pp. 242-244, March 2010.
- [65] A. Noorwali, *Performance Analysis of Channel-Aware Media Access Control Schemes*, MS dissertation, Western University, Available: <http://ir.lib.uwo.ca/etd/727>, August 2012.
- [66] S. McCanne and S. Floyd. "NS Network Simulator." Available: <http://www.isi.edu/nsnam>, 2015.
- [67] N. Bisnik and A. Abouzeid, "Delay and Throughput in Random Access Wireless Mesh Networks," Proceedings of 2006 IEEE International Conference on Communications, Istanbul, pp. 403-408, 2006.
- [68] H. Li, Y. Cheng, C. Zhou and W. Zhuang, "Minimizing End-to-End Delay: A Novel Routing Metric for Multi-Radio Wireless Mesh Networks," Proceedings of INFOCOM 2009, IEEE, Rio de Janeiro, pp. 46-54, 2009.
- [69] J. Zhou and K. Mitchell, "A Scalable Delay Based Analytical Framework for CSMA/CA Wireless Mesh Networks," Computer Networks, vol. 54, no. 2, pp. 304-318, 2010.
- [70] J. Jun and M. L. Sichitiu, "MRP: Wireless Mesh Networks Routing Protocol," Computer Communications, vol. 31, no. 7, pp. 1413 - 1435, 2008.
- [71] S. Miskovic and E. W. Knightly, "Routing Primitives for Wireless Mesh Networks: Design, Analysis and Experiments," Proceedings of 2010 IEEE INFOCOM, San Diego, CA, pp. 1-9, 2010.
- [72] A. Raniwala and T. Chiueh, "Architecture and Algorithms for an IEEE 802.11-based Multi-Channel Wireless Mesh Network," Proceedings of IEEE 24th Annual

Joint Conference of the IEEE Computer and Communications Societies, col. 3, pp. 2223-2234, 2005.

- [73] B. Sen, L. Libman, X. Zhao and S. Jha, "An End-to-End Delay metric for Multi-Rate Wireless Mesh Networks with Cooperative Retransmission," Proceedings of 2013 IEEE 38th Conference on Local Computer Networks (LCN), Sydney, NSW, pp. 296-299, 2013.
- [74] C. Seo, E. Leonardo, P. Cardieri, M. Yacoub, D. Gallego and A. de Medeiros, "Performance of IEEE 802.11 in Wireless Mesh Networks," Proceedings of SBMO/IEEE MTT-S International Conference on Microwave and Optoelectronics, pp. 363-367, 2005.
- [75] T. Liu and W. Liao, "Interference-aware QoS Routing for Multi-Rate Multi-Radio Multi-Channel IEEE 802.11 Wireless Mesh Networks," Wireless Communications, IEEE Transactions on, vol. 8, no. 1, pp. 166-175, Jan 2009.
- [76] X. Wu, J. Liu and G. Chen, "Analysis of Bottleneck Delay and Throughput in Wireless Mesh Networks," 2006 IEEE International Conference on Mobile Ad Hoc and Sensor Systems, Vancouver, BC, pp. 765-770, 2006.
- [77] A. Noorwali, R. Rao and A. Shami, "End-to-End Delay Analysis of Wireless Mesh Backbone Network in a Smart Grid," Proceedings of 2016 IEEE Canadian Conference on Electrical and Computer Engineering (CCECE), Vancouver, BC, Canada, pp. 1-6, May 2016.
- [78] J. Li, H. Kao, and J. Ke, "Voronoi-based Relay Placement Scheme for Wireless Sensor Networks," IET Communications, vol. 3, no. 4, pp. 530-538, April 2009.
- [79] C. Chou, J. Su and C. Chen, "Straight Line Routing for Wireless Sensor Networks," Proceedings of 10th IEEE Symposium on Computers and Communications (ISCC'05), pp. 110-115, 2005.
- [80] "IEEE draft standard for information technology-telecommunications and information exchange between systems-local and metropolitan area networks-specific requirements part 11: Wireless LAN medium access control (mac) and physical layer

- (phy) specifications: Amendment to IEEE P802.11-REV MCTM D4.0: Fast initial link setup,” IEEE P802.11ai D7.0, pp. 1-190, Jan 2016.
- [81] N. Maxemchuk and M. El Zarki, “Routing and Flow Control in High-Speed Wide-Area Networks,” *Proceedings of the IEEE*, vol. 78, no. 1, pp. 204-221, Jan 1990.
  - [82] D. Abensour, “High Speed Networking Evolution,” *Proceedings of Distributed Computing Systems, Second IEEE Workshop on Future Trends of*, pp. 238-244, September 1990.
  - [83] A. Noorwali, R. Rao, and A. Shami, “Modeling and Delay Analysis of Wide Area Network in Smart Grid Communications,” *Proceedings of 2016 IEEE Smart Energy Grid Engineering (SEGE)*, pp. 347-352, Aug 2016.
  - [84] G. Westfield, and R. Maher, “Optical Communications System is Setting Record for Fastest Data Transmission.” Available: <http://interestingengineering.com>, 2016.
  - [85] A. Papoulis, *Probability, Random Variables, and Stochastic Processes*. New York: McGraw-Hill, 1991.
  - [86] W. Whitt, “The Queueing Network Analyzer,” *The Bell System Technical Journal*, vol. 62, pp. 2779-2815, April 1983.
  - [87] A. Popescu and D. Constantinescu, *Network Performance Engineering*, Berlin, Heidelberg: Springer-Verlag, pp. 1-13, 2011.
  - [88] W. Marchal, “Numerical Performance of Approximate Queuing Formulae with Application to Flexible Manufacturing Systems,” *Annals of Operations Research*, vol. 3, no. 5, pp. 141-152, 1985.
  - [89] Toronto Demographics. Available: <http://www1.toronto.ca>, 2016.
  - [90] M. Daoud and X. Fernando, “On the Communication Requirements for the Smart Grid,” *Proceedings of Energy and Power Engineering Journal*, Vol. 3 No. 1, pp. 53-60, 2011.
  - [91] A. Sayeed, “Deconstructing Multiantenna Fading Channels,” *Signal Processing, IEEE Transactions on*, vol. 50, no. 10, pp. 2563-2579, October 2002.



- [92] H. Huang, H. Barani, and H. Al-Azzawi, “Network Multiple-Input and Multiple-Output for Wireless Local Area Networks,” ArXiv e-prints, February 2014.

# Curriculum Vitae

**Name:** Abdulfattah Noorwali  
**Year of Birth:** 1985

## Education:

**Ph.D.** Department of Electrical and Computer Engineering  
2012 - 2016 Western University, London, Ontario, Canada  
*Major* Communication Systems and Data Networks

**M.S.C** Department of Electrical and Computer Engineering,  
2010 - 2012 Western University, London, Ontario, Canada  
*Major* Communication Systems and Data Networks

**B.S.C** Department of Electrical Engineering  
2003- 2008 Umm Al-Qura University, Makkah, Saudi Arabia  
*Major* Electrical Engineering

## Experience:

**Teaching Assistant** Western University, London, Ontario, Canada  
2010 - 2016 Department of Electrical and Computer Engineering  
*List of courses* ES 1050 - January - April, 2011  
ES 1036 - January - April, 2012  
ECE 4457A - September - December, 2013  
SE 3314 - January - April, 2014  
ES 1036 - September - December, 2014  
ES 1036 - January - April, 2015  
ECE 3337A - September - December, 2015  
ECE 3375B - January - April, 2016

**Teaching Assistant** Umm Al-Qura University, Makkah, Saudi Arabia  
2008 - 2009 Department of Electrical Engineering

**Awards:****Fellowship**

2010 - 2016

Umm Al-Qura University

Saudi Cultural Bureau, Ottawa, Ontario, Canada

To pursue Master's and Doctoral studies at Western University

**Best Paper****Award**

IEEE International Conference on Smart Energy Grid

Engineering (SEGE'15), UOIT, Oshawa, ON, 21- 24 August, 2016

for the paper: A. Noorwali, R. Rao, and A. Shami,

"Modeling and Delay Analysis of Wide Area Network

in Smart Grid Communications," Proceedings of 2016 IEEE Smart

Energy Grid Engineering (SEGE), pp. 347-352,

Available: <http://www.sege-conference.com>.

**List of Publications:**

- [1] A. Noorwali, "Performance analysis of channel-aware media access control schemes," MSC dissertation, Western University, Available: <http://ir.lib.uwo.ca/etd/727>, 2012.
- [2] A. Noorwali, R. Rao and A. Shami, "Performance Evaluation of Channel-Aware MAC Protocol in Smart Grid," Proceedings of Electrical Power and Energy Conference (EPEC), 2015 IEEE EPEC Conference on, London, ON, pp. 429-435, 2015.
- [3] E. Shafter, A. Noorwali and R. K. Rao, "OFDM Systems with CPM Mappers for Smart Grid Applications," Proceedings of Electrical Power and Energy Conference (EPEC), 2015 IEEE, London, ON, pp. 424-428, 2015.
- [4] A. Noorwali, R. Rao and A. Shami, "Modelling and Delay Analysis of Wireless Home Area Networks in a Smart Grid," Proceedings of 2015 IEEE International Conference on Smart Grid Communications (SmartGridComm), Miami, FL, pp. 569-574, 2015.
- [5] A. Noorwali, M. Alsharef, R. Rao, and A. Shami, "Delay Analysis of Discrete-Time NoN-Preemptive Priority Queues in EDN of Smart Grids," Proceedings of the International Conference on Communications Computer Science and Information Technology (ICCCSIT), 2016 International conference on, Dubai, pp. 2-7, March 2016.
- [6] E. Shafter, A. Noorwali and R. K. Rao, "Peak-to-Average Power Ratio of OFDM Systems with CPM Mappers using PTS for Smart Grid Applications," Proceedings of the International Conference on Communications Computer Science and Information Technology (ICCCSIT), 2016 International conference on, Dubai, pp. 2-6, March 2016.
- [7] A. Noorwali, A. Hamed, R. Rao and A. Shami, "Modeling and Delay Analysis of Wireless HANs in Smart Grids Over Fading Channels Subjected to Multiple Access Schemes and Interference," Proceedings of Electrical and Computer Engineering

- (CCECE), 2016 IEEE 29th Canadian Conference on, Vancouver, BC, pp. 1-6, May 2016.
- [8] A. Noorwali, R. Rao and A. Shami, "End-to-End Delay Analysis of Wireless Mesh Backbone Network in a Smart Grid," Proceedings of Electrical and Computer Engineering (CCECE), 2016 IEEE 29th Canadian Conference on, Vancouver, BC, pp. 1-6, May. 2016.
  - [9] A. Hamed, A. Noorwali, and R. Rao, "Energy Efficient Adaptive Transmission in Generalized-K Fading Channel network," Proceedings of Electrical and Computer Engineering (CCECE), 2016 IEEE 29th Canadian Conference on, Vancouver, BC, pp. 1-16, May. 2016.
  - [10] A. Noorwali, R. Rao, and A. Shami, "Wireless EDN in Smart Grids Communication: Modelling, Prioritizing, and Delay Analysis," NNGT International Journal on Networking and Communication, vol. 5, no. 4, pp.1-12, June 2016.
  - [11] A. Noorwali, R. Rao, and A. Shami, "Modeling and Delay Analysis of Wide Area Network in Smart Grid Communications," Proceedings of 2016 IEEE Smart Energy Grid Engineering (SEGE), pp. 347-352, Aug 2016.
  - [12] A. Noorwali, R. Rao and A. Shami, "Wireless Home Area Networks in Smart Grids: Modelling and Delay Analysis," Proceedings of Smart Grid Conference (SASG), IEEE International Conference on, Jeddah, Saudi Arabia, pp. 1-7, December 2016.